Fall 1-1-2015

Severely Stressed Astrocytes Adapt to Injury and Still Protect Neighboring Neurons

Amanda Marie Gleixner

SEVERELY STRESSED ASTROCYTES ADAPT TO INJURY AND STILL PROTECT NEIGHBORING NEURONS

A Dissertation

Submitted to the Mylan School of Pharmacy

Duquesne University

In partial fulfillment of the requirements for

the degree of Doctor of Philosophy

By

Amanda Marie Gleixner

December 2015

SEVERELY STRESSED ASTROCYTES ADAPT TO INJURY AND STILL PROTECT NEIGHBORING NEURONS

By

Amanda Marie Gleixner

Approved November 2, 2015

_____	_____
Rehana K. Leak, Ph.D. Assistant Professor of Pharmacology Graduate School of Pharmaceutical Sciences Duquesne University, Pittsburgh, PA (Committee Chair)	Lauren O'Donnell, Ph.D. Assistant Professor of Pharmacology Graduate School of Pharmaceutical Sciences Duquesne University, Pittsburgh, PA (Committee Member)
_____	_____
Paula Witt-Enderby, Ph.D. Professor of Pharmacology Graduate School of Pharmaceutical Sciences Duquesne University, Pittsburgh, PA (Committee Member)	Wilson Meng, Ph.D. Associate Professor of Pharmaceutical Sciences Graduate School of Pharmaceutical Sciences Duquesne University, Pittsburgh, PA (Committee Member)
_____	_____
Sandra Hewett, Ph.D. Professor of Biology Department of Biology Syracuse University, Syracuse, NY (Committee Member)	J. Douglas Bricker, Ph.D. Dean and Professor of Pharmacology-Toxicology Mylan School of Pharmacy Graduate School of Pharmaceutical

ABSTRACT

SEVERELY STRESSED ASTROCYTES ADAPT TO INJURY AND STILL PROTECT NEIGHBORING NEURONS

By

Amanda Marie Gleixner

December 2015

Dissertation supervised by Rehana K. Leak

Neurodegenerative disorders such as Parkinson's and Alzheimer's disease are projected to affect 15.14 million people by the year 2050. All neurodegenerative diseases are characterized by protein-misfolding stress, or proteotoxicity, in both neurons and glia. However, the impact of proteotoxicity on glia is less well understood than in neurons. Astrocytes are an abundant type of glia and play an essential role in brain homeostasis by supporting neuronal functions. Therefore, one of the major goals of the present study was to identify ways to reduce the impact of proteotoxicity in astrocytes. In Aim 1, we examined natural adaptations to proteotoxic stress in astrocytes. Our studies demonstrate that the astrocytes surviving a severe proteotoxic insult are resistant to subsequent challenges due to upregulation of the antioxidant biomolecule glutathione. Prior to this body of work, only mild stressors were thought to elicit stress tolerance and severe stress was thought to only weaken cells. In contrast with traditional views of reactive

astrocytes, severely stressed astrocytes were still able to protect neighboring neurons from proteotoxic injury in our model. In Aim 2, we examined the therapeutic potential of N-acetyl cysteine, a glutathione precursor known to benefit patients with neurological disorders. We discovered that N-acetyl cysteine protected astrocytes from proteotoxic stress independent of glutathione. Instead, the protection afforded by N-acetyl cysteine was abolished by heat shock protein inhibitors, suggesting a novel mechanism of action for N-acetyl cysteine in astrocytes. It is important to promote heat shock protein activity in patients with neurodegenerative conditions because loss of chaperone defenses may contribute to proteotoxicity in the elderly. In Aim 3, we characterized the impact of aging on the expression of several heat shock proteins, many of which are expressed in astrocytes. We discovered age-related changes in multiple heat shock proteins in the substantia nigra, caudoputamen, and olfactory bulb, three regions known to develop Lewy pathology in Parkinson's disease. In conclusion, astrocytes can be protected against protein-misfolding stress by upregulation of endogenous glutathione defenses or by N-acetyl cysteine treatment. Furthermore, some heat shock proteins are increased with aging, perhaps as an endogenous defense against proteotoxic stress in older animals.

ACKNOWLEDGEMENT

My sincerest gratitude goes to my research advisor Dr. Rehana Leak. I admire your passion and dedication for research. This dissertation project has been made possible through your encouragement, knowledge, and support. Thank you for always challenging me and fully devoting your time and attention to my graduate research studies.

My committee members, Drs. Paula Witt-Enderby, Lauren O'Donnell, Wilson Meng and Sandra Hewett, were phenomenal in providing insight into different aspects of this research project. It was through their help that this project became an in-depth assessment of the literature and enhanced our understanding of astrocytic responses to protein misfolding stress.

I appreciate the help and support from my fellow graduate students, especially my lab-mates. Thank you for teaching me how to use shared instruments, providing reagents, and for our scientific discussions that helped me to look at my data with a fresh perspective. I am especially appreciative of my time spent with Jessica Posimo in the lab. Thank you for the hugs, laughs, and support. My time in graduate school was made much more enjoyable because of our time together.

My time spent at Duquesne was made more enjoyable and ran more smoothly because of the dedicated efforts by the support staff: Debbie Willson, Mary Caruso, Jackie Farrer, and Nancy Hosni. I cherish the friendships that we have developed over the years and will forever remember the support and encouragement that you have given me.

I appreciate having had the opportunity to teach and mentor many undergraduate and Doctor of Pharmacy students during my studies at Duquesne University. My passion for teaching was strengthened through my involvement in your research projects. I especially appreciate

having the opportunity to work with Ajay Unnithan and Deepti Pant. I am also truly indebted to Diane Rhodes for strengthening my teaching skills. I will forever cherish our time spent together, friendship, and all of the support and guidance that you have provided to me over the years.

I cannot put into words the gratitude and appreciation that I have for my family's support. Completion of this project would not be possible without their faith and guidance. I would not be here, completing my doctorate, if it were not for my parent's encouragement to enter into graduate school. They were my shining light when times were more challenging than I could ever imagine. I appreciate all times that my parents and siblings lent a helping hand when I could not juggle all of life's needs with my graduate studies. To Dan: Thank you for your endless support, keeping me calm when stress levels were high, and always helping me to keep life in perspective. To Natalie: thank you for motivating me to complete my studies and although you may not understand what is happening right now, thank you for being so cooperative. I love you all and thank you for every bit of help along the way.

The efforts and success of this research project were made possible through the academic and financial support provided by Dr. James K. Drennen, III and the Graduate School of Pharmaceutical Sciences in the Mylan School of Pharmacy at Duquesne University. Other financial support was provided by Commonwealth Universal Research Enhancement (C.U.R.E) program of Pennsylvania, the National Institutes of Health, and the Hillman Foundation. Many of these studies were also made possible through the donation of reagents from Drs. Patrick Flaherty, Peter Wipf, and Jeffrey Brodsky.

TABLE OF CONTENTS

Page

LIST OF FIGURES

Page

LIST OF ABBREVIATIONS

Adenosine triphosphate ..... ATP

Astrocyte-conditioned media ..... ACM

Buthionine sulfoximine ..... BSO

Glial fibrillary acidic protein ..... GFAP

Glutamate cysteine ligase ..... GCL

Glutamate cysteine ligase catalytic subunit ..... GCLC

Glutamate cysteine ligase modifier subunit ..... GCLM

Glutathione synthetase ..... GS

Glucose regulated protein, 78kDa GRP78

Heat shock factor 1 ..... HSF1

Heat shock cognate 70 ..... .Hsc70

Heat shock protein 27 ..... Hsp27

Heat shock protein 40 ..... Hsp40

Heat shock protein 60 ..... Hsp60

Heat shock protein 70 ..... Hsp70

Heat shock protein 90 ..... Hsp90

Heat shock factor 1 ..... HSF1

Heme oxygenase 1 ..... HO1

Kelch-like ECH-associated protein Keap1

Microtubule associated protein 2 ..... MAP2

N-acetyl L-cysteine ..... NAC

Nuclear factor-erythroid 2-related factor-2 ..... Nrf2

Phosphate buffered saline ..... PBS

Tris buffered saline ..... TBS

Ubiquitin proteasome system ..... UPS

Chapter 1 Introduction

1.1 Neurodegenerative diseases

Alzheimer's and Parkinson's disease are the most prevalent neurodegenerative disorders and are becoming increasingly common as the United States' population ages (Hebert, Weuve, Scherr, & Evans, 2013; Kowal, Dall, Chakrabarti, Storm, & Jain, 2013). Patients with Parkinson's disease exhibit premotor (hyposmia, rapid eye movement disturbances), motor (rigidity, resting tremor, dyskinesia), and nonmotor (depression, anxiety, psychosis) symptoms, although the motor symptoms are the most easily recognized (Chaudhuri, Healy, & Schapira, 2006; Ponsen et al., 2004). Alzheimer's patients exhibit memory loss, personality changes, and cognitive impairments (Mega, Cummings, Fiorello, & Gornbein, 1996). The etiologies of Parkinson's and Alzheimer's disease have not been established but are attributed to a combination of genetic and environmental factors (Gatz et al., 2006; Warner & Schapira, 2003). For example, residence in rural areas and chronic exposure to pesticides and herbicides are known to increase the risk for developing Parkinson's disease (McCormack et al., 2002). Parkinson's disease is more prevalent in men whereas women are at greater risk for developing Alzheimer's disease (Fratiglioni et al., 1997; Van Den Eeden et al., 2003). Both disorders place an enormous physical and emotional toll on patients and their caregivers. It is estimated that greater than 240 billion dollars are spent annually on caring for patients with these two conditions (M. D. Hurd, Martorell, & Langa, 2013; Kowal, et al., 2013). Thus, it is imperative to find treatments that will slow or halt the progression of these disorders.

1.1.1 Hallmark pathologies in Parkinson's and Alzheimer's disease

All neurodegenerative diseases are characterized by progressive cell loss in specific brain regions over the course of years, if not decades. Vulnerable brain regions in these conditions are

known to exhibit high levels of oxidative stress in postmortem analyses (Jenner, Dexter, Sian, Schapira, & Marsden, 1992; Markesbery, 1997). For example, the hippocampus and cortex exhibit increases in advanced glycation end productions, nitration, lipid peroxidation adduction, and carbonyl-modified neurofilament proteins in Alzheimer's patients (Adams, Klaidman, Odunze, Shen, & Miller, 1991; Venkateshappa, Harish, Mahadevan, Srinivas Bharath, & Shankar, 2012; Venkateshappa et al., 2012). In response to oxidative damage, numerous compensatory changes in pro-survival molecules, such as glutathione, are also evident in these disorders (Damier, Hirsch, Zhang, Agid, & Javoy-Agid, 1993; Mythri et al., 2011). Furthermore, other antioxidant defense systems, such as heme oxygenase 1 (heat shock protein 32 (Hsp32) or HO1) and superoxide dismutases are increased in neurodegenerative diseases (Jenner, 1992; Mateo et al., 2010). The upregulation of endogenous antioxidant defenses may at least partly explain the slow progression of neurodegeneration in these conditions. Thus, enhancing these cellular defenses through pharmacological methods may further delay the progression of neurodegenerative diseases.

Besides evidence of oxidative stress, another major hallmark of neurodegenerative conditions is the stereotyped, progressive accumulation of protein aggregations in specific brain regions (Braak, Ghebremedhin, Rub, Bratzke, & Del Tredici, 2004; Braak, Rub, Gai, & Del Tredici, 2003; Braak, Rub, Schultz, & Del Tredici, 2006; Braak, Sastre, & Del Tredici, 2007). For example, Parkinson's patients exhibit alpha-synuclein^{+} Lewy bodies and Lewy neurites and Alzheimer's patients exhibit extracellular beta-amyloid plaques and intracellular neurofibrillary tangles containing hyperphosphorylated tau (Hardy & Selkoe, 2002; Spillantini, Crowther, Jakes, Hasegawa, & Goedert, 1998). The buildup of misfolded proteins in both conditions is thought to inhibit the activity of the proteasomal and lysosomal protein degradation systems (Keller, Hanni,

& Markesbery, 2000a; McNaught, Belizaire, Isacson, Jenner, & Olanow, 2003; McNaught & Jenner, 2001). Thus, both Parkinson's and Alzheimer's disease are characterized by severe and inexorable loss of protein homeostasis. This loss of protein homeostasis is also known as proteotoxicity and is thought to propel and propagate oxidative stress (Alexandrova, Petrov, Georgieva, Kirkova, & Kukan, 2008a; Morimoto, 2008). Conversely, reactive oxygen species can oxidize proteins, disrupt their native conformations, and promote the formation of protein aggregates (Davies, 1987; Floyd & Carney, 1992; Salvi, Carrupt, Tillement, & Testa, 2001). As a result, normal protein functions may be impaired, leading to amplification of proteotoxicity and further loss of homeostasis. In sum, restoration of redox and protein homeostasis may be essential for the prevention of neurodegenerative diseases.

1.1.2 Astrocyte pathology in neurodegenerative conditions

Parkinson's and Alzheimer's pathologies are known to affect both neurons and glia, although the neuronal changes have been investigated more thoroughly. Specifically, the impact of neurodegeneration on astrocytes is less well understood. In Parkinson's disease, astrocytes contain alpha-synuclein^{+} protein aggregations in a topographic pattern that mimics the staged appearance of neuronal inclusions across specific brain regions (Braak, et al., 2007; Guo, Wharton, Moseley, & Shi, 2007; Wakabayashi, Hayashi, Yoshimoto, Kudo, & Takahashi, 2000). As alpha-synuclein is a neuronal protein, these astrocytes are thought to engulf alpha-synuclein from the extracellular space (Miyata et al., 2012). Astrocytes have also been observed to accumulate beta-amyloid (1-42) in Alzheimer's disease (Acunzo, Katsogiannou, & Rocchi, 2012). In both diseases, there is a robust increase in glial fibrillary acidic protein (GFAP), a marker of astrocyte activation (Le Prince et al., 1993; Mythri, et al., 2011). Other neurodegenerative diseases, such as Huntington's disease and amyotrophic lateral sclerosis may

also negatively impact astrocytes. Regions associated with neurodegeneration and glial activation in Huntington's disease exhibit an increase in small heat shock protein defenses (Seidel et al., 2012). For example, astrocytes exhibit increased reactivity in the spinal cord of amyotrophic lateral sclerosis patients compared to control subjects(Aronica, Catania, Geurts, Yankaya, & Troost, 2001).

Astrocytes are known to be less susceptible than neurons to loss of protein homeostasis and cell death than neurons in these conditions. For example, studies of primary neurons and astrocytes reveal that neurons are more susceptible to proteasome inhibitors than astrocytes (Dasuri et al., 2010). However, both neurons and astrocytes are known to increase heat shock protein expression in response to proteotoxicity (Morimoto, 2008). These observations suggest that both cell types can respond to and defend against proteotoxic stress. However, astrocytes may mount better defenses than neurons because their role is to support damaged neurons and build scar tissue in areas of severe injury. Alternatively, unlike most adult neurons, injured astrocytes may continue to proliferate in order to maintain glial population numbers.

1.2 Ubiquitin proteasome system

1.2.1 Ubiquitin proteasome system structure and function

The ubiquitin proteasome system (UPS) is one of the major protein degradation systems in eukaryotic cells. The UPS maintains protein homeostasis by degrading damaged proteins into peptides that are then recycled into amino acids by peptidases. Both ubiquitin-conjugated and oxidized proteins are degraded by the UPS (Lecker, Goldberg, & Mitch, 2006; Shringarpure, Grune, Mehlhase, & Davies, 2003). Degradation of proteins through the UPS occurs within the catalytic 26S proteasome particle and is dependent upon adenosine triphosphate (ATP) (Ciechanover & Schwartz, 1994). The 26S proteasome consists of one 20S and two 19S protein

complexes. The 19S subunits recognize proteins tagged for degradation with ubiquitin side-chains. The ubiquitin-conjugated proteins are then linearized to facilitate their entrance into the barrel-like structure of the 20S subunit. Efficient enzymatic degradation of proteins into peptides occurs in the 20S subunit by chymotrypsin-, trypsin-, and caspase-like enzymatic activities (D. H. Lee & Goldberg, 1998).

Cytosolic proteins destined for degradation by the UPS are tagged with ubiquitin through three enzymatic steps (Pickart, 2001). Ubiquitin activating enzymes are designated as E1 enzymes and hydrolyze ATP and adenylate the ubiquitin molecule. After adenylation of ubiquitin by E1, ubiquitin conjugating enzymes, designated as E2 enzymes, transfer ubiquitin to the cysteine residues of the misfolded protein. Subsequently, ubiquitin ligating enzymes designated as E3 enzymes catalyze the transfer of ubiquitin from E2 to the target protein. The target protein must be labeled with at least four ubiquitin molecules prior to its recognition by the proteasome (Deveraux, Ustrell, Pickart, & Rechsteiner, 1994). Finally, proteins destined for proteasomal degradation are tagged by ubiquitin molecules that are linked through lysine 48 of the adjacent ubiquitin, also known as K48-linked ubiquitin (Jacobson et al., 2009). Because of the essential nature of the UPS, inhibitors of this protein clearance system elicit protein aggregations and cell death.

1.2.2 Impact of Parkinson's and Alzheimer's disease on the ubiquitin proteasome system

Impairment of the UPS has been observed in postmortem tissue from Parkinson's disease and Alzheimer's disease patients. For example, chymotrypsin, trypsin, and caspase enzymatic activity are decreased in the substantia nigra of Parkinson's disease patients relative to age matched controls (Cook & Petrucelli, 2009; McNaught & Jenner, 2001). Similarly, chymotrypsin activity of the proteasome was decreased (relative to age-matched controls) in the hippocampus

of brains obtained from Alzheimer's disease patients (Keller, Hanni, et al., 2000a). Furthermore, the substantia nigra of Parkinson's disease patients harbors fewer proteasomal subunits than in control patients (Cook & Petrucelli, 2009). Alpha-synuclein, a major component of Lewy bodies and Lewy neurites, is known to inhibit the activity of the UPS and to propagate proteotoxicity (Lindersson et al., 2004). Under some conditions, impaired UPS activity may cause the cells to shift towards autophagic degradation of proteins (Cecarini et al., 2014). However, in neurodegenerative disorders, autophagic protein clearance is also compromised, leading to severe loss of protein homeostasis (Anglade et al., 1997; Cuervo, Stefanis, Fredenburg, Lansbury, & Sulzer, 2004; Nixon et al., 2005).

1.2.3 Modeling impairments in the ubiquitin proteasome system

Pharmacological inhibitors targeting the UPS elicit proteasome impairment and proteotoxicity and are used to model neurodegenerative diseases *in vitro* and *in vivo* (Rideout, Larsen, Sulzer, & Stefanis, 2001; Rideout & Stefanis, 2002; Sawada et al., 2004; F. Sun et al., 2006). MG132 (carbobenzoxy-L-leucyl-L-leucyl-L-leucinal) is a peptide aldehyde that reversibly inhibits the chymotrypsin-like activity of the 26S proteasome (Alexandrova, Petrov, Georgieva, Kirkova, & Kukan, 2008b; Braun et al., 2005; Kisselev & Goldberg, 2001). Although MG132 has also been shown to inhibit proteases such as cathepsin A, cathepsin B, and calpain (Ostrowska, Wojcik, Omura, & Worowski, 1997; Rivett & Gardner, 2000; Shirley et al., 2005), all of these effects converge to elicit loss of protein homeostasis or proteotoxicity. Thus, experiments using MG132 are thought to model proteotoxic stress and not merely proteasome inhibition. Additional proteasome inhibitors with different mechanisms of action include lactacystin. Lactacystin is a cyclic amide that covalently binds β2 of the 20S subunit of the proteasome and irreversibly inhibits UPS protein clearance (D. H. Lee & Goldberg, 1998). As

with all inhibitors, the effects of lactacystin are not limited to the proteasome because lactacystin also inhibits cathepsin B (D. H. Lee & Goldberg, 1998).

1.3 Heat shock proteins

1.3.1 Heat shock protein biology and defense against proteotoxicity

In response to proteotoxicity, cells are known to upregulate pro-survival molecules that reduce loss of protein homeostasis and combat cell death. Heat shock proteins are molecular chaperones that refold misfolded proteins, aid in protein degradation by the UPS and lysosome, and activate the unfolded protein response in the endoplasmic reticulum (Walter & Ron, 2011). Heat shock proteins also inhibit caspase-mediated apoptosis. Heat shock proteins can be constitutively expressed (e.g. heat shock cognate 70 (Hsc70)) or stress induced (e.g. heat shock protein 70 (Hsp70) and heat shock protein 27 (Hsp27)). These proteins are typically grouped into high molecular weight (e.g. Hsp70 and heat shock protein 90 (Hsp90)) and small heat shock proteins (e.g. Hsp27). Typically, the high molecular weight heat shock proteins are ATP-dependent whereas the small heat shock proteins are ATP-independent (Lanneau, Wettstein, Bonniaud, & Garrido, 2010).

Hsp70 is the best-studied member of the heat shock protein family and is comprised of three interdependent domains: N-terminal ATPase domain, peptide binding domain, and a helical lid domain (Lanneau, et al., 2010). The coordinated functions of these protein domains determine Hsp70 folding activity. A number of co-chaperones drive Hsp70-mediated protein degradation or protein refolding. For example, Hsp70-mediated protein degradation is facilitated by binding to the co-chaperones BAG1 and CHIP. BAG1 binds to the ATPase domain while CHIP, a ubiquitin ligase, binds to the substrate-binding domain. Alternatively, the

co-chaperone heat shock protein 40 (Hsp40) binds to the ATPase domain of Hsp70 to stimulate the refolding of proteins bound to the Hsp70-misfolded protein complex.

In addition to refolding misfolded proteins and promoting intracellular protein degradation, Hsp70 attenuates oxidative stress and may be released by exosomes to work in the extracellular space (Taylor, Robinson, Gifondorwa, Tytell, & Milligan, 2007). For example, astrocytes are known to release Hsp70, which may offer protection against the proteotoxicity in neighboring cells (Taylor, et al., 2007). Hsp70 may also attenuate cellular damage by upregulating glutathione defenses. For example, Guo and colleagues have shown that over-expression of Hsp70 increases glutathione reductase and glutathione peroxidase activity after oxygen glucose deprivation (Guo, et al., 2007). Hsp70, unlike Hsc70, is susceptible to oxidation at cysteine residues (Miyata, et al., 2012). These findings suggest that Hsp70 may be sensitive to oxidative stress and regulate redox cycling and glutathione defenses in additional to its traditional chaperone functions. Hsp70 is also known to inhibit caspase-mediated apoptosis (Beere et al., 2000; Ravagnan et al., 2001). Hsp27 (or the murine form Hsp25) is able to attenuate apoptosis in addition to its role in enhancing catalytic activity of the proteasome (Acunzo, et al., 2012; Lanneau, et al., 2010).

As mentioned above, disruption of protein homeostasis usually occurs in association with oxidative stress. Some heat shock proteins are known to decrease oxidative stress. HO1 (also known as Hsp32) is involved in antioxidant defense and breaks down toxic heme into the reactive oxygen species scavenger biliverdin and the prosurvival molecule carbon monoxide (Schipper, 2011). Many studies have shown that HO1 is increased in astrocytes in neurodegenerative conditions, possibly as a compensatory response (Schipper, 2011; Schipper, Liberman, & Stopa, 1998).

Proteotoxicity is often measured in the cytoplasm. However, proteotoxicity is also observed in the endoplasmic reticulum and can be reversed through the unfolded protein response. Glucose-regulated protein 78 kDa (GRP78) is a member of the same chaperone family as Hsp70 and mediates the unfolded protein response (Walter & Ron, 2011). Heat shock protein 60 (Hsp60) is typically associated with mitochondrial proteotoxicity and is responsible for refolding misfolded proteins (Saibil, 2013), (Clare & Saibil, 2013).

1.3.2 Inhibition of heat shock protein activity

In order to study the role of heat shock proteins, several small molecules inhibitors have been developed to decrease heat shock protein activity. Inhibition of Hsp70 activity can occur via blockade of the ATPase and/or substrate binding domains. There are three major classes of Hsp70 inhibitors. VER155008, an adenosine-derived inhibitor, binds to the active site of Hsp70 and Hsc70 to inhibit ATPase activity (Chatterjee et al., 2013; Massey et al., 2010; Schlecht et al., 2013). MAL3-101 is an allosteric Hsp70 inhibitor and interferes with the interaction of Hsp40 and the ATPase domain of Hsp70 (Adam et al., 2014; Fewell et al., 2004; Huryn et al., 2011). 2-phenylethynsulfonimide (PES or pifithrin-μ) is a small molecule inhibitor and binds to the substrate binding domain of Hsp70 to attenuate chaperone activity (Granato et al., 2013; Kondoh & Osada, 2013; Leu, Pimkina, Frank, Murphy, & George, 2009; Leu, Pimkina, Pandey, Murphy, & George, 2011). HO1 activity can be inhibited by tin protoporphyrin IX (SnPPx), which competes with heme for the active site of the enzyme (Drummond & Kappas, 1981; Yoshinaga, Sassa, & Kappas, 1982).

1.3.3 *Heat shock protein changes in Parkinson's disease*

As neurodegenerative diseases are characterized by the accumulation of misfolded proteins, heat shock proteins are often upregulated in these conditions and bound to protein

aggregations. For example, Hsp70 is found in Lewy bodies and Lewy neurites in Parkinson's patients (McNaught, Shashidharan, Perl, Jenner, & Olanow, 2002). Increases in Hsp27 and HO1 have been observed in astrocytes in Parkinson's disease (Renkawek, Stege, & Bosman, 1999; Schipper et al., 2006). Although heat shock protein levels are increased in neurodegenerative conditions, their activity may not be sufficient to fully attenuate or reverse proteotoxicity. On the other hand, it seems likely that they are partly responsible for the slow progression of these disorders given their established roles in protein folding and degradation.

1.3.4 Heat shock protein changes with aging

Aging is thought to be the major risk factor for neurodegenerative diseases, perhaps because of accrual of oxidative and proteotoxic damage. Age-related increases in cellular stress may be attributed to a decline in proteasome and autophagic systems and an increase in mitochondrial dysfunction (Keller, Gee, & Ding, 2002; Keller, Huang, & Markesbery, 2000; H. C. Lee & Wei, 2012; Martinez-Vicente, Sovak, & Cuervo, 2005). In normal aging, protein aggregations often appear in the olfactory bulb (Attems, Lintner, & Jellinger, 2005). Aging has also been associated with degeneration of dopaminergic neurons in the substantia nigra and a decline in striatal dopamine levels, although other studies have failed to observe age-related decreases in dopamine neurons (Gibb & Lees, 1991; Kish, Shannak, Rajput, Deck, & Hornykiewicz, 1992; McCormack et al., 2004). Furthermore, striatal volume is known to decrease with age (Raz et al., 2003).

There are conflicting reports of changes in heat shock proteins with aging. Calabrese and colleagues observed an age-related increase in Hsp70 in the cortex, striatum, and hippocampus, whereas Arumugam and colleagues observed an age-related decrease in Hsp70 in the cortex and striatum (Arumugam et al., 2010; V. Calabrese et al., 2004). However, many studies are in

agreement that Hsp25/Hsp27 expression is increased with natural aging (Dickey et al., 2009; Gupte et al., 2010; Schultz et al., 2001). Advancing age is associated with a decrease in GRP78 in the cortex, striatum, and hippocampus but an increase in the substantia nigra (Alladi et al., 2010; Arumugam, et al., 2010; Hussain & Ramaiah, 2007; Paz Gavilan et al., 2006). Hsc70 is reported to increase with aging in the pons, medulla, striatum, thalamus, and substantia nigra (V. Calabrese, et al., 2004; Unno et al., 2000). Declines in heat shock proteins may contribute to disruption of protein homeostasis associated with aging while increases may help mitigate age-related proteotoxic stress.

1.4 Astrocyte biology

1.4.1 Neurosupportive role

Astrocytes, once thought to be merely "brain glue," are essential for many neuronal and extraneuronal functions (Allen & Barres, 2009). For example, astrocytes are the primary source of glutathione in the brain and can robustly upregulate heat shock protein defenses (Dringen, 2000; Dringen, Gutterer, & Hirrlinger, 2000; Schipper, et al., 2006; Schipper, et al., 1998). As mentioned above, astrocytes are also known to release Hsp70 into the extracellular space via exosomes (Taylor, et al., 2007). Some authors have argued that astrocytes play a toxic role (Gouix et al., 2014; Jana & Pahan, 2010). Although this may be the case in some disease states, it seems likely that astrocytes are more often protective given their overwhelmingly supportive nature. In other words, if astrocytes were absent from the diseased brain, one would expect even greater neuronal injury.

1.4.2 Primary source of brain glutathione

Neurons and glia are both equipped to synthesize glutathione. Nevertheless, astrocytes are the primary source of glutathione in the central nervous system (Dringen, 2000). Astrocytes

can promote neuronal glutathione synthesis by releasing glutathione and glutathione precursors into the extracellular space. Glutathione precursors, such as glutamate and cysteine, are then taken up by neurons for *de novo* glutathione synthesis (Dringen, et al., 2000; Dringen, Pfeiffer, & Hamprecht, 1999).

1.5 Glutathione

Glutathione is the most abundant antioxidant found throughout the body and can exist in millimolar concentrations (Aquilano, Baldelli, & Ciriolo, 2014; Meister & Anderson, 1983). Glutathione plays an important role in the metabolism of xenobiotics via glutathione S-transferase, enzymatic elimination of peroxides, and reduction of free radicals through the cysteine thiol.

1.5.1 Synthesis and regulation

Glutathione is a tripeptide molecule comprised of glutamate, cysteine, and glycine. Glutathione production relies on the availability of synthetic enzymes (glutamate cysteine ligase and glutathione synthetase) and glutathione substrates. The transcription factor nuclear factor (erythroid-derived 2)-like 2 (Nrf2) regulates glutamate cysteine ligase (GCL) and glutathione synthetase (GS) transcription. Under basal conditions (no oxidative stress), Nrf2 is bound to Kelch-like ECH-associated protein (Keap1). Reactive oxygen species can react with the cysteines on Keap1 to elicit its dissociation from Nrf2 (Fourquet, Guerois, Biard, & Toledano, 2010; D. D. Zhang & Hannink, 2003). Upon dissociation from Keap1, Nrf2 translocates to the nucleus and induces GCL and GS transcription, among other genes. If glutathione substrate and synthetic enzyme levels are sufficient, the first step of glutathione synthesis can proceed and GCL ligates glutamate and cysteine. GCL activity is regulated by modifier (GCLM) and catalytic (GCLC) subunits. GCLM has been shown to promote the enzymatic efficiency of GCLC (S. C.

Lu, 2009). In the final synthetic step, glycine is incorporated into the glutamate-cysteine molecule by GS (S. C. Lu, 2013).

Cysteine availability is a rate-limiting factor in glutathione synthesis. The membrane transporter system x_c^- is responsible for importing cystine or cysteine while exporting glutamate. Once imported, cystine can be converted to cysteine by cystine reductase. Astrocytes are known to express system x_c^- and thereby obtain the cysteine necessary for glutathione synthesis. The prodrug *N*-acetyl L-cysteine (NAC) can provide the L-cysteine for the glutathione synthetic pathway (Zhou et al., 2015). NAC can also activate system x_c^- and thereby promote glutathione synthesis (Baker et al., 2003).

The amino acid cysteine can exist in two isomeric forms: L-cysteine and D-cysteine. L-cysteine is the highly abundant form of cysteine and can be incorporated into glutathione. D-cysteine cannot be used in glutathione synthesis and is not readily found in cells. However, both L- & D-cysteine can decrease reactive oxygen species through their sulfhydryl group. The sulfhydryl group donates a hydrogen molecule and neutralizes free radicals. D-amino acid oxidase and D-aspartate oxidase interconvert L- & D-amino acids (Friedman & Levin, 2012; Sacchi et al., 2008). D-amino acid oxidase is thought to convert D-cysteine to L-cysteine to increase glutathione synthesis. Thus, D-cysteine-mediated protection in the absence of D-amino acid oxidase activity would be suggestive of thiol-mediated effects.

Glutathione synthesis is a tightly regulated process. Upon exposure to oxidative stress, there is rapid activation of Nrf2, as outlined above, and this promotes transcription and translation of the enzymes that synthesize glutathione (Taguchi, Motohashi, & Yamamoto, 2011). Conversely, cells also negatively regulate glutathione synthesis in the presence of excess glutathione. For example, high levels of glutathione inhibit further glutathione synthesis by

blocking GCL activity (Franklin et al., 2009). This process of glutathione synthesis blockade can be replicated with buthionine sulfoximine (BSO), a reversible, competitive inhibitor of GCL (Griffith, 1982; Griffith & Meister, 1979). Methionine sulfoximine and etanidazole also inhibit glutathione synthesis but are thought to be less specific than BSO (Griffith, 1982).

Aside from synthesizing glutathione, astrocytes are known to tightly regulate the oxidized and reduced form of glutathione. Glutathione becomes oxidized when glutathione peroxidase converts hydrogen peroxide into water and oxygen. This enables astrocytes to prevent oxidative damage from the production and accumulation of hydrogen peroxide. The oxidized form of glutathione is readily converted back to the reduced form by glutathione reductase. Glutathione is primarily found in the reduced form, permitting it to exert antioxidant effects (Owen & Butterfield, 2010).

1.5.2 Changes in glutathione defenses associated with neurodegenerative diseases

Table 1 highlights some of the changes in glutathione and glutathione-related proteins in various neurodegenerative diseases (Adams, et al., 1991; Damier, et al., 1993; Maher, 2005; Mythri, et al., 2011; Pearce, Owen, Daniel, Jenner, & Marsden, 1997; Sian et al., 1994). A net decrease in glutathione relative to age-matched control patients has been observed in brain regions highly susceptible to Parkinson's disease, such as the substantia nigra (Pearce, et al., 1997; Sian, et al., 1994; Sofic, Lange, Jellinger, & Riederer, 1992). An early decrease in reduced glutathione in neurons of the substantia nigra may exacerbate subsequent cell death in this region in Parkinson's disease. Despite the net decrease in glutathione in degenerating brain regions, a 3-5 fold increase in total glutathione has been observed in less susceptible brain regions in Parkinson's patients such as the frontal cortex, caudate nucleus, and putamen (Mythri, et al., 2011). Furthermore, glutathione peroxidase^{+} astrocytes are significantly increased in the

Table 1: Changes in glutathione defenses in neurodegenerative diseases				
Measure of Glutathione	Brain Region	Change	Disease	Citation
Total glutathione	Substantia nigra	-	Parkinson's Disease	Sian et al. 1994 Maher et al. 2005
Total glutathione	Frontal cortex, caudate, putamen	+ (3-5 fold)	Parkinson's disease	Mythri et al. 2011
Reduced glutathione in neurons	Substantia nigra	-	Parkinson's disease	Pearce et al. 1997
Oxidized glutathione	Substantia nigra	No change	Parkinson's disease	Sian et al. 1994
Glutathione peroxidase^{+} cells	Substantia niga/ventral tegmental area	+	Parkinson's disease	Damier et al. 1993
Reduced glutathione	Lateral globus pallidus	+ (2-fold)	Multiple system atrophy	Sian et al. 1994
Oxidized Glutathione	Lateral globus pallidus	-	Multiple system atrophy	Sian et al. 1994
Reduced glutathione	Cerebral cortex, caudate nucleus, substantia nigra zona compacta	No change	Huntington's disease	Sian et al. 1994
Oxidized glutathione	Caudate nucleus	-	Huntington's disease	Sian et al. 1994
Reduced glutathione	Midbrain	+	Alzheimer's disease	Adams et al. 1991
Reduced glutathione	Hippocampus	+	Alzheimer's disease	Adams et al. 1991
Reduced glutathione	Hippocampus	+	Alzheimer's & Parkinson's disease	Adams et al. 1991

substantia nigra in Parkinson's patients relative to age-matched control subjects (Damier, et al., 1993). Therefore, astrocytes seem to engage in some compensatory responses in neurodegenerative conditions. However, the compensatory increase in glutathione defenses in astrocytes is not sufficient to halt disease progression. Future explorations of therapies that enhance astrocytic glutathione defense at earlier stages of neurodegeneration or lead to even greater increases in glutathione defenses are highly warranted.

The family of cytosolic glutathione S-transferase enzymes is subdivided into classes based upon N-terminal domain amino acid sequence (Mazzetti, Fiorile, Primavera, & Lo Bello, 2015). Two of the cytosolic glutathione S-transferase classes are π and μ. Glutathione S-transferase μ is primarily found in astrocytes under physiological conditions whereas glutathione

S-transferase π, normally found in oligodendrocytes, is found in reactive astrocytes (Arumugam, et al., 2010; V. Calabrese, et al., 2004; Unno, et al., 2000). Glutathione S-transferase is primarily recognized for its conjugation of glutathione to xenobiotics, thereby eliciting cellular protection (Mazzetti, et al., 2015). Glutathione S-transferase π and μ can also be protective through regulation of the stress kinase pathways (Adler et al., 1999; Cho et al., 2001). Both π and μ classes of glutathione S-transferase may be important for decreasing the oxidative stress associated with Parkinson's and Alzheimer's disease. Polymorphisms in glutathione S-transferase π have been associated with an increased risk for developing Parkinson's disease in individuals who smoke (Hussain & Ramaiah, 2007). Furthermore, loss of glutathione S-transferase π activity is associated with increased susceptibility of dopaminergic neurons in a mouse model of Parkinson's disease (Paz Gavilan, et al., 2006). Alterations in the glutathione S-transferase π 1 gene sequence are linked to earlier cognitive decline in Alzheimer's disease patients (Alladi, et al., 2010). The glutathione S-transferase μ 1 null genotype is associated with an earlier onset of Parkinson's disease (V. Calabrese, et al., 2004). In addition, a significant association between glutathione S-transferase μ 1 null polymorphisms and Parkinson's disease has been observed in Chilean populations with a strong American genetic component (Arumugam, et al., 2010). Consistent with these observations, a combination of the glutathione S-transferase μ 1 null genotype and prior exposure to pesticides is more frequently observed in Parkinson's disease patients than in control subjects (McCormack, et al., 2004). Furthermore, Piacentini and colleagues found a positive association between glutathione S-transferase μ 1 null genotypes and late onset Alzheimer's disease (Raz, et al., 2003). Thus, glutathione S-transferase may be a reasonable target to slow or halt neurodegenerative disease progression.

1.5.3 Therapeutic approaches to increasing glutathione

Several clinical trials have explored increasing glutathione levels as a therapeutic approach to blunting the progression of neurodegenerative diseases. For example, clinical trials have shown that NAC increases blood and brain glutathione levels in Parkinson's patients (Holmay et al., 2013). Adair and colleagues showed that NAC improved some aspects of cognitive function in Alzheimer's disease patients (Adair, Knoefel, & Morgan, 2001). Similarly, NAC dramatically improved the resolution of neurological symptoms in soldiers that experienced traumatic brain injury in combat settings (M. E. Hoffer, Balaban, Slade, Tsao, & Hoffer, 2013). NAC has also been shown to improve some of the clinical symptoms of schizophrenia and bipolar disorder (Attems, et al., 2005; Gibb & Lees, 1991). The beneficial effects of NAC in neurodegenerative and psychiatric diseases may result from enhanced glutathione synthesis and decreases in oxidative damage.

1.6 N-acetyl L-cysteine

1.6.1 Up-regulation of antioxidant response element and heat shock factor 1

Because NAC contains a sulfhydryl group and participates in thiol exchange reactions, it may interact with the cysteine residues in Keap1 and heat shock factor 1 (HSF1). HSF1 activation results in its translocation to the nucleus and Hsp70 gene induction. This hypothesis is consistent with previous work showing that NAC upregulates Hsp70 in neuroblastoma cells under conditions of proteotoxic stress (Jiang et al., 2013). As mentioned above, Keap1 modification via thiol exchange reactions enhances Nrf2 activity and subsequent transcription of genes such as those that encode for Hsp70 and those under the control of the antioxidant response element (Hu et al., 2006; Kwak et al., 2003). Thus, NAC may have protective effects through direct antioxidant activity, as a glutathione prodrug, and through thiol exchanges with Keap1 and HSF1 that lead to the induction of pro-survival genes.

1.7 Adaptations to cellular stress

1.7.1 Preconditioning

Cellular adaptations to stressors are often studied in the context of low level, subtoxic stress. Exposure to subtoxic stress often promotes endogenous defenses that improve survival following subsequent challenges. This phenomenon is known as preconditioning or tolerance (E. J. Calabrese et al., 2007). Self-protection in response to cellular stress depends both on the concentration and duration of the injury (Leak, 2014). Exposure to subtoxic insults may elicit the upregulation of endogenous defensive molecules such as Nrf2 and HO1 (Bell et al., 2011; Garnier et al., 2001; Xu et al., 2014).

Many studies have established that astrocytes can be preconditioned by subtoxic stress. For example, hypoxic preconditioning of astrocytes enhances their neuroprotective properties (Sen et al., 2011). Astrocyte-mediated neuroprotection may be facilitated by an increase in glutamate uptake following ischemic insults. Astrocytes can then convert glutamate to glutamine and decrease excitotoxicity (Maragakis & Rothstein, 2006). Furthermore, transfer of astrocyte-conditioned media from preconditioned astrocytes to neurons decreases neuron apoptosis (Saibil, 2013). In sum, astrocytes exposed to low level cellular stressors are protected against subsequent insults and maintain their ability to support neuronal functions.

Although it is well established that astrocytes and other cells can adapt to low level stress, it is not known if cells can adapt to severe proteotoxic stress such that they are protected against subsequent challenges. Instead, high levels of cellular stressors are generally thought to elicit additive or synergistic toxicity, as predicted by the dual hit hypothesis of neurodegeneration (Boger, Granholm, McGinty, & Middaugh, 2010; Sulzer, 2007; Unnithan, Choi, Titler, Posimo, & Leak, 2012; Zhu, Lee, Perry, & Smith, 2007). As astrocytes are known to be a highly resilient

cell type, they seem well suited to test the hypothesis that some cells can adapt to both subtoxic and toxic stress, with the latter being defined as stress that is lethal to some fraction of the cellular population (Walter & Ron, 2011). The slow and progressive nature of neurodegenerative disorders is consistent with the notion that some severely stressed cells are able to resist subsequent challenges better than stress-naïve cells. This process might enrich the affected brain region in cells that become increasingly difficult to kill, thereby delaying the progression of the disease, perhaps for decades. Whether severely stressed astrocytes mitigate or exacerbate neuronal injury is also not well understood. However, this is an important question to answer because if astrocytes can adapt to severe stress conditions, they might be able to support neighboring neurons more effectively.

Chapter 2 Materials and Methods

Cortical astrocyte cultures Use of animal tissue was conducted in accordance with the *NIH Guide for the Care and Use of Laboratory Animals* following Institutional Animal Care and Use Committee approval. Primary cortical astrocytes were harvested as previously published (Titler, Posimo, & Leak, 2013). Briefly, the cerebral cortex of postnatal day 1-2 Sprague-Dawley rats (Charles River, Wilmington, MA) was dissected under sterile conditions and incubated in 0.25% Trypsin-EDTA (Cat. no. 25200, Gibco Life Technologies, Grand Island, NY) at 37 °C for 7 min before washes and dissociation with a 5 mL serological pipet. For dual hit studies (part I), the cell culture medium was comprised of Basal Medium Eagle (Cat. No. B1522, Sigma-Aldrich) supplemented with bovine calf serum (Cat. No. 2151, HyClone Thermo Scientific), 35 mM glucose (Cat. No. G8769, Sigma-Aldrich, St. Louis, MO), 1 mM L-glutamine (Cat. No. 25030-081, Gibco, Life Technologies), 50 Units/mL penicillin, and 50 µg/mL streptomycin (Cat. No. 15140-122, Gibco, Life Technologies). For dual hit studies (part II) and the N-acetyl cysteine studies, the cell culture medium was composed of Dulbecco's modified Eagle medium (DMEM, Cat. no. 12100061, Gibco Life Technologies) with 10% Fetal Clone III (Cat. no. SH30109.03, Thermo Scientific Hyclone, Logan UT), penicillin and streptomycin (50 U/mL and 50 µg/mL, respectively; Cat. no. 15070, Gibco Life Technologies). Dissociated cells were counted under Trypan blue exclusion and 24 x 10^6 cells were plated on T175 flasks coated with poly-D-lysine (10 µg/mL; Cat. no. P0899, Sigma-Aldrich). Flasks were incubated at 37°C and 5% CO_2 for 7-10 days and non-astrocytic cells were removed by orbital shaking at 260 revolutions per minute overnight at 37°C. The media was removed from these flasks and replaced with fresh cell culture medium as described above. Astrocyte cultures were then incubated for an additional 2-3 days before trypsinization and plating for experimental procedures, at which point they might be

considered secondary astrocyte cultures. Astrocyte cultures were maintained and used for experiments for up to one month.

For Part I of the dual-hit studies, astrocytes were plated at 40,000 cells/well in 96-well plates for viability experiments. For Part II of the dual hit studies and the investigation of N-acetyl cysteine (NAC), cells were plated at a density of 20,000 cells/well in 96-well plates for viability experiments and 6.8×10^5 cells/well in 6-well plates for Western blotting (Costar, Corning Incorporated, Corning, NY). Under both conditions, the astrocytes formed a confluent monolayer at the time of experimentation.

Primary neuron cultures Neocortical tissue was harvested from postnatal day 1-2 Sprague Dawley pups as previously published (Posimo, Titler, Choi, Unnithan, & Leak, 2013). Briefly, primary neuronal cultures were prepared by first incubating neocortical tissue in 10 Units/mL papain (Cat. No. P3125, Sigma-Aldrich) for 30 min at 37 °C. The tissue was then transferred to 10% type II-O trypsin inhibitor (Cat. No. T9253, Sigma-Aldrich) at room temperature followed by mechanical dissociation in Basal Medium Eagle (Cat. No. B1522, Sigma-Aldrich) supplemented with 10% bovine calf serum (BME/BCS, Cat. No. 2151, HyClone Thermo Scientific), 35 mM glucose (Cat. No. G8769, Sigma-Aldrich), 1 mM L-glutamine (Cat. No. 25030-081, Gibco, Life Technologies), 50 Units/mL penicillin, and 50 µg/mL streptomycin (Cat. No. 15140-122, Gibco, Life Technologies). Cells were then plated at a density of 80,000 cells/well in Opti-MEM (Cat. No. 51985-034, Gibco, Life Technologies) with 20 mM glucose on a 96 well plate coated with poly-D-lysine (1 µg/mL) and laminin (Cat. No. 354232, 1.88 µg/mL, Corning Incorporated). After a 2 hour incubation at 37 °C, Opti-MEM was replaced with Neurobasal A medium (Cat. No. 10888-022, Gibco Life Technologies) supplemented with 2%

v/v B27 (Cat. No. 17504-044, Invitrogen Life Technologies) and L-glutamine (1:50, Cat. No. 25030-081, Gibco Life Technologies). Neuronal cells were treated two days after plating.

Neuron-astrocyte co-cultures Purified cortical astrocytes (as described above) were plated and treated with the 1st MG132 hit or vehicle in astrocyte cell culture medium. Primary neocortical neurons were plated on top of cortical astrocytes in Neurobasal-A Medium. Two days after plating the neurons, the 2nd MG132 hit was delivered. Neuron-astrocyte co-cultures were assayed for viability 48 hours after the 2nd MG132 hit. For astrocyte-conditioned media experiments, astrocytes were treated with 1st MG132 hit for 24 hours. Astrocyte-conditioned media from MG132 and vehicle-treated astrocytes were directly transferred (never frozen) to neocortical neurons in a 1:1 dilution in neuronal media.

Dual-hit protocol The 1st MG132 hit or MG132 pretreatment was delivered as a 10x stock to astrocytes that had been plated the day before. Following a 24-hour incubation in the 1st MG132 hit, the medium was removed and the 2nd MG132 hit or MG132 post-treatment was delivered at a 1x concentration in a full media exchange, which served to remove all previously applied MG132. After a 24-hour incubation in the 2nd MG132 hit, astrocyte viability was measured by blinded counts of Hoechst-stained nuclei counts or ATP levels as described in the "Cell viability and immunocytochemistry" and "ATP assay" sections, respectively. All experiments involved a 24-hour period between the 1st and 2nd MG132 hits and a 24-hour incubation between the 2nd MG132 hit and the assay, with the exception of data presented in Figure 9D-I and Figure 9J-L.

MG132, N-acetyl L-cysteine, D-cysteine, and L-cysteine treatments Proteotoxic stress was induced 24 hours after plating with the proteasome inhibitor MG132 (Cat. No. 474790, EMD Millipore, Billerica, MA). MG132 was added at a final concentration of 0.1 to 0.8 μM in the presence or absence of 3 mM NAC (Cat. No. 160280250, Acros, Geel, Belgium). On the

following day, fresh NAC was added for an additional 24 h, after which cell viability was assessed as described below. The same procedure was followed for studies on 3 mM L-cysteine (Cat. No. C12, 180-0, Aldrich Chemical Company, Milwaukee, WI) and D-cysteine (Cat. No. C1329, Tokyo Chemical Industry, Tokyo, Japan).

Pharmacological inhibitors Buthionine sulfoximine was used as a competitive inhibitor of the rate limiting enzyme glutamate-cysteine ligase (Cat. No. 309475000, Acros) (Griffith & Meister, 1979). Ammonium chloride was used to inhibit all types of autophagy by increasing the lysosomal pH (NH_4Cl, 20 mM; Acros Organics, Somerset NJ). VER155008 (Cat. No. 3803, Tocris Bioscience, Minneapolis, MN) was used as an ATPase activity inhibitor of Hsp70/Hsc70 (Chatterjee, et al., 2013; Massey, et al., 2010; Saykally et al., 2012). Pifithrin-μ (2-phenylethynesulfonamide, Cat. No. 506155, EMD Millipore) was used to bind and inhibit the substrate-binding domain of Hsp70/Hsc70 (Balaburski et al., 2013; Granato, et al., 2013; Kondoh & Osada, 2013; Leu, et al., 2009; Leu, et al., 2011; Schlecht, et al., 2013). The third Hsp70/Hsc70 inhibitor, MAL3-101 (provided by Drs. Peter Wipf and Jeffrey Brodsky), interferes with Hsp40-mediated ATP hydrolysis by Hsp70/Hsc70 (Adam, et al., 2014; Braunstein et al., 2011; Hatic, Kane, Saykally, & Citron, 2012; Huryn, et al., 2011; Kilpatrick et al., 2013). Sodium benzoate (Cat. No. AC447802500, Acros) and used to inhibit the conversion between D- and L-cysteine by D-amino acid oxidase (Katane et al., 2013). Tin (IV) protoporphyrin IX dichloride (SnPPx, Cat. no. Sn749-9, Frontier Scientific, Logan, Utah), competes for heme at the heme oxygenase 1 active site and therefore inhibits the conversion of heme into bilirubin and carbon monoxide (Drummond & Kappas, 1981; Yoshinaga, et al., 1982). Pharmacological inhibitors were added at the same time as MG132 and NAC.

Cell viability and immunocytochemistry Cell viability was measured following nuclear staining with the Hoechst reagent. Upon the completion of the experiment, astrocytes were fixed in 3% paraformaldehyde (Cat. No. 9990244, Thermo Scientific, Pittsburgh, PA) and 3% sucrose (Cat. No. 0389, Sigma-Aldrich, St. Louis, MO) in phosphate buffer for 20 min at room temperature and washed three times with 10 mM PBS. Cells were then stained with Hoechst 33258 (5 µg/mL, bisBenzimide, Sigma-Aldrich) diluted in PBS for 20 min. Images of Hoechst-stained nuclei were captured on an EVOS microscope (Model #AMF 4301 US, Advanced Microscopy Group, Bothell WA) in the 3 o'clock and 9 o'clock position in each well. ImageJ software (NIH Image, Bethesda, MD) was then used for blinded cell counts of the number of Hoechst-stained nuclei at 200x magnification.

For immunocytochemistry, astrocyte cultures and neuron-astrocyte co-cultures were washed in PBS, and blocked for 30 min in Odyssey Block (LI-COR Bioscience, Lincoln, NE) diluted 1:1 in PBS. Primary antibodies were prepared in Odyssey Block/PBS (1:1) with 0.3% Triton X-100 as indicated in **Table 2**. Cells were incubated in primary antibody solutions overnight at 4 ^{o}C. On the following day, cells were washed three times with PBS. Secondary antibodies (see **Table 3**) were diluted in 1:1 Odyssey Block/PBS and 0.3% Triton X-100 and applied to cells for 1 hour at room temperature. Finally, the secondary antibody was removed by three washes before microscopy on the EVOS microscope or LI-COR Odyssey Imager.

ATP assay ATP levels were measured by the luminescent CellTiter-Glo Assay with minor modifications (Cat. no. G7572, Promega, Madison, WI), as previously published (Posimo et al., 2014; Titler, et al., 2013). Astrocytes were lysed and incubated in CellTiter-Glo reagent at a 1:2 ratio in astrocyte cell culture medium (25 µL CellTiter-Glo: 50 µL media). Luminescence was

measured on a luminometer (VICTOR3 1420 multilabel counter; PerkinElmer, Waltham, MA) after a 15 min incubation period.

Total and reduced glutathione measures. The In-Cell Western technique was used to assess total glutathione levels. Glutathione measures were expressed as a fraction of α-tubulin signal and Hoechst- or DRAQ5-stained nuclei in the same well to account for differences in cell density. Reduced glutathione levels were measured by the luminescent GSH-Glo assay according to the manufacturer's instructions (Cat. no. V6911, Promega, Madison, WI). Reduced glutathione levels were expressed as a function of Hoechst-stained nuclei on parallel plates to account for differences in cell density.

Immunoblotting. Whole cell lysates were collected in cell lysis buffer (recipe from Cell Signaling Technologies, Danvers, MA, Cat. no. 9803) supplemented with protease inhibitor cocktail (1:50; Cat. no. P8340, Sigma-Aldrich) and 10 mM sodium fluoride (Leak, Castro, Jaumotte, Smith, & Zigmond, 2010), 24 h or 48 h following treatments. The samples were then sonicated with a probe and protein concentrations were measured by the bichinchoninic assay. Ten micrograms of each sample were loaded on a 10% polyacrylamide gels and subjected to electrophoresis. Separated proteins were then transferred to Immobilon-FL polyvinylidene fluoride or nitrocellulose membranes (EMD Millipore). Following the transfer, membranes were subjected to three Tris-buffered saline (TBS) washes before the blocking step in 5% nonfat dry milk in TBS or Odyssey block diluted 1:1 in TBS (Cat. no. 927-40000, LI-COR). Primary antibodies (**Table 2**) were prepared in TBS with 0.1% Tween and 5% bovine serum albumin fraction V (Research Products International, Mount Prospect, IL) or Odyssey block diluted 1:1 in TBS with 0.1% Tween. Secondary antibodies (**Table 3**) were diluted in TBS with 5% nonfat dry milk and 0.1% Tween or in Odyssey block diluted 1:1 in TBS with 0.1% Tween. Immunolabeled

blots were then washed in TBS with 0.1% Tween and fluorescent signal was assessed on a LI-COR Odyssey Imager. The data was quantified by Odyssey software (Ver 3.0; LI-COR) or Image Studio Lite software (LI-COR).

Tissue collection for *in vivo* aging study Protocols for obtaining tissue in this study were approved by the Duquesne University Institutional Animal Care and Use Committee and conducted in compliance with the *NIH Guide for the Care and Use of Laboratory Animals*. Female Sprague Dawley rats (Charles River, Wilmington, MA) were generated in an in-house breeding colony and aged to 22 months. Animals were sacrificed by 22 months of age due to poor health at older ages. Animals were anesthetized with 5% isoflurane immediately prior to decapitation and tissue microdissection. The boundaries of the olfactory bulb, substantia nigra, and striatum were defined according to the Paxinos rat atlas (George Paxinos, 1998). All animals were sacrificed within 48 h of each other and processed together. In addition, three young female rats (2-4 months old) were perfused with 4% paraformaldehyde for immunofluorescent staining of heat shock proteins. Fixed brains were cryoprotected in 30% sucrose in phosphate-buffered saline and cut at 40 microns on a freezing microtome (Microm HM450, Thermo Scientific, Pittsburgh, PA) (Crum et al., 2015b; Gleixner et al., 2014).

Immunohistochemistry Coronal sections through the substantia nigra were immunolabeled with Hsp25, Hsp60, and HO1 antibodies in conjunction with antibodies raised against the dopaminergic phenotype marker tyrosine hydroxylase. All sections were blocked with Odyssey Block diluted in 1:1 in PBS for 1h at room temperature. Sections were then incubated overnight at 4ºC in primary antibodies diluted in PBS with 0.3% Triton X-100. Unbound primary antibodies were washed off with three exchanges of PBS before incubation in secondary antibodies for 1hr at room temperature. After the secondary antibody incubations, tissue sections

were washed, mounted onto glass slides, and coverslipped with Fluoromount-G (Cat. no. 0100-01, Southern Biotech, Birmingham, AL). A confocal microscope was used to examine protein expression patterns (Leica TCS SP2, Wetzlar, Germany). For the primary and secondary antibody dilutions and sources, please see Tables 2 and 3. The following controls were used for each antibody examined by immunohistochemistry: 1) exposure to all solutions except both primary antibodies and 2) exposure to one primary antibody only, followed by exposure to both secondary antibodies (Crum, et al., 2015b).

Statistical analyses Statistical significance was determined with SPSS Statistics (IBM, Version 10.0, Armonk, NY) or GraphPad Prism (Version 6, La Jolla, CA) software. Data were subjected once to the Grubb's outlier test. For experiments with two groups, the Student's *t* test was used and for experiments with more than two groups a two- or three-way ANOVA with the Bonferroni *post hoc* correction was employed. Each experiment was conducted on at least three separate occasions. Furthermore, each experiment was conducted in triplicate or quadruplicate wells. Triplicate or quadruplicate data were averaged for an n=1 only. For Western blotting experiments, samples were collected on a minimum of three separate occasions. Changes were only deemed significant when $p \leq 0.05$. All data are presented as the mean ± standard error of the mean.

Table 2: Primary Antibodies							
Antibody	Source	Company	Catalog #	Lot #	Western blot dilution	Immunofluorescence dilution	Study
α-tubulin	Mouse	Sigma-Aldrich	T5168	078K4781		1:10,000	Dual Hit Part I
α-tubulin	Mouse	Sigma-Aldrich	T5168	078K4781	1:200,000		Dual Hit Part II MG132 + NAC
α-tubulin	Mouse	Sigma-Aldrich	T5168	078K4781	1:20,000		Olfactory bulb aging Nigra & striatum aging
β-actin	Mouse	Sigma-Aldrich	A5441	028K4826	1:20,000		Dual Hit Part I
β-actin	Mouse	Sigma-Aldrich	A5441	030M4788	1:50,000		Dual Hit Part II MG132 + NAC
β-actin	Mouse	Sigma-Aldrich	A5441	030M4788	1:20,000		Olfactory bulb aging
CHIP	Rabbit	Cell Signaling Technology	2080	07/2012	1:1000		Olfactory bulb aging
GAPDH	Rabbit	Cell Signaling Technology	2118S	8	1:1000		MG132 + NAC
GAPDH	Rabbit	Cell Signaling Technology	2118S	8	1:1000		Olfactory bulb aging Nigra & striatum aging
GAPDH	Rabbit	Cell Signaling Technology	2118S	8	1:5000		Dual Hit Part II
GFAP	Rabbit	Dako	Z0334	00059584	1:5000	1:1000	MG132 + NAC Dual Hit Part I Dual Hit Part II
Glutamate cysteine ligase catalytic subunit	Rabbit	Sigma-Aldrich	AV54576	QC226721	1:1000		Dual Hit Part II
Glutamate cysteine ligase modifier subunit	Rabbit	Sigma-Aldrich	SAB210090	QC23487	1:1000		Dual Hit Part II
Glutathione	Rabbit	EMD Millipore	AB5010	NG1870405		1:300	Dual Hit Part I MG132 + NAC
Glutathione	Rabbit	EMD Millipore	AB5010	2379274		1:300	Dual Hit Part II
Glutathione S-transferase							
Glutathione s-transferase							
Grp78	Rabbit	Abcam	ab21685	GR127425-1			Nigra & striatum aging
Heme oxygenase-1 (HO1)	Rabbit	Sigma-Aldrich	H4535	081M1122	1:200		Dual Hit Part II MG132 + NAC Olfactory bulb aging Nigra & striatum aging
Hip	Rabbit	Cell Signaling Technology	2723	1	1:1000		Dual Hit Part II Olfactory bulb aging
HOP	Rabbit	Cell Signaling Technology	4464	1	1:1000		Olfactory bulb aging Nigra & striatum aging
Hsc70	Rat	Enzo Life Sciences	ADISPA815	04231339	1:5000		Dual Hit Part II MG132 + NAC Nigra & striatum aging
Hsp25	Goat	Santa Cruz	sc-1048	D0312	1:1000	1:100	Dual Hit Part II MG132 + NAC Olfactory bulb aging Nigra & striatum aging
phospho-Hsp25	Rabbit	Cell Signaling Technology	2401	11	1:1000		Dual Hit Part II MG132 + NAC
phospho-Hsp25	Rabbit	Cell Signaling Technology	2401	11	1:500		Olfactory bulb aging
Hsp40	Rabbit	Cell Signaling Technology	4868	2	1:1000		MG132 + NAC Olfactory bulb aging
Hsp40	Rabbit	Cell Signaling Technology	4868	2	1:2000		Dual Hit Part II
Hsp60	Rabbit	Cell Signaling Technology	4870	2	1:1000		Nigra & striatum aging
Hsp70	Mouse	Calbiochem	386032	D00126860	1:1000		MG132 + NAC
Hsp70	Rabbit	EMD Millipore	AB9920	NG1571180	1:5000		Dual Hit Part I
Hsp70	Rabbit	EMD Millipore	AB9920	2278555	1:1000		Dual Hit Part II
Hsp70	Rabbit	Cell Signaling Technology	386032	3	1:1000		Olfactory bulb aging
Hsp90	Rabbit	Cell Signaling Technology	4877	3	1:1000		MG132 + NAC
Hsp90	Rabbit	Cell Signaling Technology	4877	3	1:2000		Dual Hit Part II Olfactory bulb aging Nigra & striatum aging
LAMP2a	Rabbit	Abcam	ab18528	GR29029-1		1:200	Dual Hit Part I
MAP2	Mouse	Sigma-Aldrich	M9942	069K4770		1:2000	MG132 + NAC Dual Hit Part II
mtHsp70	Rabbit	Cell Signaling Technology	2816	1	1:1000		Olfactory bulb aging
PA28α	Rabbit	Calbiochem	539146	D00092184	1:1000		MG132 + NAC
PA700	Rabbit	EMD Millipore	539147	D00110930	1:1000		MG132 + NAC
S100β	Mouse	Sigma-Aldrich	S2532	070M4767		1:1000	MG132 + NAC Dual Hit Part I Dual Hit Part II
Tyrosine Hydroxylase	Mouse	Millipore	MAB318	NG1723972		1:2000	Nigra & striatum aging
Ubiquitinated proteins	Mouse	Santa Cruz	sc-8017	D0412	1:500		MG132 + NAC Dual Hit Part II
K48-linked ubiquitinated proteins	Rabbit	Millipore	05-1307	2299608	Dilution needed		Nigra & striatum aging

Table 3: Secondary Antibodies					
Secondary Antibody	Company	Catalog #	Western blot dilution	Immunofluorescence dilution	Study
Donkey anti-rabbit 680	LI-COR Biosciences	926-32223	1:20,000		MG132 + NAC Dual Hit Part II
Donkey anti-rabbit 680	LI-COR Biosciences	926-68073	1:10,000		Nigra & striatum aging
Donkey anti-rabbit 800	LI-COR Biosciences	926-32213	1:20,000	1:1000	MG132 + NAC Dual Hit Part I Dual Hit Part II
Donkey anti-rabbit 800	LI-COR Biosciences	926-32213	1:10,000		Olfactory bulb aging
Donkey anti-rabbit 800	Jackson ImmunoResearch	711-655-152	1:30,000		Dual Hit Part II
Goat anti-rabbit 800	LI-COR Bioscience	926-32211	1:10,000		Nigra & striatum aging
Donkey anti-mouse 680	LI-COR Biosciences	926-32222	1:20,000		MG132 + NAC Dual Hit Part II
Donkey anti-mouse 680	LI-COR Biosciences	926-32222	1:10,000		Olfactory bulb aging
Donkey anti-mouse 680	LI-COR Biosciences	926-32222	1:10,000		Dual Hit Part I
Donkey anti-mouse 680	LI-COR Biosciences	926-68072	1:10,000		Nigra & striatum aging
Goat anti-mouse 800	LI-COR Biosciences	926-32210	1:20,000	1:2000	MG132 + NAC Dual Hit Part I Dual Hit Part II
Goat anti-mouse 800	LI-COR Biosciences	926-32210	1:10,000		Olfactory bulb aging
Donkey anti-goat 800	LI-COR Biosciences	926-32214	1:20,000		MG132 + NAC Dual Hit Part II
Donkey anti-goat 800	LI-COR Biosciences	926-32214	1:10,000		Olfactory bulb aging
Goat anti-rat 800	LI-COR Biosciences	926-32219	1:20,000		Dual Hit Part II
Donkey anti-mouse 488	Life Technologies	A21202		1:1000	Nigra & striatum aging Olfactory bulb aging
Goat anti-mouse 488	Life Technologies	A1101		1:500	Dual Hit Part I
Goat anti-mouse 488	Life Technologies	A11029		1:1000	MG132 + NAC Dual Hit Part II
Goat anti-rabbit 555	Life Technologies	A21429		1:1000	MG132 + NAC Dual Hit Part I Dual Hit Part II
Donkey anti-goat 546	Life Technologies	A11056		1:1000	Nigra & striatum aging Olfactory bulb aging

Chapter 3 Results

3.1 Exposure to severe proteotoxic stress elicits tolerance in surviving astrocytes and does not abolish their neuroprotective role

Part I.

Characterization of cortical astrocyte cultures

We began these studies by developing a model of proteotoxic stress in cortical astrocyte cultures harvested from postnatal rat pup brains. In order to characterize the purity of the cortical astrocyte cultures, cells were immunolabeled for glial markers glial fibrillary acidic protein (GFAP) and S100β and stained with the nuclear marker Hoechst (Fig 1a-d lower magnification, Fig 1e-h higher magnification). Large, Hoechst$^+$ nuclei stained positive for GFAP and S100β or for S100β alone (long-stemmed arrows), whereas smaller nuclei were only GFAP$^+$ (short-stemmed arrows). Shrunken, condensed nuclei did not stain for either glial marker, perhaps because they were undergoing apoptosis and lost the glial phenotype (Fig. 1g). The purity of the astrocyte cultures was then determined by counting the number of GFAP$^+$ cells, S100β$^+$ cells, and cells that did not stain for either glial cell marker, all expressed as a percentage of total Hoechst$^+$ cell numbers. Primary cultures derived by the abovementioned protocol contained 83% GFAP$^+$ cells and 87% S100β$^+$ cells, whereas 8% of the cells did not stain positive for either astrocyte marker (Fig 1i).

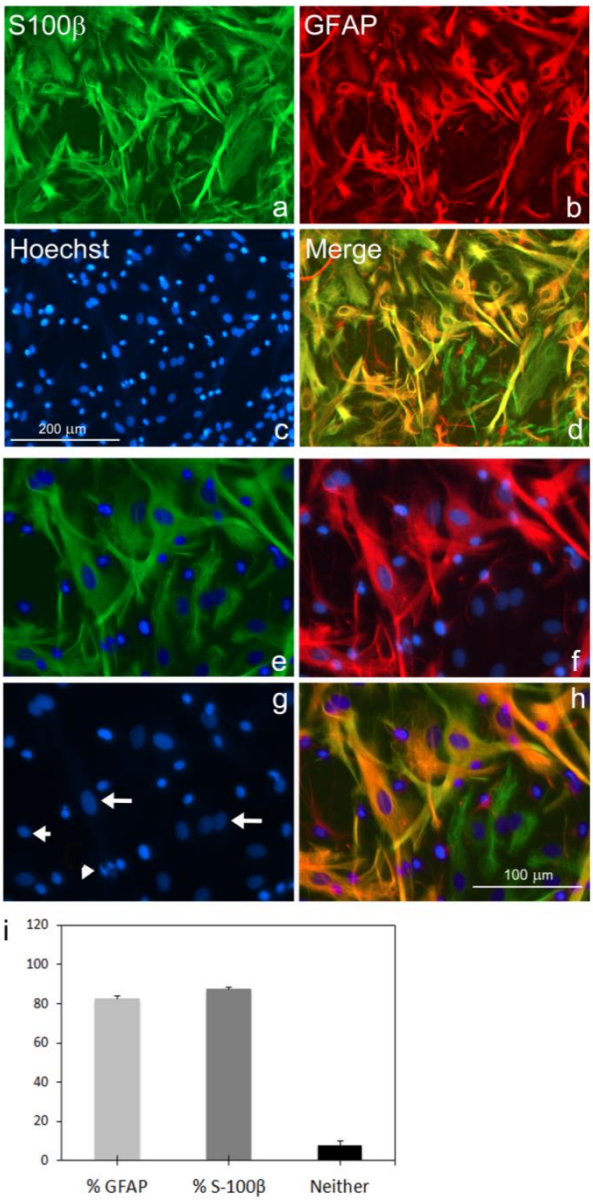

Figure 1. Cortical astrocyte culture purity in Basal Medium Eagle. a-h Astrocytes were immunocytochemically labeled for S100β (**a** and **e**; green) and GFAP (**b** and **f**; red) as well as stained for nuclear marker Hoechst (**c** and **g**; blue). The center of the image in a-d was photographed at a higher magnification in **e-h**. Cellular morphologies fell into three anatomical categories. Cells with large, flat nuclei were labeled with both S100β and GFAP or only with S100β (long-stemmed arrows, **g**). Cells with smaller and brighter nuclei were positive for GFAP only (short-stemmed arrow). Condensed, fragmented nuclei lacked both markers, perhaps because they were apoptotic cells that lost their normally glial phenotype (arrowhead). **i:** Quantification of Hoechst-labeled nuclei that were positive for either GFAP (light gray bar) or S100β (dark gray bar), or negative for either marker (black bar). n=3 independent experiments. Reprinted from "Astrocyte plasticity revealed by adaptations to severe proteotoxic stress," by A. M. Titler, 2013, *Cell Tissue Research, 352*, 427-443. Copyright [2013] by A.M Titler. Reprinted with permission.

Proteotoxic stress elicits stress tolerance in astrocytes

Stress adaptations are often studied in the context of low-level or subtoxic stressors. For example, exposure to subtoxic ischemic insults decreases astrocyte susceptibility to subsequent ischemic insults, a phenomenon known as preconditioning or stress tolerance (Pang et al., 2015). In contrast, severe stress is generally thought to weaken cells and to exacerbate the toxic response to subsequent insults. We define severe stress as stress that kills some fraction of the cellular population under study. Because astrocytes are more resistant than many other types of brain cells, we hypothesized that astrocytes surviving severe stress may mount adaptive defenses and tolerate subsequent insults better than naïve astrocytes. If this hypothesis were supported, it would suggest that stress can elicit protective and not always toxic stress responses even when the stress is high in concentration. This hypothesis lies in contrast with traditional views of the stress response, which hold that cells can only mount adaptive defenses against mild stress (E. J. Calabrese, 2008).

In order to test whether astrocytes that survive high levels of proteotoxic stress would be more or less susceptible to subsequent insults, we developed a dual hit model. Proteotoxic stress, or stress associated with loss of protein homeostasis, was induced with the proteasome inhibitor MG132. MG132 was chosen because proteotoxicity is a major hallmark of all neurodegenerative disorders (Gundersen, 2010; Keller, Hanni, et al., 2000a; Morimoto, 2008) and it is a well characterized and commonly used toxin (D. H. Lee & Goldberg, 1998). Cortical astrocytes were first exposed to toxic concentrations of MG132; this is referred to as the MG132 pretreatment. In order to assess the effect of the initial MG132 insult, the surviving glial population was challenged a second time with

toxic concentrations of MG132 to see if the astrocytes were resistant to subsequent insults. The second exposure to MG132 is referred to as the MG132 post-treatment.

Increasing concentrations of MG132 pretreatment elicited morphological changes consistent with astrocyte stress reactivity, as visualized by increases in GFAP and S100β immunostaining (Fig 2a). Similarly, increasing concentrations of MG132 post-treatment led to cytoskeletal condensation and retraction of astrocytic processes (Fig 2b), suggestive of cellular stress (Sofroniew & Vinters, 2010; Tynan et al., 2013). Quantification of the number of $Hoechst^{+}$ cells revealed that MG132 pre- and post-treatment alone led to a significant decrease in astrocyte viability (48h or 24h after treatment, respectively) (Fig 2c & d). As expected, astrocytes that survived MG132 pretreatment were resistant to 60 and 80 μM MG132 post-treatment. In other words, there was no additional decrease in viability in response to MG132 post-treatment when astrocytes had been pretreated with MG132. However, previously stressed astrocytes were unable to tolerate the toxicity associated with 160 μM MG132 post-treatment. These data suggest that stressed astrocytes are resistant to subsequent insults but that there is a threshold beyond which they no longer maintain tolerance. In order to determine whether severe proteotoxic stress was eliciting significant loss in cell numbers at the time of post-treatment, astrocyte viability was assessed 24h after MG132 pretreatment (Fig 2e). As expected, MG132 pretreatment (0.20-0.80 μM) significantly decreased astrocyte viability at the time of MG132 post-treatment. Furthermore, there was no significant difference in viability between 24 and 48h after MG132 pretreatment. These findings suggest that the weaker astrocytes have already died at the time of delivery of post-treatment and that there is no additional cell loss in the next 24h interval.

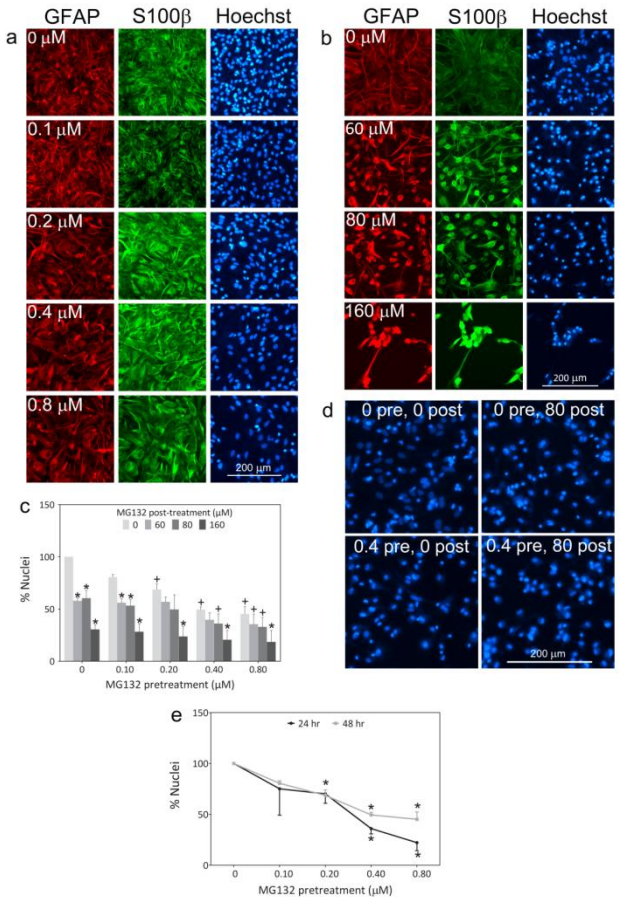

Figure 2. Severe proteotoxic stress renders astrocytes protected against subsequent insults **a:** Photomontage of GFAP, S100β and Hoechst labeled astrocytes following treatment with indicated concentrations of MG132. MG132 was applied the day after plating (pretreatment or 1st hit paradigm). Two days later, cells were fixed, immunostained, and photographed. Cell loss was apparent at concentrations of 0.2 μM and beyond. **b:** Photomontage of GFAP, S100β and Hoechst labeled astrocytes following treatment with indicated concentrations of MG132. Cells were treated with MG132 two days after plating (post-treatment or 2nd hit paradigm). Much higher concentrations of MG132 (60 μM and beyond) were needed to elicit cell loss in the post-treatment paradigm, perhaps because cells had been plated 2 days before and were much better attached. **c:** MG132 pretreatments and post-treatments were combined and viability assessed with counts of Hoechst-positive nuclei. Increasing shades of gray indicate higher concentrations of MG132 post-treatment. The lightest gray bars indicate pretreatment alone (0 μM MG132 post-treatment). **d:** A representative photomontage of cells treated with 0.4 μM pretreatment, 80 μM post-treatment, and the combination of both is shown on the right of the quantification. Cells pretreated with an LC_{50} concentration of 0.4 μM MG132 were protected against additional loss of nuclei when post-treated with a normally LC_{50} concentration of 80 μM MG132. **e:** Cells were pretreated with indicated concentrations of MG132 and assayed either 24 h later or 48 h later for viable nuclei. There was no difference in viability between cells collected at the two timepoints. n=3 independent experiments. * $p \leq 0.05$ versus MG132 pretreatment alone (0 μM post-treatment), + $p \leq 0.05$ versus MG132 post-treatment alone (0 μM MG132 pretreatment), two-way ANOVA followed by Bonferroni *post hoc* test. Reprinted from "Astrocyte plasticity revealed by adaptations to severe proteotoxic stress," by A. M. Titler, 2013, *Cell Tissue Research, 352*, 427-443. Copyright [2013] by A.M Titler. Reprinted with permission.

Stress tolerance is associated with preservation of metabolic function

ATP levels reflect metabolic health and are often used as an indicator of cell viability (Crouch, Kozlowski, Slater, & Fletcher, 1993; Petty, Sutherland, Hunter, & Cree, 1995; Unnithan, et al., 2012). Therefore, we used a luminescent assay for ATP levels, CellTiter Glo, to complement the Hoechst cell count data. However, changes in ATP did not precisely coincide with changes in the number of $Hoechst^+$ nuclei in this model, consistent with other reports from our group (Posimo, et al., 2014). For example, ATP levels were not decreased by MG132 pretreatment alone as had been shown for $Hoechst^+$ cell numbers (Fig 3a). However, a concentration-dependent decrease in ATP was observed in response to MG132 post-treatment in cells that had not been previously stressed. In contrast, MG132-pretreated astrocytes showed no significant decrease in ATP levels in response to MG132 post-treatment, except in the 0.10 μM pretreatment and 80 μM post-treatment groups. These data suggest that severe proteotoxic stress prevents the loss of ATP in response to MG132 post-treatment, consistent with stress-induced protection of metabolic function. In order to force ATP loss, we also applied 100-fold higher MG132 pretreatment concentrations (Fig 3b). Even at these extremely high concentrations of MG132 pretreatment (10 to 80 μM MG132; sufficient to yield ATP loss), previously stressed astrocytes were able to maintain ATP levels in response to post-treatment (80 μM MG132).

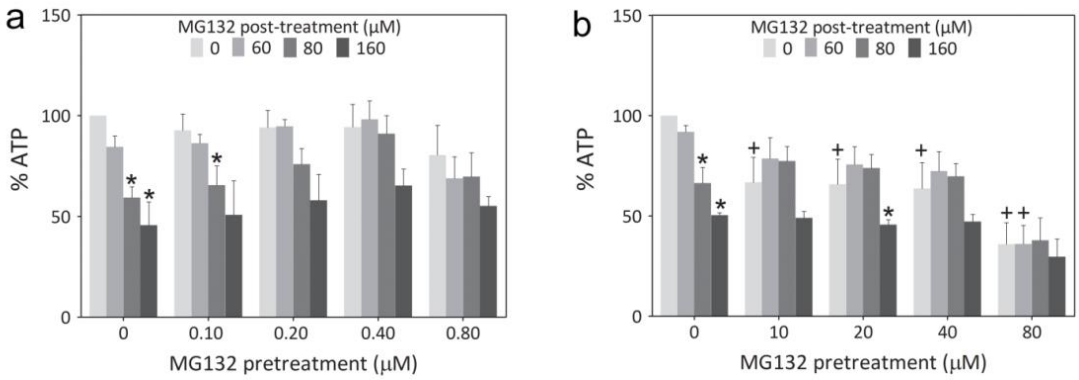

Figure 3. Impact of severe proteotoxic stress on ATP a: Viability following pretreatment and post-treatment was assessed with the Cell Titer Glo assay for ATP. ATP levels did not fall with pretreatment even though cell number was lower by parallel counts of Hoechst stained nuclei in Figure 2. However, ATP levels did fall with post-treatment under control conditions (no pretreatment). In contrast, cells that were pre-stressed with MG132 were protected against the ATP loss caused by post-treatment. n=3 independent experiments. **b:** ATP assay following 10-fold higher pretreatment concentrations of MG132 that *did* elicit ATP loss. Pretreated cells were completely protected against the usual loss of ATP in response to 80 μM MG132. n=3 independent experiments. * $p \leq 0.05$ versus MG132 pretreatment alone (0 μM post-treatment), + $p \leq 0.05$ versus MG132 post-treatment alone (0 μM MG132 pretreatment), two-way ANOVA followed by Bonferroni *post hoc* test. Reprinted from "Astrocyte plasticity revealed by adaptations to severe proteotoxic stress," by A. M. Titler, 2013, *Cell Tissue Research, 352*, 427-443. Copyright [2013] by A.M Titler. Reprinted with permission.

Severe proteotoxic stress leads to upregulation of cellular defenses

We hypothesized that high concentrations of MG132 would elicit proteotoxic stress and the upregulation of cellular defenses. As an indicator of proteotoxicity, we measured ubiquitin-conjugated proteins by Western blot analysis. Ubiquitin is attached to misfolded proteins in order to tag them for proteasomal degradation (Lecker, et al., 2006). Application of proteasomal inhibitors, such as MG132, is expected to elicit an increase in ubiquitinated proteins because the tagged proteins can no longer be degraded. In cells not exposed to MG132 pretreatment, MG132 post-treatment elicited a dramatic increase in ubiquitin-conjugated proteins, demonstrating proteotoxic stress (Fig 4a). Furthermore, there was an even greater increase in ubiquitin-conjugated proteins in response to the dual hits. These findings suggest that astrocytes respond to MG132 post-treatment with a sharp increase in protein misfolding, and that this response is still evident and even greater when cells have been previously exposed to MG132 pretreatment. Thus, previously stressed astrocytes are resistant to subsequent proteotoxic insults despite evidence of severe proteotoxic stress. Importantly, the results also show that previously stressed astrocytes are not simply refractory to the MG132 toxin and can still respond to continued proteotoxic stress. For example, we have not simply enriched our cultures in cells that fail to take up the MG132 toxin and so do not respond to the post-treatment either. Further evidence that severely stressed astrocytes still respond to post-treatment was gathered by measurements of HO1, which is known to be induced by cellular stress and to engage in antioxidant defense (Fig 4b) (Schipper, et al., 2006; Schipper, et al., 1998; Schipper, Song, Zukor, Hascalovici, & Zeligman, 2009). MG132 post-treatment elicited a dramatic increase in HO1 in MG132-pretreated astrocytes

whether or not they had been exposed to MG132 pretreatment. Again, these results are inconsistent with the notion that stressed astrocytes are refractory to further MG132 toxicity. These data also demonstrate that the stressed astrocytes mount active defenses against protein misfolding stress. In sum, the HO1 and ubiquitin-conjugated proteins data confirm that previously stressed astrocytes still take up MG132 and respond to post-treatment, but nevertheless resist additional cell death.

It has been known for many decades that the folding chaperone Hsp70 is upregulated in response to protein misfolding stress (Mayer & Bukau, 2005). This was also observed in our studies as MG132 post-treatment significantly increased Hsp70 levels (Fig 4c). However, MG132 pretreatment blunted the effect of MG132 post-treatment on Hsp70 levels. Similar to HO1 and Hsp70, GFAP is a highly stress-responsive protein (Middeldorp & Hol, 2011). As an additional measure of cellular stress in our model, we investigated the effect of MG132 pre- and post-treatment on GFAP levels. MG132 pretreatment significantly increased GFAP as expected (Fig 4d). No additional effect of post-treatment on GFAP was observed in pretreated cells. These results show that the impact of post-treatment on two stress-responsive proteins, Hsp70 and GFAP, is blunted by pretreatment.

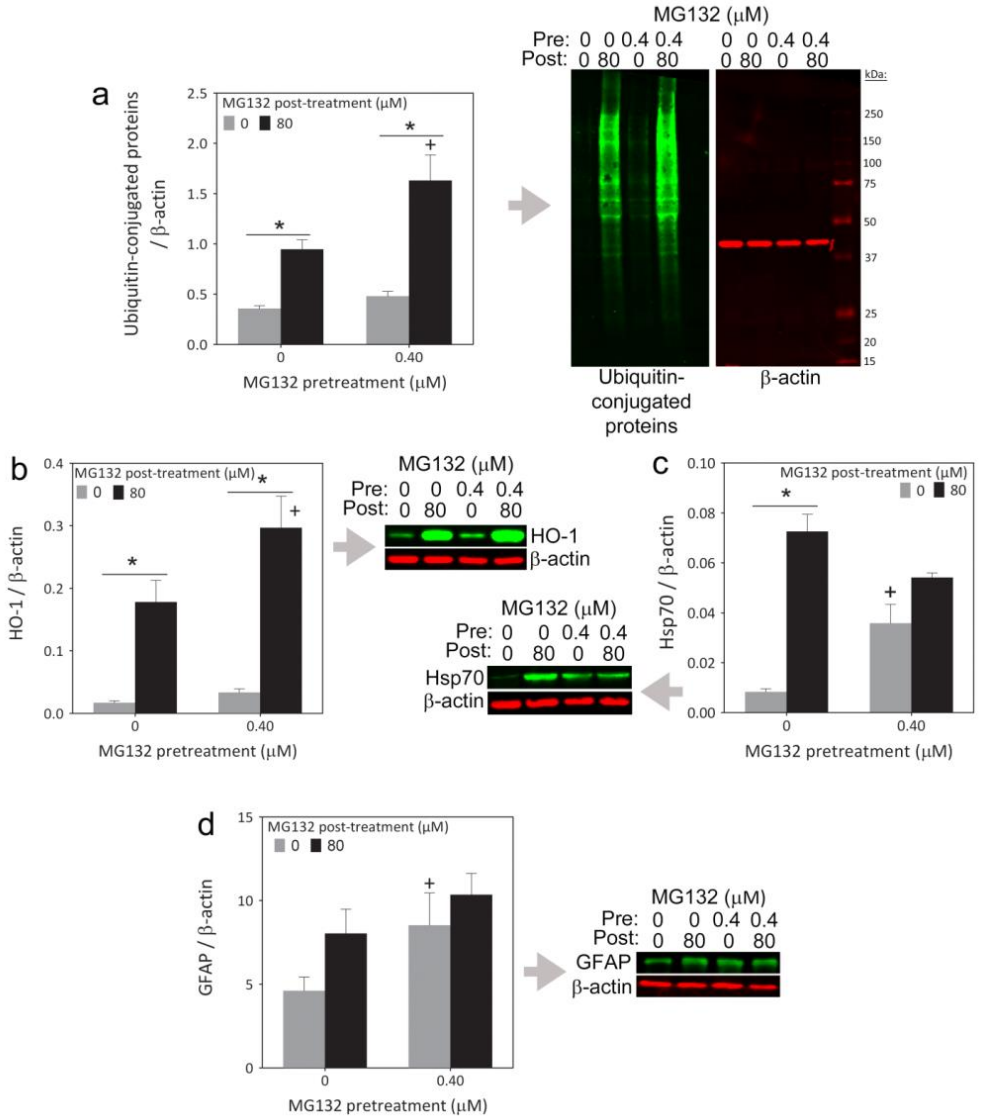

Figure 4. Severe proteotoxic stress elicits the upregulation of protein defenses. Western immunoblotting on astrocytes treated with 0.4 μM MG132 pretreatment, 80 μM MG132 post-treatment, and the combination of two hits. Representative infrared images of protein bands were pseudocolored red or green and are shown adjacent to the quantification (see arrows) for ubiquitin-conjugated proteins (**a**, n=6 independent experiments), heme oxygenase 1 (**b**, HO-1; n=6 independent experiments), heat shock protein 70 (**c**, Hsp70, n=6 experiments), and GFAP (**d**, n=3 independent experiments). Gray bars indicate 0 μM MG132 post-treatment. Black bars indicate 80 μM MG132 post-treatment. All proteins are expressed as a fraction of cytoskeletal β-actin levels. * $p \leq 0.05$ for 0 μM versus 80 μM MG132 post-treatment, + $p \leq 0.05$ versus MG132 post-treatment alone (0 μM MG132 pretreatment), two-way ANOVA followed by Bonferroni *post hoc* test. Reprinted from "Astrocyte plasticity revealed by adaptations to severe proteotoxic stress," by A. M. Titler, 2013, *Cell Tissue Research, 352*, 427-443. Copyright [2013] by A.M Titler. Reprinted with permission.

Autophagy inhibition does not reduce stress tolerance in astrocytes

Autophagy is an alternative clearance system that removes misfolded proteins and damaged organelles (Arias & Cuervo, 2011). Proteasome inhibition is known to upregulate autophagy as a compensatory response (Ding et al., 2007; Korolchuk, Menzies, & Rubinsztein, 2010). This raises the possibility that stressed astrocytes can tolerate subsequent MG132 post-treatment because they transition from protein degradation by the UPS to autophagy at times of UPS inhibition. Thus, astrocytes were stained for a marker of chaperone-mediated autophagy, LAMP2a (Fig 5a-d) (Kaushik & Cuervo, 2012). Qualitative assessments of LAMP2a levels reveal that this protein was increased in the dual hit group. This suggests that stressed astrocytes may upregulate autophagic systems to defend against subsequent proteotoxic stress. Therefore, we inhibited all forms of autophagy with ammonium chloride and assessed astrocyte viability (R. Sun et al., 2015). However, inhibition of autophagy did not decrease the stress-induced resilience in our model (Fig 5e). These findings suggest that stressed astrocytes do not rely on autophagy for stress tolerance.

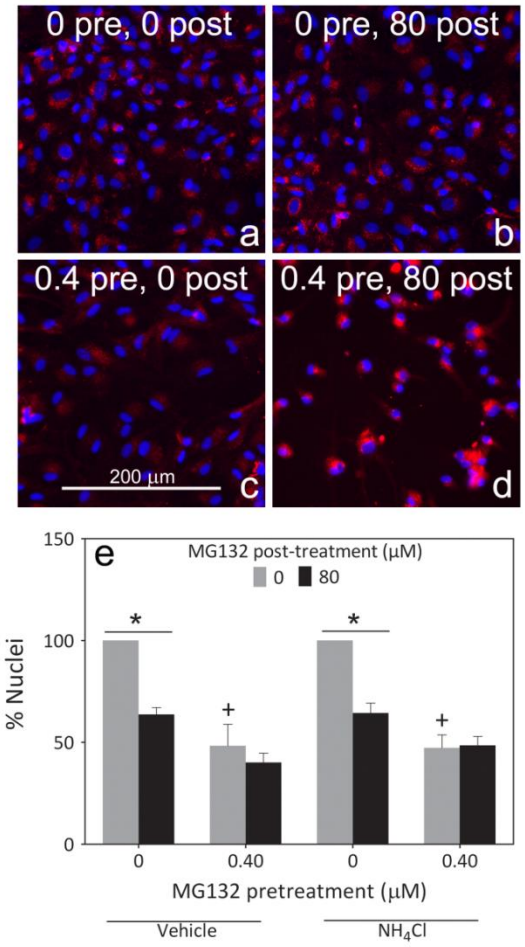

Figure 5. Astrocytes do not rely on autophagy for resilience. a-d Immunocytochemistry for lysosome-associated membrane protein type-2a (LAMP2a, red) in astrocytes treated with 80 µM MG132 post-treatment **(b)**, 0.4 µM MG132 pretreatment **(c)**, and the combination of two hits **(d)**. Nuclei were stained with Hoechst (blue). LAMP2a was found in a perinuclear anatomical location, as expected from a lysosomal marker, and was highest in the astrocytes treated with two hits (0.4 µM pretreatment + 80 µM post-treatment). **e:** Nuclear viability of astrocytes treated with 0.4 µM MG132 pretreatment, 80 µM MG132 post-treatment, and the combination of two hits, in the presence or absence of autophagy inhibitor ammonium chloride (20 mM NH_4Cl). Gray bars indicate 0 µM MG132 post-treatment. Black bars indicate 80 µM MG132 post-treatment. Pretreated astrocytes did not respond to post-treatment with additional cell loss and NH_4Cl had no effect on this pattern. n=3 independent experiments. * $p \leq 0.05$ for 0 µM versus 80 µM MG132 post-treatment, + $p \leq 0.05$ versus MG132 post-treatment alone (0 µM MG132 pretreatment), two-way ANOVA followed by Bonferroni *post hoc* test. Reprinted from "Astrocyte plasticity revealed by adaptations to severe proteotoxic stress," by A. M. Titler, 2013, *Cell Tissue Research, 352*, 427-443. Copyright [2013] by A.M Titler. Reprinted with permission.

Inhibition of glutathione synthesis attenuates stress tolerance in astrocytes

Glutathione is one of the most abundant cellular antioxidants and astrocytes are the primary source of glutathione in the brain (Dringen, 2000; Makar et al., 1994; Slivka, Mytilineou, & Cohen, 1987). In Parkinson's disease, astrocytes retain and/or upregulate glutathione levels despite loss of glutathione in neighboring neurons (Damier, et al., 1993; Mythri, et al., 2011). Therefore, we hypothesized that astrocytes rely on glutathione to defend against severe proteotoxic stress. In order to test the importance of glutathione in the dual hit model, glutathione synthesis was inhibited with buthionine sulfoximine (BSO) (Griffith, 1982; Griffith & Meister, 1979). BSO successfully decreased total glutathione levels at subtoxic concentrations (Fig 6a-c). MG132 pretreatment completely prevented the loss of total glutathione in response to MG132 post-treatment, suggesting that stressed astrocytes may rely on glutathione to survive a second challenge and BSO abolished this effect (Fig 6d-f). As expected, loss of glutathione sensitized MG132-pretreated astrocytes to MG132 post-treatment. In other words, previously stressed astrocytes showed a 42% decrease in viability in response to MG132 post-treatment under conditions of glutathione loss (Fig 7a-i). This suggests that stressed astrocytes rely on glutathione synthesis to tolerate subsequent MG132 insults. BSO did not alter ATP levels in stressed astrocytes (Fig 7j). Thus, ATP levels again failed to coincide with the number of $Hoechst^{+}$ nuclei.

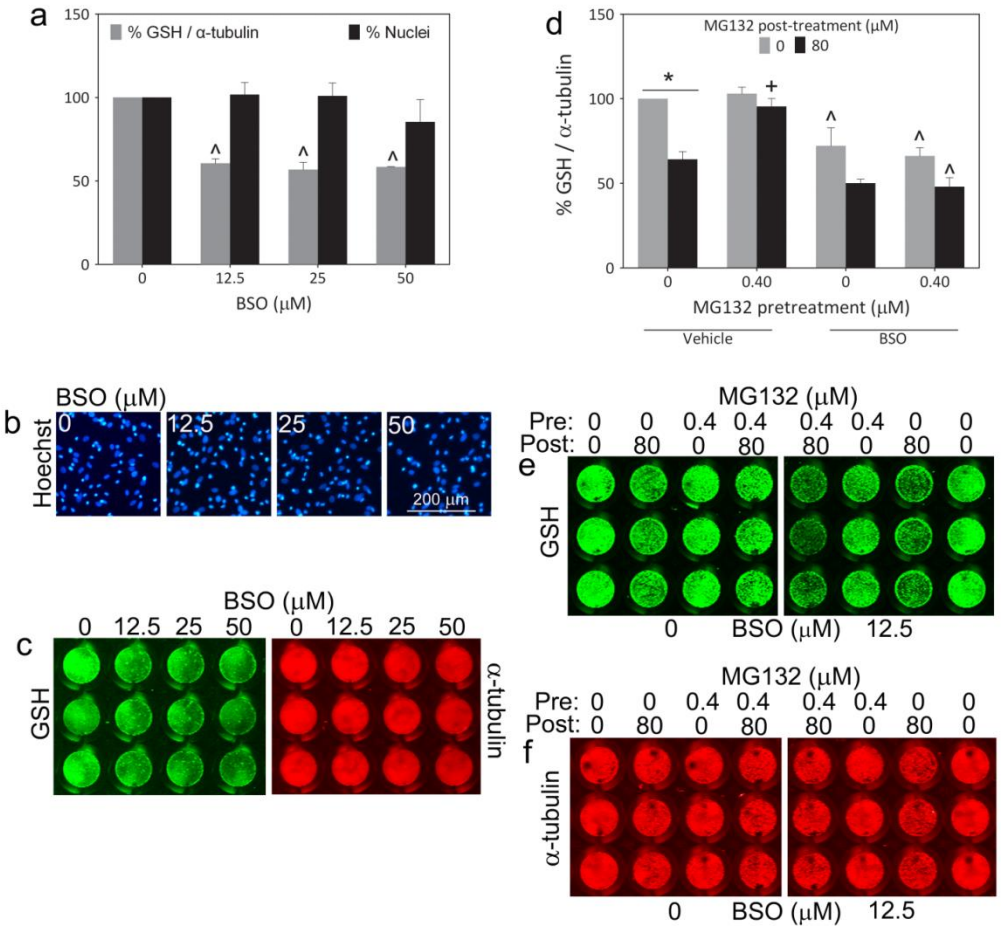

Figure 6. Buthionine sulfoximine attenuates the rise in glutathione with proteotoxic stress. a Impact of buthionine sulfoximine (BSO), an inhibitor of glutathione (GSH) synthesis, on glutathione levels (expressed as a fraction of cytoskeletal α-tubulin levels; gray bars) and on nuclear viability (black bars). n=3 independent experiments. Representative images of Hoechst-stained nuclei treated with indicated concentrations of buthionine sulfoximine are illustrated in **b**. Representative infrared images of the glutathione assay (pseudocolored green) and α-tubulin levels (pseudocolored red) are shown in **c**. From these data, the 12.5 μM buthionine sulfoximine concentration was chosen for subsequent experiments because it reduced glutathione levels without causing any cell death. **d:** Glutathione levels (expressed as a fraction of α-tubulin) in astrocytes treated with 0.4 μM MG132 pretreatment, 80 μM MG132 post-treatment, and the combination of two hits, in the absence or presence of 12.5 μM buthionine sulfoximine. Gray bars indicate 0 μM MG132 post-treatment. Black bars indicate 80 μM MG132 post-treatment. Glutathione levels fell with 80 μM MG132 post-treatment, but were completely rescued by pretreatment with 0.4 μM MG132 in the absence of buthionine sulfoximine. In the presence of buthionine sulfoximine, glutathione levels were depressed in all groups except the 80 μM post-treatment alone group. n=3 independent experiments. Representative infrared images of glutathione (green) and α-tubulin levels (red) are shown in **e** and **f**, respectively. * $p \leq 0.05$ 0 μM versus 80 μM MG132 post-treatment, + $p \leq 0.05$ versus MG132 post-treatment alone (0 μM MG132 pretreatment), and ^ $p \leq 0.05$ versus 0 μM buthionine sulfoximine (H_2O vehicle), two-way ANOVA followed by Bonferroni *post hoc* test. Reprinted from "Astrocyte plasticity revealed by adaptations to severe proteotoxic stress," by A. M. Titler, 2013, *Cell Tissue Research, 352*, 427-443. Copyright [2013] by A.M Titler. Reprinted with permission.

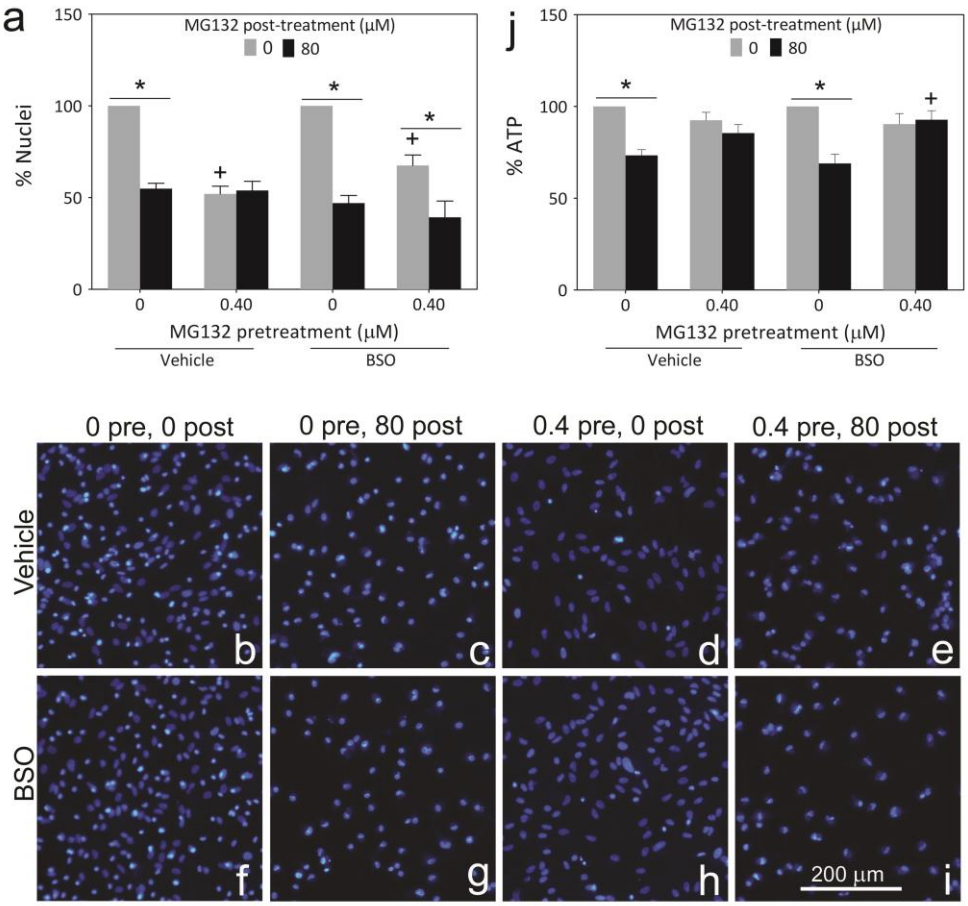

Figure 7. Stressed astrocytes rely on glutathione in order to remain resilience. a Nuclear viability in astrocytes treated with 0.4 μM MG132 pretreatment, 80 μM MG132 post-treatment, and the combination of two hits, in the absence or presence of 12.5 μM buthionine sulfoximine. Gray bars indicate 0 μM MG132 post-treatment. Black bars indicate 80 μM MG132 post-treatment. Buthionine sulfoximine rendered pretreated cells sensitive to 80 μM MG132 post-treatment, as they were no longer protected against additional cell loss. n=4 independent experiments. **b-i**: Representative images of Hoechst-stained nuclei in astrocytes treated with 0.4 μM MG132 pretreatment, 80 μM MG132 post-treatment, and the combination of two hits, in the absence or presence of 12.5 μM buthionine sulfoximine. Note the enhancement of the toxicity of two hits in the presence of buthionine sulfoximine. **j:** ATP levels of astrocytes treated in the same format as in **a**. Astrocytes were still protected against additional ATP loss even in the presence of buthionine sulfoximine. n=3 independent experiments. * $p \leq 0.05$ 0 μM versus 80 μM MG132 post-treatment, and + $p \leq 0.05$ versus MG132 post-treatment alone (0 μM MG132 pretreatment), two-way ANOVA followed by Bonferroni *post hoc* test. Reprinted from "Astrocyte plasticity revealed by adaptations to severe proteotoxic stress," by A. M. Titler, 2013, *Cell Tissue Research, 352*, 427-443. Copyright [2013] by A.M Titler. Reprinted with permission.

Part II.

Our next set of dual hit studies was conducted at a lower plating density due to rapid cell growth and in a less expensive cell culture medium. Therefore, astrocyte cultures were reevaluated in this new model, in collaboration with an undergraduate student, Deepti Pant. Astrocyte culture purity was slightly higher with the new protocol: 89.6% of the cells were $GFAP^+$, 91.8% were $S100\beta^+$, and 6.1% of the cells did not stain positive for either marker (Fig 8). As described in Part I, viable astrocytes were quantified by measuring the number of $Hoechst^+$ cells. In the dual hit studies of Part II we used the automated cell counting function in ImageJ software (NIH Image). $Hoechst^+$ cells undergoing cell death typically display shrunken, condensed nuclei. Therefore, $Hoechst^+$ nuclei with areas less than 350 pixels (53 μm^2) were excluded in the viability measurements. Representative images of such cells are illustrated in Figure 8C &D.

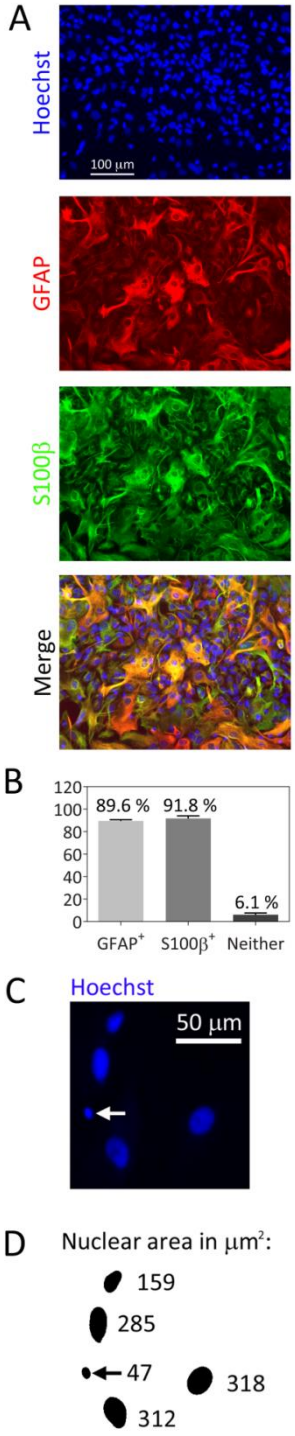

Figure 8. Cortical astrocyte culture purity in Dulbecco's Modified Eagle Medium. A) Cortical astrocytes were stained with the nuclear marker Hoechst and immunolabeled for the glial markers glial fibrillary acid protein (GFAP) and S100β. **B)** The percentage of Hoechst$^+$ cells that were immunolabeled for GFAP or S100β proteins or were immunonegative were quantified. **C)** Representative image of Hoechst-stained nuclei in untreated astrocytes. White arrow points to one cell with a condensed nucleus. **D)** The image in C was converted to a binary image using the threshold function in Image J. Nuclear cross-sectional areas appear next to each cell in square microns. Cells with nuclear areas under 350 pixels (53 µm^2, see black arrow) were excluded from the counts of viable cells in subsequent figures. Reprinted from "Astrocytes surviving severe stress can still protect neighboring neurons from proteotoxic stress," by A. M. Gleixner, 2015, *Molecular Neurobiology, Epub ahead of print*. Copyright [2015] by A.M Gleixner. Reprinted with permission.

Long-lasting stress tolerance in astrocytes

In addition to reevaluating astrocyte cultures with the new protocol, the LC_{50} concentrations of MG132 also had to be reevaluated. For the sake of simplicity, we changed the name of the pretreatment to the 1st MG132 hit and the post-treatment to the 2nd MG132 hit. Toxic 1st and 2nd MG132 hit concentrations first had to be identified in the new dual hit protocol. Despite several protocol modifications, toxic concentrations of the 1st hit (0.16-0.64 μM) still elicited tolerance against a toxic 2nd hit (3.125 μM) (Fig 9A-C). The 2nd hit concentration in these studies was lower than that used in the Part I dual hit studies. However, both MG132 concentrations decreased astrocyte viability by approximately 50% in previously naïve cells. When we expressed the data from Fig 9A as a function of the 0 μM 2nd MG132 hit (i.e., all gray bars were expressed as a percentage of the adjacent black bars), the attenuation of the toxicity of the 2nd hit in previously stressed astrocytes became evident (Fig 9B). Consistent with the MG132 data, astrocytes surviving toxic concentrations of a different proteasome inhibitor, lactacystin, were also resistant to subsequent lactacystin insults (Fig 10). Lactacystin and MG132 have distinct mechanisms of action, although both converge on the chymotrypsin-like activity of the proteasome particle and increase the cellular burden of misfolded proteins (D. H. Lee & Goldberg, 1998).

In order to determine whether the effect of the 1st MG132 hit on the 2nd MG132 hit was long lasting, the duration between the 1st and 2nd hit was increased from 24h to 48h (Fig 9D-F) and 96h (Fig 9G-I). Astrocytes that survived the toxic 1st hit remained protected against the 2nd hit for up to 96 hours. These findings suggest that the 1st hit does not elicit transient protective effects. In addition, we also examined the duration of the

protective effect by increasing the interval between the 2nd hit and the time of viability assay from 24 to 72h. As expected, astrocytes exposed to two severe proteotoxic insults remained viable for up to 72h after the 2nd hit (Fig 9J-L). All of these findings are consistent with the notion that stress-induced tolerance in this model is not fleeting in nature.

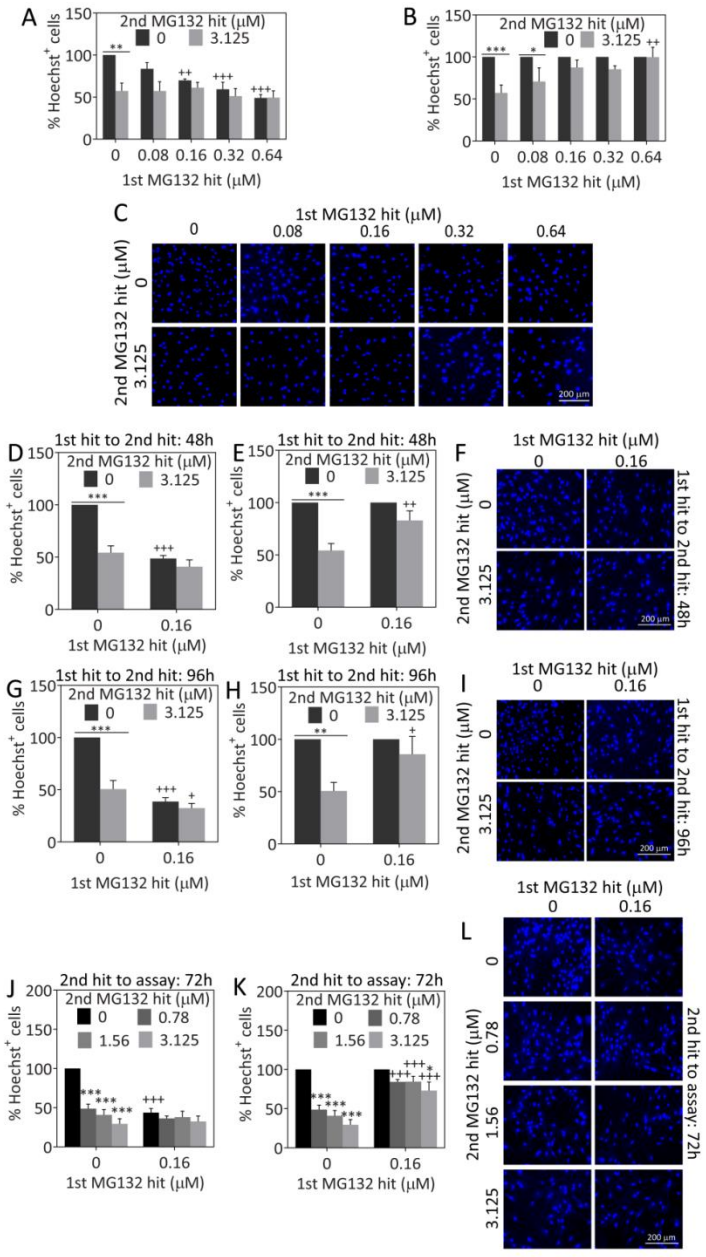

Figure 9. Severe proteotoxic stress preconditions astrocytes against subsequent insults. A) Cortical astrocytes were treated with indicated concentrations of the proteasome inhibitor MG132 one day after plating (1st hit) or an equal v/v of vehicle. Twenty-four hours later, astrocytes were challenged with a 2nd hit of MG132 (3.125 μM) or vehicle. Astrocyte viability was assessed 24h after the 2nd hit by counting viable Hoechst+ nuclei in blinded fashion. **B**) Data in panel A were expressed as a percentage of each 0 μM 2nd MG132 hit group (i.e., each gray bar was expressed as a percentage of the adjacent black bar). **C**) Representative images of Hoechst-stained astrocyte nuclei from the groups shown in A. The interval between the 1st hit and the 2nd hit was prolonged to 48h in **D-F** and to 96h in **G-I**. E and H represent data in D and G, respectively, expressed as a percentage of the 0 μM 2nd MG132 hit group. Representative Hoechst-stained nuclei are shown in F and I. **J-K)** The interval between the 2nd hit and the assay was extended to 72h. The data in panel J were expressed as a percentage of the 0 μM 2nd MG132 hit group and presented in panel K. **L)** Representative images of Hoechst-stained nuclei from groups shown in J. * $p \leq 0.05$, ** $p \leq 0.01$, *** $p \leq 0.001$ vs 0 μM 2nd MG132 hit, + $p \leq 0.05$, ++ $p \leq 0.01$, +++ $p \leq 0.001$ vs 0 μM 1st MG132 hit, two-way ANOVA followed by Bonferroni *post hoc* correction. Reprinted from "Astrocytes surviving severe stress can still protect neighboring neurons from proteotoxic stress," by A. M. Gleixner, 2015, *Molecular Neurobiology, Epub ahead of print*. Copyright [2015] by A.M Gleixner. Reprinted with permission.

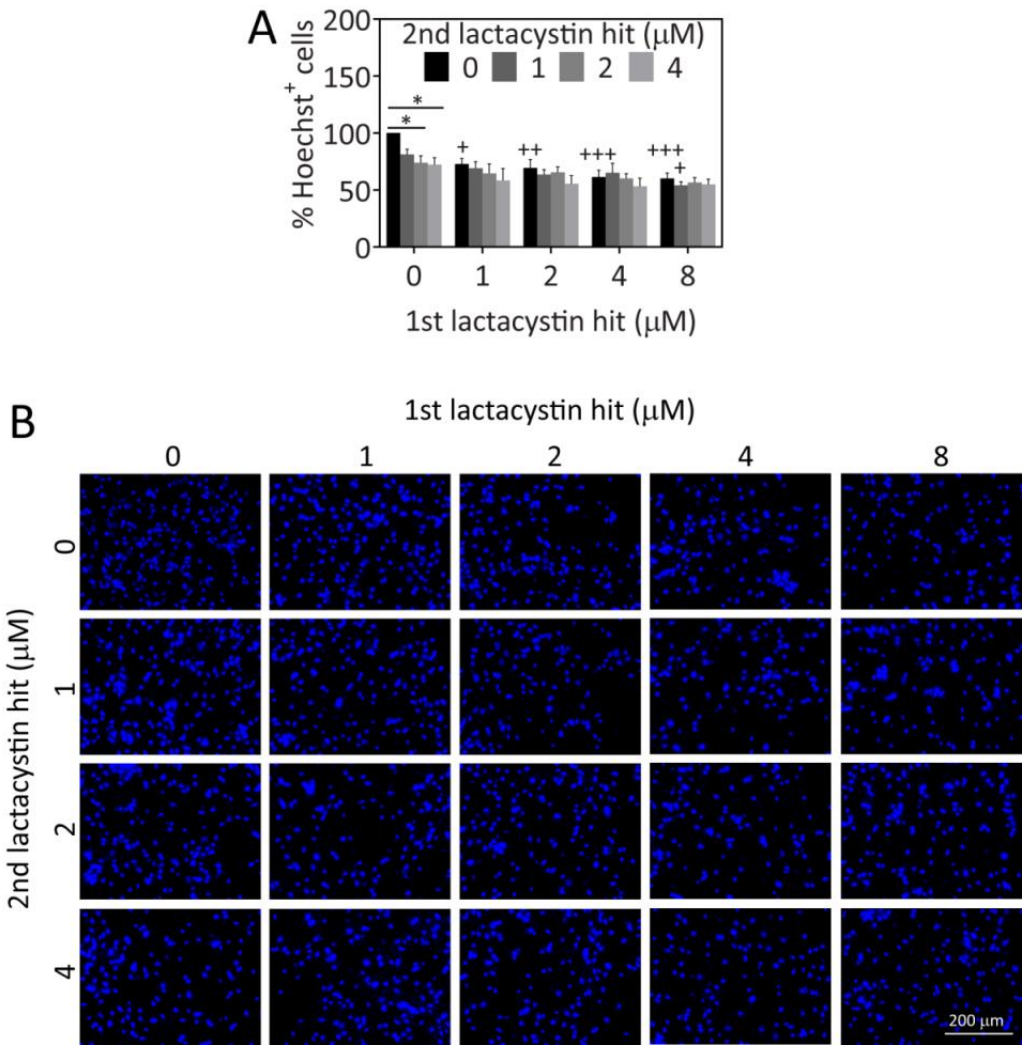

Figure 10. Lactacystin-mediated severe proteotoxic stress preconditions astrocytes against subsequent insults. A) Five days after plating, astrocytes were treated with various concentrations of lactacystin or an equivalent v/v of vehicle (phosphate buffered saline) as the 1st hit. On the following day, the astrocytes were treated with vehicle or a 2nd hit of lactacystin at the indicated concentrations. Viability was assayed 24h after the 2nd hit by counting Hoechst-stained nuclei. **B)** Representative images of Hoechst-stained nuclei for experiments shown in panel A. * $p \leq 0.05$ vs 0 μM 2nd lactacystin hit; + $p \leq 0.05$, ++ $p \leq 0.01$, +++ $p \leq 0.001$ vs 0 μM 1st lactacystin hit, two-way ANOVA followed by Bonferroni post hoc correction Reprinted from "Astrocytes surviving severe stress can still protect neighboring neurons from proteotoxic stress," by A. M. Gleixner, 2015, *Molecular Neurobiology, Epub ahead of print*. Copyright [2015] by A.M Gleixner. Reprinted with permission.

Astrocytes surviving the 1st hit do not exhibit characteristics of apoptosis

Hoechst or DAPI-stained cells undergoing apoptosis are often characterized by increased staining intensity and condensed nuclear area relative to non-apoptotic cells (Tone et al., 2007; Yu et al., 2002). Thus, we assessed nuclear area and staining intensity in astrocytes treated with 1st, 2nd, and dual MG132 hits in order to determine if the 1st hit left behind nuclear profiles exhibiting signs of cell death. The frequency distribution of the number of cells corresponding to specific nuclear sizes is shown in Figure 11A-C. No decrease in median nuclear size was found with the 1st, 2nd, or dual MG132 hits, supporting the view that most apoptotic cells had died and washed off the plate at the time of the viability assays. However, a slight decrease in average nuclear size was observed in astrocytes exposed to dual MG132 hits, even when excluding cells with nuclear areas less than 53 μm^2 (Fig 11D & E). Representative images of Hoechst-stained nuclei are shown in Figure 11F. Similar to the nuclear area analysis, no shift in median nuclear staining intensity was observed in astrocytes treated with 1st, 2nd and dual MG132 hits (Fig 11G-I). Furthermore, no change in average nuclear staining intensity with 1st, 2nd, and dual MG132 hits was observed either. These findings suggest that cells undergoing dual hits show a slight decrease in nuclear area but not staining intensity, but that the effect size is very small. Most importantly, these measurements reveal that cells surviving the 1st hit alone have viable nuclei with no change in average nuclear size.

As mentioned above, cells undergoing apoptosis are often described as having shrunken nuclei with increased Hoechst staining intensity (Tone, et al., 2007). Therefore, we assessed the relationship between nuclear size and Hoechst-staining intensity in the 1st hit, 2nd hit, and both hit groups. According to the scatterplots, MG132 treatment

eliminated a population of cells with small brightly stained nuclei [nuclear size 50-150 μm^2 and nuclear staining intensity greater than 20 arbitrary units (A.U.) for the mean gray value measurements] (Fig 11L-O). Therefore, we compared the effect of MG132 on the small, brightly stained nuclei to the effect of MG132 on cells with large nuclei (larger than 150 μm^2). MG132 eliminated a greater percentage of Hoechst-stained nuclei in the small, brightly stained nuclei group relative to the larger nuclei group (Fig 11P). These data are normalized to the vehicle group because the number of nuclei in the large nuclei group is significantly greater than the number of nuclei in the small, brightly stained nuclei group. The raw, untransformed data that show these differences are illustrated in Figure 12. Thus, small, brightly stained nuclei are most vulnerable to proteotoxic stress, as might be expected because they already show signs of injury.

Double-stranded DNA breaks are indicative of cells undergoing apoptosis. The TUNEL (terminal deoxynucleotidyl transferase dUTP nick end labeling) stain is a well-established marker of apoptosis (Elmore, 2007; Gavrieli, Sherman, & Ben-Sasson, 1992). Terminal deoxynucleotidyl transferase incorporates fluorescently labeled dUTP onto the exposed 3'-OH ends of the double-stranded DNA breaks in apoptotic cells. We counted the number of $TUNEL^+$ cells in our dual hit model in order to determine the number of cells undergoing apoptosis at the time that our viability assays were conducted. Less than 10% of the total number of cells present at the time of fixation (24h after the 2^{nd} hit) were $TUNEL^+$ in the 2^{nd} MG132 hit group (Fig 11Q). The 0.16 μM 1^{st} MG132 hit did not elicit any increase in the number of $TUNEL^+$ cells by itself in comparison to the 0 μM 1^{st} MG132 hit. The 1^{st} hit also did not change the number of $TUNEL^+$ cells in response to the 2^{nd} MG132 hit. Due to very low numbers of $TUNEL^+$ cells, there was high inter-

experimental variability of the data. Thus, we also expressed the number of TUNEL$^+$ cells as a fold change over control values. Here we found that both naïve and stressed astrocytes showed a significant increase in TUNEL staining in response to the 2nd MG132 hit (Fig 11R). Representative images of TUNEL$^+$ cells are displayed in Figure 11S. It is noteworthy that the number of TUNEL$^+$ profiles was low at the time of the assay, suggesting that we are mostly counting live cells at the time that our viability assays are conducted. Furthermore, our data confirm that the 1st hit does not increase the number of TUNEL$^+$ profiles in response to the 2nd hit, suggesting that cell death is not enhanced despite a slight shrinkage of nuclear surface area in the dual hit group. In sum, these data are consistent with the analyses of nuclear size and Hoechst-staining intensity and demonstrate that the 1st hit does not increase vulnerability to the 2nd hit when measuring either live or dead cells because the fold change in TUNEL$^+$ cells is similar between naïve and stressed cells. It is important to note that by far the majority of cells that we are counting in the dual hit group are not TUNEL$^+$ and that they continue to survive for at least 72h after the 2nd hit is administered (see Figure 9J-L), suggesting that they are indeed survivors despite a slight decrease in average nuclear size. It is also important to note that the TUNEL stain labels small, dying cells that are excluded from our viable cell counts by the threshold function in ImageJ anyway. From the scatterplots in Figure 11O it is further evident that the dual hits kill the brightest, smallest cells (0-150 microns in size) and that the majority of remaining cells are clustered around nuclear sizes of 150 to 300 microns instead of a wider spread from 0 to 400 microns in the untreated group (Figure 11L). The clustering of cells in the scatterplot data readily explain the small decrease in average nuclear size in the dual hit group Figure 11E and

the *lack* of change in median nuclear area in the dual hit group in Figure 11C. The clustering effect is also apparent in the shape of the dual hit histogram in Figure 11C.

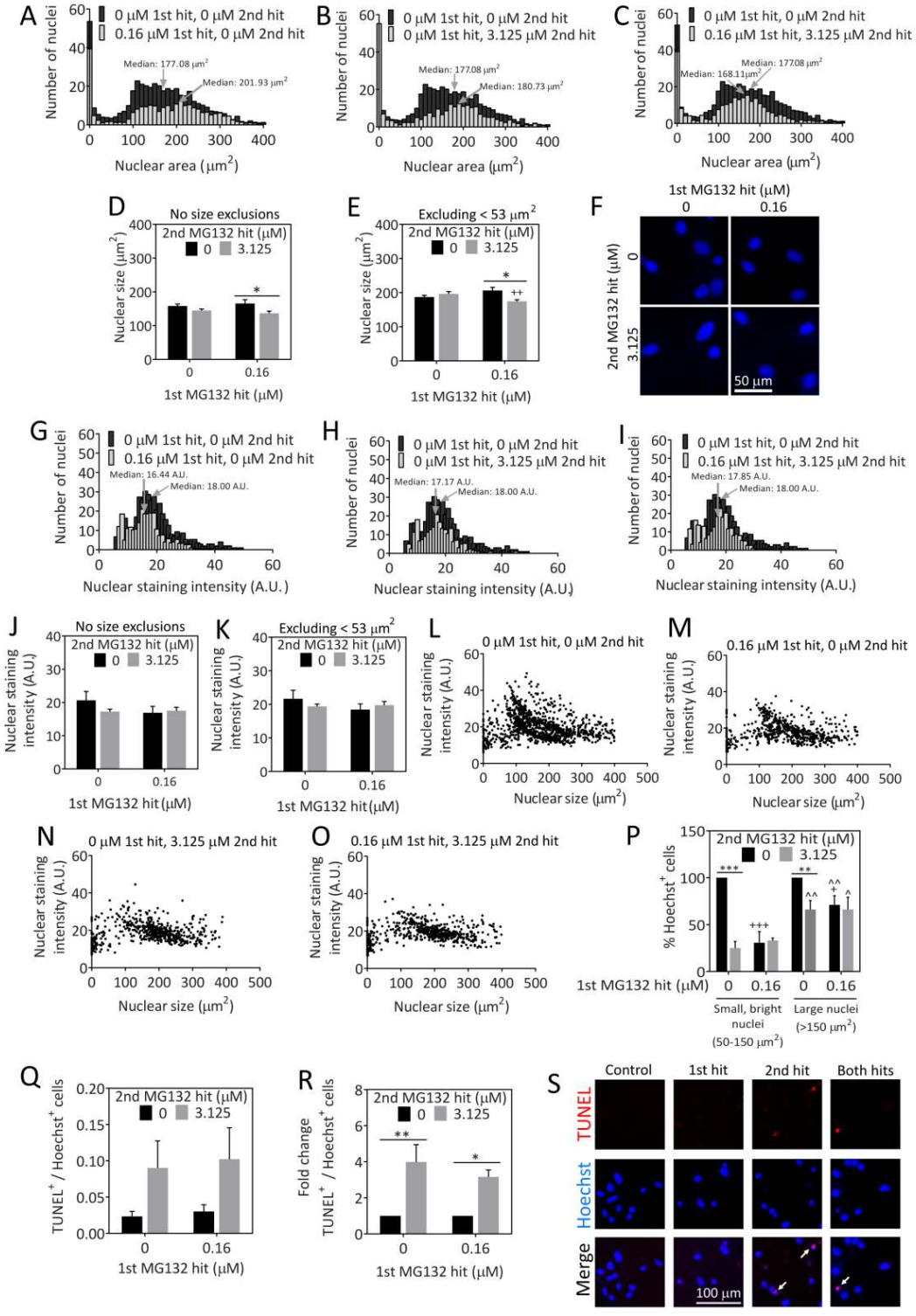

Figure 11. See below for figure legend

Figure 11. Nuclear viability in stressed astrocytes. Astrocytes were treated with the indicated concentrations of MG132 24h (1st hit) and 48h (2nd hit) after plating. On the third day, astrocytes were stained with the nuclear marker Hoechst and analyzed by a blinded observer using ImageJ software. **A-C)** Frequency distributions of the number of nuclei corresponding to the indicated nuclear area. The vehicle-treated group is included on all three figures for comparison. **D)** Average nuclear size of all cellular profiles. **E)** Average size of all nuclei except those smaller than 53 μm^2. **F)** Representative high-power image of Hoechst-stained nuclear profiles. **G-I)** Frequency distribution of the number of nuclei as a function of Hoechst nuclear staining intensity. The vehicle-treated group is included on all three figures for comparison. **J)** Average nuclear staining intensity of all cellular profiles. **K)** Average nuclear staining intensity of all profiles except cells with nuclei smaller than 53 μm^2. **L-O)** Nuclear staining intensity as a function of nuclear size. **P)** Astrocytes were divided into two groups: those with small, bright nuclei (50-150 μm^2; staining intensity greater than 20 arbitrary units for the mean gray value measurements) or large nuclei (greater than 150 μm^2; all staining intensities). Raw data is presented in Figure 12. **Q)** Number of $TUNEL^+$ cells relative to the total number of $Hoechst^+$ nuclei. **R)** Data presented in panel Q were expressed as a function of the 0 μM 2nd MG132 hit groups. **S)** Representative images of TUNEL staining. * $p \leq 0.05$, ** $p \leq 0.01$ vs 0 μM 2nd MG132 hit; + $p \leq 0.05$, ++ $p \leq 0.01$, +++ $p \leq 0.001$ vs 0 μM 1st MG132 hit; ^ $p \leq 0.05$, ^^ $p \leq 0.01$ vs small, bright nuclei; two- or three-way ANOVA followed by Bonferroni post hoc correction. Reprinted from "Astrocytes surviving severe stress can still protect neighboring neurons from proteotoxic stress," by A. M. Gleixner, 2015, *Molecular Neurobiology, Epub ahead of print*. Copyright [2015] by A.M Gleixner. Reprinted with permission.

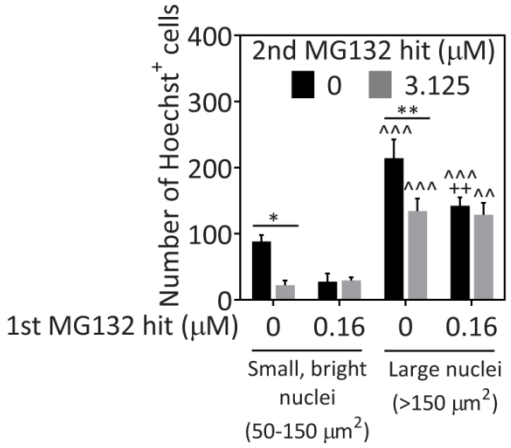

Figure 12. MG132 treatment is more lethal to small, bright nuclei than large nuclei. A) Hoechst-stained nuclei were categorized into two groups: those exhibiting small, brightly stained nuclei (50-150 μm^2 in size and staining intensity greater than 20 arbitrary units for the mean gray value measurements) or large nuclei (greater than 150 μm^2; all staining intensities). Raw counts of the numbers of nuclei per microscopic field of view (200× magnification) are shown here to supplement the transformed data in Figure 3P. * $p \leq 0.05$, ** $p \leq 0.01$ vs 0 μM 2nd MG132 hit; ++ $p \leq 0.01$ vs vs 0 μM 1st MG132 hit; ^^ $p \leq 0.01$, ^^^ $p \leq 0.001$ vs small, bright nuclei, three-way ANOVA followed by Bonferroni *post hoc* correction**.** Reprinted from "Astrocytes surviving severe stress can still protect neighboring neurons from proteotoxic stress," by A. M. Gleixner, 2015, *Molecular Neurobiology, Epub ahead of print*. Copyright [2015] by A.M Gleixner. Reprinted with permission.

Severe proteotoxic stress increases the expression of multiple defensive proteins

As we had switched protocols, we reexamined ubiquitinated protein and Hsp70 levels after dual hits in the new model in order to assess the effect of severe proteotoxicity on astrocytes. A significant increase in ubiquitinated proteins was observed 24h after the 1st MG132 hit, at the time of delivery of the 2nd hit (Fig 13A). These findings confirm that the 1st hit elicits proteotoxic stress. Forty-eight hours after the 1st hit, there was no significant difference in the levels of ubiquitinated proteins between the 0 and 0.16 μM 1st MG132 hit groups, supporting the view that the increase in ubiquitinated proteins was transient. Furthermore, the 2nd MG132 hit elicited a significant increase in ubiquitinated proteins in both naïve and stressed astrocytes 24h later (Fig 13B). Unlike in our initial studies (see Fig 4a), the two hits of MG132 were not synergistic in their impact on ubiquitinated protein levels, perhaps because the concentrations of MG132 were much lower in the new model. Nevertheless, these findings are still consistent with the hypothesis that previously stressed astrocytes are not simply refractory to the effects of MG132 and still respond to proteasomal inhibition by the 2nd hit with a dramatic increase in ubiquitin-conjugated proteins. The transient increase in ubiquitinated proteins after the 1st hit is also not consistent with the view that the MG132 survivors do not even take up the MG132 poison or are refractory to its effects.

Next we examined heat shock protein levels after the 1st hit. Depending upon the heat shock protein examined, the 1st MG132 hit yielded varying effects on protein levels 24h after treatment (Fig 13C-L). Some heat shock proteins, such as pHsp27 and Hsp70, were significantly upregulated 24h after the 1st MG132 hit. Trends towards increases in

Hsp40 (p = 0.093), HO1 (p = 0.058), and Hsc70 (p = 0.070) were also observed 24h after the 1st MG132 hit. However, several other defensive proteins were not altered by the 1st MG132 hit (DJ-1, Hsp27, Hsp90 and Hip). Similar to the ubiquitinated protein pattern, Hsp70 and HO1 were significantly increased by the 2nd MG132 hit in both naïve and stressed astrocytes (Fig 13M & N). These findings suggest that astrocytes can still mount defenses against subsequent proteotoxic insults despite prior exposure to severe stress. Another important finding is that there is an increase in Hsp70 24h after the 1st hit alone (Figure 13L) that wanes within 48h (or 24h after the 2nd hit in Figure 13M). Thus, the 1st hit elicits a transient rise in Hsp70 as shown with the ubiquitin data. This finding suggests that the 1st hit elicits active defenses in the cells that manage to survive and is not consistent with the view the 1st hit simply leaves behind cells that have higher expression of protective proteins to begin with and do not respond with any additional adaptive changes in response to MG132. In conclusion, our data show that stressed astrocytes that survive the 1st hit are not simply refractory to the MG132 poison and respond actively to proteotoxicity, otherwise there could not be a transient rise in Hsp70

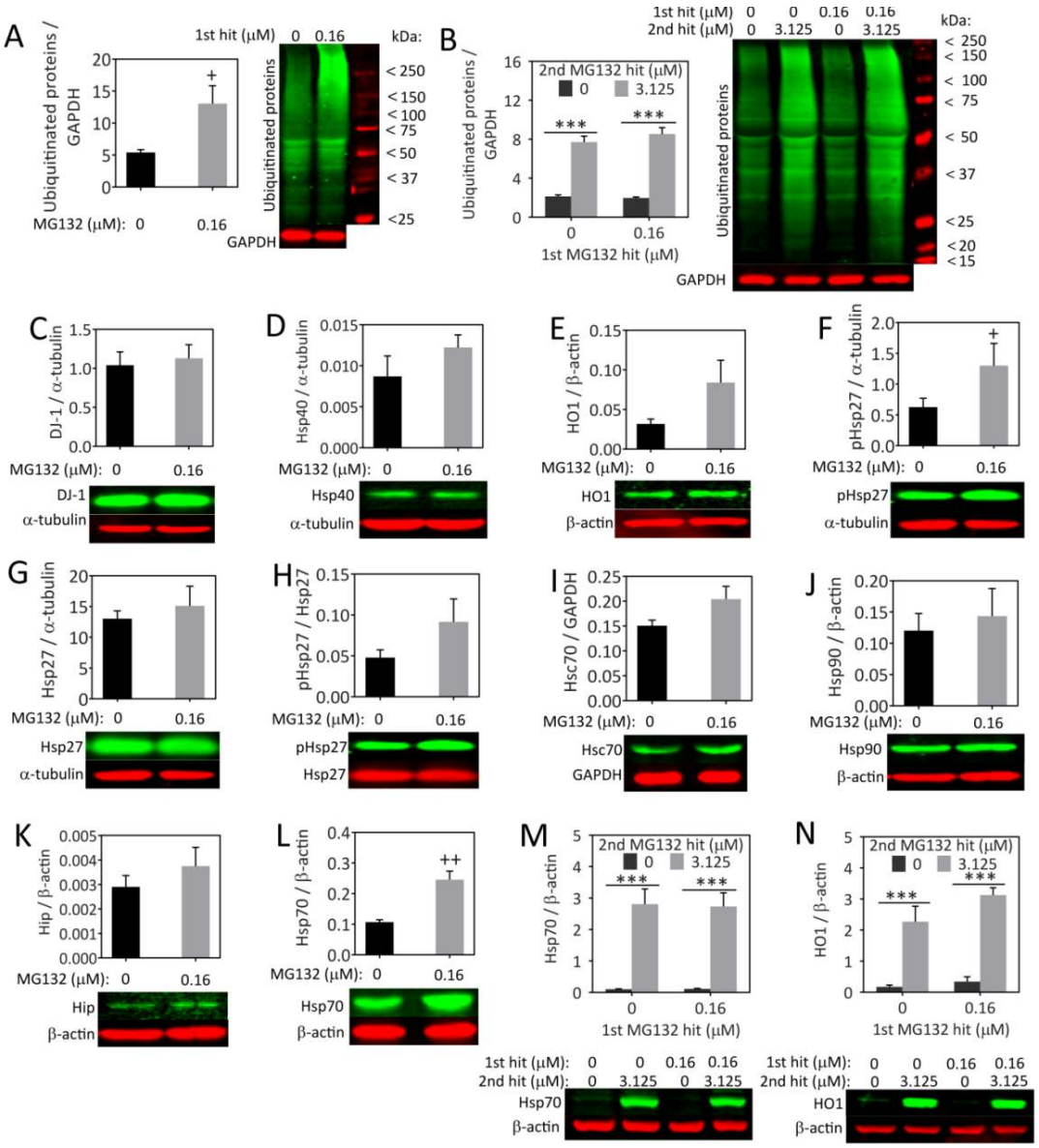

Figure 13. MG132 increases protein misfolding stress and upregulates Hsp70 and HO1 levels. Astrocytes were treated with indicated concentrations of MG132 (1st hit) and probed for a number of stress-sensitive proteins 24h later (**A, C-L**). Astrocytes were treated with single or dual hits of MG132 and assayed for levels of ubiquitinated proteins and heat shock proteins Hsp70 and HO1 24h after the 2nd hit (**B, M-N**). *** $p \leq 0.001$ vs 0 μM 2nd MG132 hit, + $p \leq 0.05$, ++ $p \leq 0.01$ vs 0 μM 1st MG132 hit, two-way ANOVA followed by Bonferroni *post hoc* correction for B, M, and N. The one-tailed, paired Student's *t-test* was used for A, C-L. Reprinted from "Astrocytes surviving severe stress can still protect neighboring neurons from proteotoxic stress," by A. M. Gleixner, 2015, *Molecular Neurobiology, Epub ahead of print*. Copyright [2015] by A.M Gleixner. Reprinted with permission.

Glutathione but not Hsp70 defenses are essential for stress tolerance in astrocytes

Thus far, we showed that the 1st MG132 hit upregulates Hsp70 levels at 24h, at the time of delivery of the 2nd MG132 hit. Hsp70 overexpression has been shown to increase glutathione peroxidase and reductase activity (Guo, et al., 2007), and our previous study had shown that glutathione is essential for stress tolerance in astrocytes (Titler, et al., 2013). Therefore, we hypothesized that Hsp70 may contribute to the protective effects of glutathione in stressed astrocytes. Thus, we inhibited Hsp70 and glutathione defenses both individually and together. Our results were not consistent with the hypothesis that Hsp70 mediates tolerance in our model because a pharmacological inhibitor of Hsp70, VER155008, did not alter the resistance of previously stressed astrocytes to subsequent proteotoxic insults (Fig 14A-C). However, as observed previously, glutathione synthesis inhibition by BSO did attenuate resistance to the 2nd MG132 hit in previously stressed astrocytes. Simultaneous inhibition of Hsp70 activity and glutathione synthesis elicited a significant decrease in basal viability (as observed with VER155008 alone) and increased susceptibility of previously stressed astrocytes to a 2nd MG132 hit (as observed with BSO alone; Fig 14A). As expected, when the data are expressed as a function of the 0 μM 2nd MG132 hit group, they reveal increased susceptibility of previously stressed astrocytes to the 2nd hit in the presence of BSO but not VER155008 (Fig 14B). Figure 14C shows representative images of Hoechst-stained cells corresponding to the data presented in Figure 14A. These findings reveal that glutathione loss unmasks the toxic impact of the 2nd hit and are not consistent with the hypothesis that the astrocytes surviving the 1st hit of MG132 are simply refractory to any of its effects. In other words, if there were no defenses against MG132 in the surviving

astrocytes, they would not become vulnerable to MG132 upon loss of glutathione defenses.

Because glutathione was an important mediator of stress tolerance in our model, we measured total glutathione levels and found that the 2nd MG132 hit significantly increased glutathione (Fig 14D). There was also a trend towards an increase in the 1st hit group ($p = 0.059$). Total glutathione levels were even higher when Hsp70 activity was inhibited by VER155008. Therefore, Hsp70 may not be a positive regulator of glutathione synthesis in our model, but may reduce the need for this antioxidant. As expected, BSO attenuated the effect of MG132 on total glutathione levels (Fig 14D & E). The assay for total glutathione levels measures both the reduced and oxidized forms of the thiol tripeptide. However, glutathione exists primarily in the reduced state (Owen & Butterfield, 2010), which suggests that total glutathione measures are likely to coincide with the reduced glutathione levels. To confirm this, reduced glutathione levels were measured by the GSH-Glo assay. Twenty-four hours after delivery of the 1st MG132 hit (or at the same time point as the 2nd hit delivery) reduced glutathione was significantly increased intracellularly but not in the extracellular space (Fig 14F & G, respectively). Forty-eight hours after the 1st hit, the 1st and 2nd MG132 hits alone significantly increased intracellular reduced glutathione levels. No additional increase in reduced glutathione was observed in the dual hit group (Fig 14H). These results are consistent with the view that feedback inhibition on the rate limiting enzyme glutamate cysteine ligase prevents any additional rise in glutathione levels in response to dual hits (C. S. Huang, Chang, Anderson, & Meister, 1993). No additional increase may be evident after the 2nd MG132 hit because the 1st hit has already upregulated those defenses and there is no further need

for a stress-induced rise in antioxidant defenses. The pattern of glutathione measurements was similar for the In-Cell Western and GSH-Glo assays, as expected, suggesting that most glutathione is in the reduced form.

In order to understand how glutathione defenses may be boosted in stressed cells, glutamate cysteine ligase levels were examined by Western blot analysis. Glutamate cysteine ligase is comprised of two subunits: the catalytic and modifier subunits. Glutamate cysteine ligase modifier subunit (GCLM) levels were elevated 24h after the 1st MG132 hit (Fig 14I). However, no significant increase was observed in glutamate cysteine ligase catalytic subunit levels (Fig 15A). GCLM has been shown to increase the catalytic efficiency of GCLC (Franklin, et al., 2009). Therefore, higher GCLM levels may be sufficient to permit an increase in glutathione synthesis. We also measured a third glutathione enzyme, glutathione S-transferase, which eliminates xenobiotics. The class of glutathione S-transferase enzymes is divided according to the composition of their N-terminal domain (Mazzetti, et al., 2015). Glutathione S-transferase π and μ have both been identified in astrocytes (Abramovitz et al., 1988; Cammer & Zhang, 1993; Johnson, el Barbary, Kornguth, Brugge, & Siegel, 1993). Therefore, we assessed the effect of 1st MG132 hit on glutathione S-transferase π and μ. The 1st MG132 hit significantly raises glutathione S-transferase μ such that it is upregulated at the time of the 2nd MG132 hit (Fig 14J). However, no significant increase in glutathione S-transferase π with the 1st MG132 hit was observed (Fig 15B). In summary, glutamate cysteine ligase modifier subunit and glutathione S-transferase μ may promote glutathione defenses in our model.

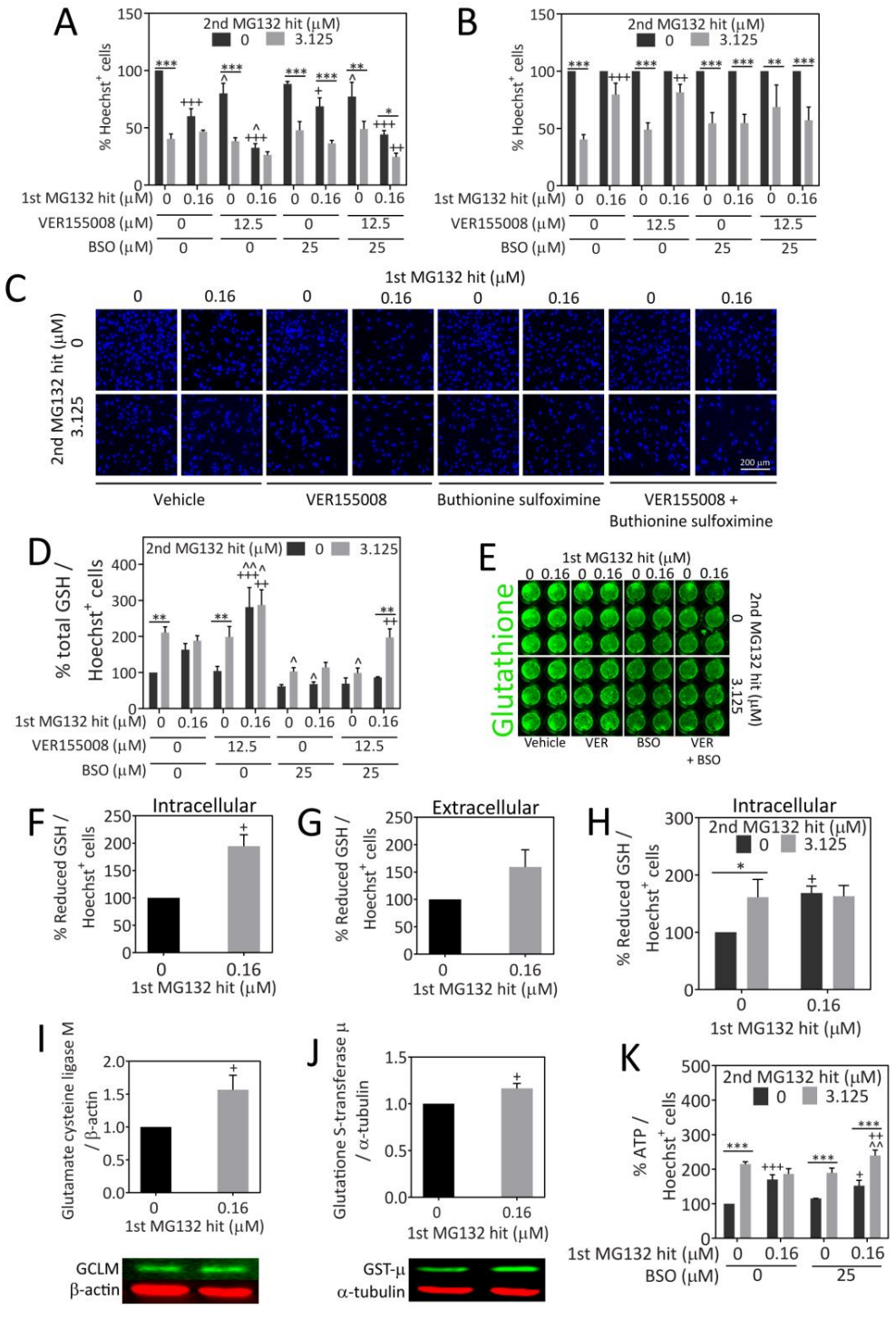

Figure 14. See below for figure legend

Figure 14. Inhibition of glutathione synthesis but not Hsp70/Hsc70 activity abolishes stress-induced protection against the 2nd MG132 hit. A) Cortical astrocytes were treated with the indicated concentrations of MG132 in the absence or presence of the Hsp70/Hsc70 inhibitor VER155008 and glutathione synthesis inhibitor buthionine sulfoximine (BSO). Viable Hoechst$^+$ nuclei were quantified 24h after the 2nd hit to measure viability. **B)** Data from panel A were expressed as a percentage of the 0 μM 2nd MG132 hit groups (i.e. all gray bars were expressed as a percentage of the adjacent black bars). **C)** Representative images of Hoechst-stained nuclei from data shown in panel A. **D)** Total glutathione levels were measured 24h after the 2nd MG132 hit by the In-Cell Western technique and expressed as a function of the corresponding number of Hoechst$^+$ nuclei to control for differences in cell density. **E)** Representative image of total glutathione In-Cell Western. **F-H)** Reduced glutathione levels were measured intracellularly and in the extracellular media by the Glutathione-Glo assay and luminescence was expressed as a function of the number of Hoechst$^+$ nuclei on parallel plates. All glutathione assays in F-H were performed 24h after the final MG132 hit. **I-J)** Western blot analysis of glutamate cysteine ligase modifier subunit (GCLM) and glutathione S-transferase μ (GST-μ) in lysates collected 24h after the 1st MG132 hit. **K)** Astrocytes were treated with single and dual hits of MG132 in the absence or presence of BSO and ATP levels were measured by the CellTiter-Glo assay 24h after the 2nd MG132 hit. ATP levels are expressed as a function of Hoechst$^+$ cell numbers on parallel plates. * $p \leq 0.05$, ** $p \leq 0.01$, *** $p \leq 0.001$ vs 0 μM 2nd MG132 hit; + $p \leq 0.05$, ++ $p \leq 0.01$, +++ $p \leq 0.001$ vs 0 μM 1st MG132 hit; ^ $p \leq 0.05$, ^^ $p \leq 0.01$ vs 0 μM VER155008 and/or 0 μM BSO, two- or three-way ANOVA followed by Bonferroni *post hoc* correction. For F-G and I-J, the two-tailed paired Student's *t* test was employed. Reprinted from "Astrocytes surviving severe stress can still protect neighboring neurons from proteotoxic stress," by A. M. Gleixner, 2015, *Molecular Neurobiology, Epub ahead of print*. Copyright [2015] by A.M Gleixner. Reprinted with permission.

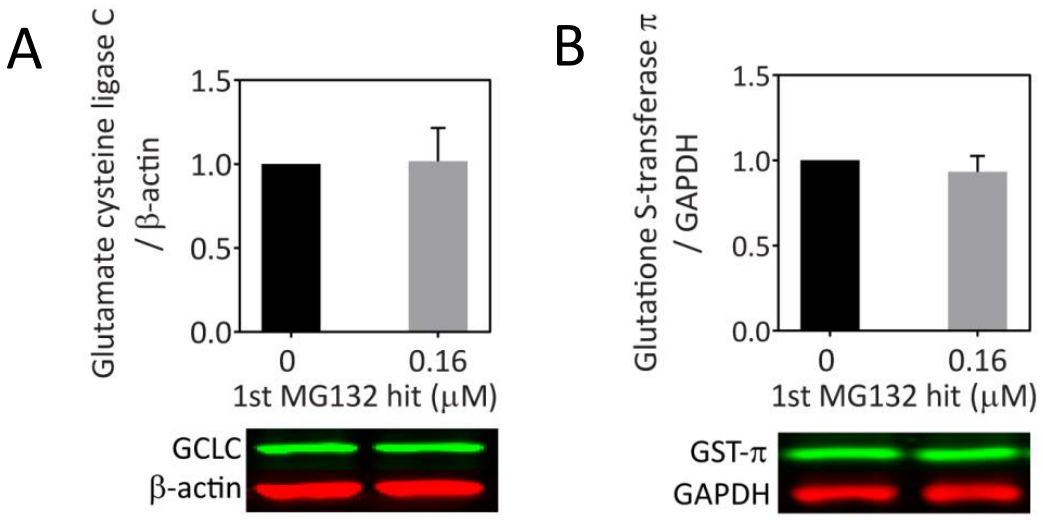

Figure 15. Impact of 1st hit on glutathione-related enzymes. Astrocytes were treated with the 1st MG132 hit or vehicle and the following glutathione-related proteins were measured in lysates collected 24h later: **A)** glutamate cysteine ligase catalytic subunit (GCLC), **B)** glutathione S-transferase π (GST-π). No significant difference was determined with the two-tailed paired Student's *t* test. Reprinted from "Astrocytes surviving severe stress can still protect neighboring neurons from proteotoxic stress," by A. M. Gleixner, 2015, *Molecular Neurobiology, Epub ahead of print*. Copyright [2015] by A.M Gleixner. Reprinted with permission.

Glutathione synthesis inhibition increases ATP levels in severely stressed astrocytes

ATP is important for fueling defensive responses in cells, and supplies energy for glutathione synthesis and heat shock protein activity (Bukau & Horwich, 1998; S. C. Lu, 2009; Mayer & Bukau, 2005). Therefore, we measured ATP levels in our model. ATP levels were increased in astrocytes treated with the 1st, 2nd, and dual MG132 hits (Fig 14K). The pattern in Figure 14K appears different from the pattern in Figure 3a in our previous model because we expressed ATP as a function of cell numbers. The data were expressed in this manner because Figure 3a does not take into consideration changes in astrocyte numbers; ATP loss might therefore mean loss of cell numbers, a drop in ATP output per cell, or both. BSO promoted a large increase in ATP levels in the dual hit group. Despite this increase in ATP, previously stressed astrocytes were susceptible to the 2nd MG132 hit in the presence of BSO, suggesting that the increase in ATP was not sufficient for protecting astrocytes. On the other hand, it is also possible that in the absence of the BSO-mediated rise in ATP, the stressed astrocytes would have been all the more vulnerable to MG132.

System x_c^- may not mediate protection in severely stressed astrocytes

Cysteine availability is often the rate-limiting component of glutathione synthesis and is determined partly by the system x_c^- glutamate/cysteine antiporter (Bannai & Kitamura, 1980; Jackman, Melchior, Hewett, & Hewett, 2012; Sato et al., 2002). Thus, we tested the hypothesis that system x_c^- would contribute to the stress-induced tolerance in this model. However, LY367385, a system x_c^- and metabotropic glutamate receptor inhibitor (mGluR1), did not attenuate the resistance of previously stressed astrocytes to subsequent insults. To control for potential off-target effects of LY367385, YM298198, a

specific mGluR1 inhibitor, was also used. YM298198 did not attenuate the tolerance of previously stressed astrocytes towards subsequent MG132 insults, as expected (Fig 16A & B). Therefore, system x_c^- may not contribute to glutathione-mediated protection of stressed astrocytes against subsequent proteotoxic insults. Further studies are nevertheless warranted, because of the possibility that both inhibitors only acted on mGluR1.

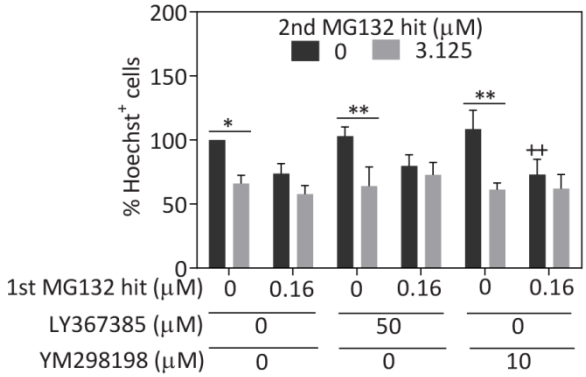

Figure 16. System x_c^- is not essential for resilience in severely stressed astrocytes. Cortical astrocytes were treated with the indicated 1st and 2nd MG132 hit in the absence and presence of pharmacological inhibitors LY367385 and YM298198. **A)** Viability was assessed by blinded cell counts of Hoechst$^+$ nuclei. **B)** Representative images of Hoechst-stained nuclei * $p \leq 0.05$, ** $p \leq 0.01$ vs 0 μM 2nd MG132 hit, ++ $p \leq 0.01$, vs 0 μM 1st MG132 hit three-way ANOVA followed by Bonferroni *post hoc* correction. Reprinted from "Astrocytes surviving severe stress can still protect neighboring neurons from proteotoxic stress," by A. M. Gleixner, 2015, *Molecular Neurobiology, Epub ahead of print*. Copyright [2015] by A.M Gleixner. Reprinted with permission.

Heme oxygenase 1 activity is not essential for stress tolerance in astrocytes

As mentioned above, HO1 is a highly stress responsive protein that prevents cell death in response to oxidative injury (Schipper, et al., 2009). Furthermore, oxidative stress can be propagated by proteasome inhibition (Maharjan, Oku, Tsuda, Hoseki, & Sakai, 2014). Thus, we hypothesized that HO1 also contributes to the stress-induced tolerance in our model. As described above, the 1st MG132 hit elicited a trend towards an increase in HO1 protein levels (see Fig 13E). A competitive inhibitor of HO1 activity, tin protoporphyrin IX, did not alter the effect of MG132 on astrocytes in the dual hit model (Fig 17A & B). Pilot data show that the inhibitor does reduce HO1 activity (data not shown). Therefore, HO1 may not be responsible for the stress-induced protection in our model, although further studies to verify the efficacy of the HO1 inhibitor are in order.

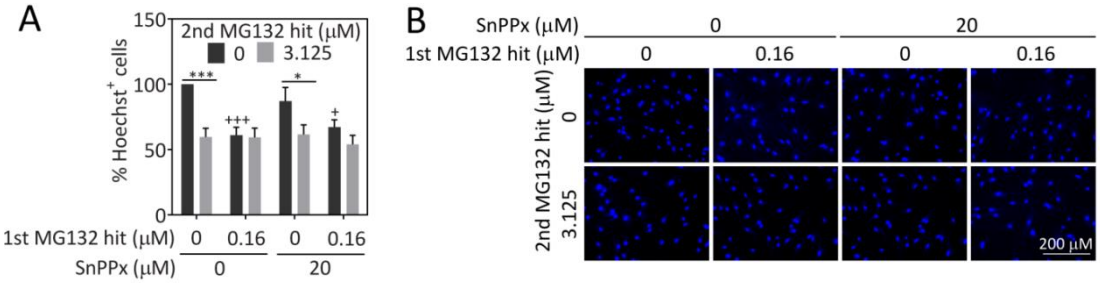

Figure 17. Stressed astrocytes can resist dual hits despite HO1 inhibition. A) Astrocytes were treated with the 1st and 2nd MG132 hits 24h apart in the absence or presence of the heme oxygenase 1 inhibitor SnPPx. Viability was assayed 24h after the 2nd hit. **B)** Representative images of Hoechst stained nuclei. * $p \leq 0.05$, *** $p \leq 0.001$ vs 0 μM 2nd MG132 hit, + $p \leq 0.05$, +++ $p \leq 0.001$ vs 0 μM 1st MG132 hit, two-way ANOVA followed by Bonferroni *post hoc* correction. Reprinted from "Astrocytes surviving severe stress can still protect neighboring neurons from proteotoxic stress," by A. M. Gleixner, 2015, *Molecular Neurobiology, Epub ahead of print*. Copyright [2015] by A.M Gleixner. Reprinted with permission.

Severely stressed astrocytes can still blunt proteotoxic cell death in neurons, even in the absence of glutathione and Hsp70/Hsc70 defenses

As shown above, glutathione synthesis is essential for protecting stressed astrocytes from subsequent proteotoxic insults. Astrocytes are known to provide glutathione precursors for neighboring neurons, which may prevent neuronal death during stress exposure (Dringen, et al., 2000; Dringen, et al., 1999). Therefore, we investigated whether severely stressed astrocytes can decrease proteotoxic stress in neighboring neurons and whether glutathione synthesis is essential for this effect. Neuron-astrocyte co-cultures were developed to answer this question and were conducted in collaboration with Dr. Jessica Posimo. Astrocytes were stressed with a 1st MG132 hit and the MG132 was then removed before neurons were plated in direct contact with the glial cells. The neuron-astrocyte contact co-cultures were then administered a 2nd MG132 hit (2nd hit in reference to astrocytes). Neuron viability was measured by In-Cell Western analysis for the neuronal marker MAP2 (Caceres, Banker, Steward, Binder, & Payne, 1984; Posimo, et al., 2014). Other studies have verified that the MAP2 In-Cell Western assay is a sensitive measure of neuronal viability (Posimo, et al., 2014). Primary neurons plated alone were highly susceptible to MG132 (Fig 18A & B). There was a trend towards neuroprotection against MG132 in the presence of unstressed astrocytes ($p=0.067$) (Fig 18A). In contrast, the severely stressed astrocytes attenuated neuronal death in response to the 2nd MG132 hit in a statistically significant manner. Surprisingly, inhibition of glutathione synthesis by BSO did not alter the effect of MG132 toxicity on neurons or the protective effects of astrocytes on neuronal viability. In order to verify that BSO was eliciting the expected decrease in glutathione, glutathione levels were measured

in the neuron-astrocyte co-cultures. The results show that 1) the presence of astrocytes significantly increased overall glutathione levels, 2) the 2nd MG132 hit significantly increased glutathione levels in a concentration-dependent manner, and 3) BSO abolished these effects (Fig 18C-E). These findings indicate that stressed co-cultures increase glutathione synthesis. We conclude that glutathione is not essential for astrocyte-mediated protection of neurons from proteotoxicity although it is essential for protection of previously stressed astrocytes from subsequent insults.

Finally, we measured GFAP levels in co-cultures treated with BSO and MG132, as GFAP is a phenotypic marker of astrocytes. Some GFAP was detected in the neuron-only group, because our primary neuronal cultures are derived from postnatal day 1-2 rat pups (a time at which astrocyte births peak) and contain 9.5% astrocytic cells (F. D. Miller & Gauthier, 2007). As expected, GFAP levels were dramatically higher in the co-culture groups (Fig 18F & G). It is worth noting here that GFAP levels are not always in proportion to the number of cells because GFAP is a reactive stress marker. Therefore, we cannot use GFAP in an In-Cell Western analysis as a measure of astrocyte numbers.

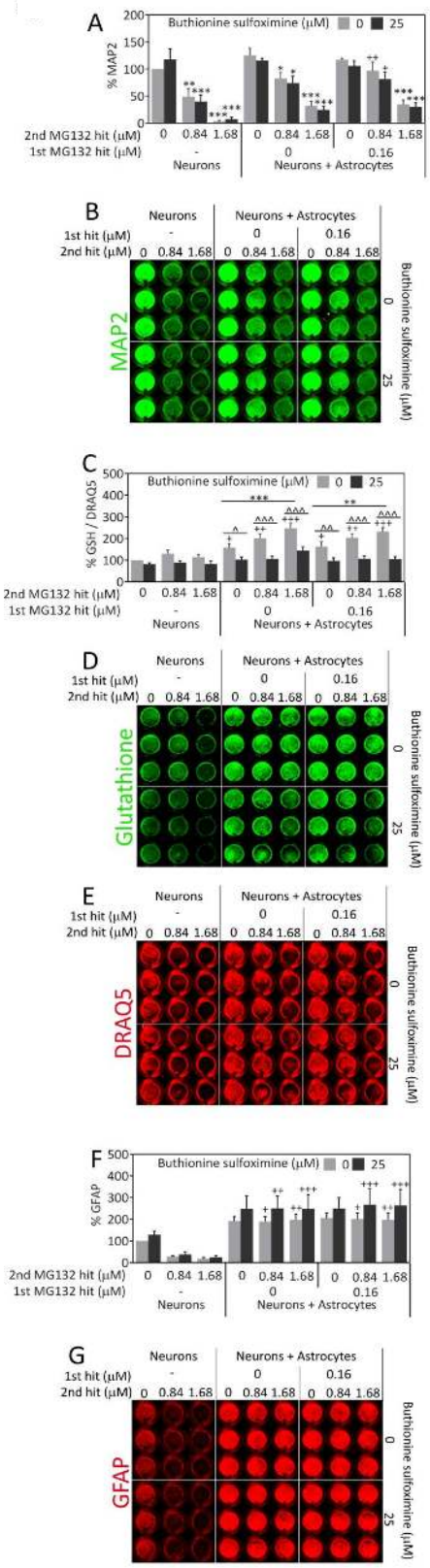

Figure 18. Severely stressed astrocytes can protect neurons from proteotoxic stress. A) Astrocytes were treated with the 1st MG132 hit 24h prior to introduction of neocortical neurons, in the absence or presence of the glutathione synthesis inhibitor buthionine sulfoximine (BSO). Two days after the introduction of neurons, the neuron/astrocyte co-cultures were treated with MG132 as a 2nd hit in the absence or presence of BSO. Two days after the 2nd hit, neuronal viability was measured by the In-Cell Western assay for the specific neuronal marker MAP2. **B)** Representative image of MAP2 In-Cell Western. **C)** Changes in glutathione levels were measured by In-Cell Western analyses and expressed as a function of the infrared nuclear stain DRAQ5. Representative images of glutathione immunostaining **(D)** and DRAQ5 levels **(E)**. **F)** The astrocytic marker GFAP was measured by In-Cell Western analysis in neuron/astrocyte co-cultures 48h after the 2nd MG132 hit in the absence or presence of BSO. **G)** Representative image of GFAP In-Cell Western. ** $p \leq 0.01$, *** $p \leq 0.001$ vs 0 μM 2nd MG132 hit, + $p \leq 0.05$, ++ $p \leq 0.01$, +++ $p \leq 0.001$ vs neurons, ^ $p \leq 0.05$, ^^ $p \leq 0.01$, ^^^ $p \leq 0.001$ vs 0 μM BSO, three-way ANOVA followed by Bonferroni *post hoc* correction. Reprinted from "Astrocytes surviving severe stress can still protect neighboring neurons from proteotoxic stress," by A. M. Gleixner, 2015, *Molecular Neurobiology, Epub ahead of print*. Copyright [2015] by A.M Gleixner. Reprinted with permission.

Astrocytes robustly protect neurons against the synergistic toxicity of proteasome and Hsp70 inhibition

Although stressed astrocytes do not rely on Hsp70 activity for protection against subsequent proteotoxic insults, Hsp70 may be released from astrocytes via exosomes in order to protect neighboring cells, such as neurons, from proteotoxicity (Lancaster & Febbraio, 2005; Taylor, et al., 2007; Zhan et al., 2009). Therefore, we tested the hypothesis that the Hsp70 inhibitor VER155008 would attenuate the neuroprotection afforded by astrocytes. As before, MG132 significantly decreased neuron viability in the neuron-only group. Furthermore, naïve and previously stressed astrocytes both attenuated MG132 toxicity in neurons. Significant protection against MG132 toxicity in neurons by naïve astrocytes may have been observed in these experiments and not the previous experiments in Figure 18 because MG132 was less toxic in the later experiments. The variability in MG132 toxicity may be attributed to differences in MG132 stock solutions or the quality of the neuronal cultures. However, all the trends in the two sets of data are identical and speak to the reproducibility of the neuroprotective properties of stressed astrocytes. In the neuron-only group, Hsp70 inhibition by VER155008 and proteasome inhibition by MG132 elicited a synergistic decrease in neuron viability (Fig 19A-C). Naïve and previously stressed astrocytes significantly protected neurons against the synergistic toxicity of MG132 and VER155008, an effect that is also evident when the data are expressed as a percentage of the 0 μM VER155008 group (Figure 19B). As observed in the earlier co-culture studies, GFAP levels were higher in the neuron-astrocyte co-culture group, and some GFAP was detected in the neuron-only group (Fig 19D & E).

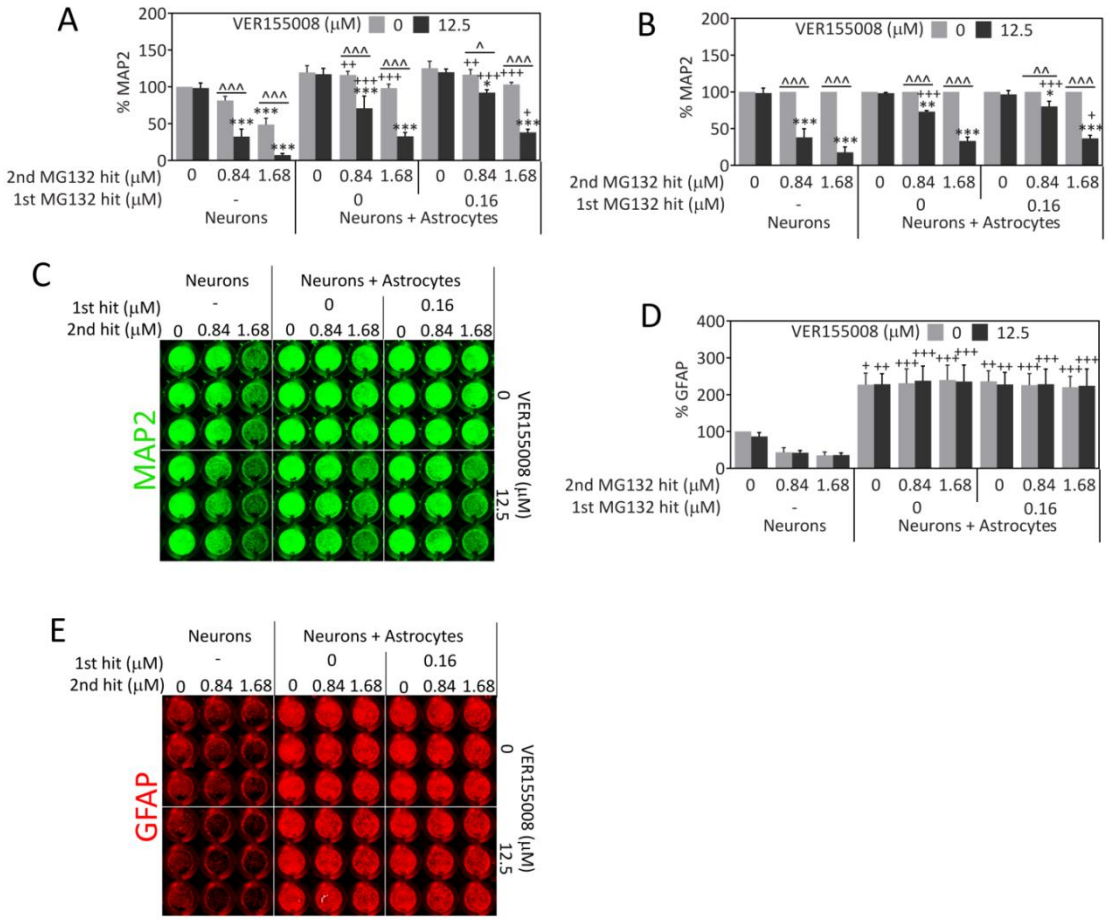

Figure 19. Stressed astrocytes prevent the synergistic toxicity of proteasome and Hsp70/Hsc70 inhibitors. A) Astrocytes were treated with the 1st MG132 hit 24h prior to introduction of neocortical neurons, in the absence or presence of the Hsp70/Hsc70 inhibitor VER155008. Two days after the introduction of neurons, the neuron/astrocyte co-cultures were treated with MG132 as a 2nd hit in the absence or presence of VER155008. Two days after the 2nd hit, neuronal viability was measured by the In-Cell Western assay for MAP2. **B)** Data from panel A were expressed as a percentage of the 0 μM VER155008 groups to illustrate the exacerbation of MG132 toxicity by VER155008. **C)** Representative image of MAP2 In-Cell Western. **D)** The astrocytic marker glial fibrillary acidic protein (GFAP) was analyzed by In-Cell Western analyses 48h after the 2nd hit in the same neuron/glia co-cultures as shown in panels A-C. **E)** Representative image of GFAP In-Cell Western. * $p \leq 0.05$, *** $p \leq 0.001$ vs 0 μM 2nd MG132 hit, + $p \leq 0.05$, ++ $p \leq 0.01$, +++ $p \leq 0.001$ vs neurons, ^ $p \leq 0.05$, ^^ $p \leq 0.01$, ^^^ $p \leq 0.001$ vs 0 μM VER155008, three-way ANOVA followed by Bonferroni *post hoc* correction. Reprinted from "Astrocytes surviving severe stress can still protect neighboring neurons from proteotoxic stress," by A. M. Gleixner, 2015, *Molecular Neurobiology, Epub ahead of print*. Copyright [2015] by A.M Gleixner. Reprinted with permission.

Astrocytes-mediated neuroprotection is dependent upon physical contacts

Astrocytes are known to support neurons by providing metabolic precursors, antioxidants, and trophic factors (Allen & Barres, 2009). Thus, we sought to determine whether astrocytes release a diffusible factor in order to protect neurons against proteotoxicity using astrocyte-conditioned media (ACM). First, astrocytes were treated with MG132 for 24h. The ACM was then added to neuron growth media (at a dilution of 1:1) in primary neuron cultures. Neurons with or without ACM were then treated with an MG132 insult (2^{nd} MG132 hit) and neuron viability was measured 24h later. As expected, neuron viability was decreased by the 2^{nd} MG132 hit, but conditioned media from either stressed or unstressed astrocytes completely failed to alter the effect of MG132 on neuron viability (Fig 20A & B). Because the diffusible factors may have been too dilute with our protocol, ACM was also concentrated by centrifugation and delivered to neurons at a 10× concentration. However, concentrated ACM also did not alter the effect of MG132 on neuron viability either (data not shown).

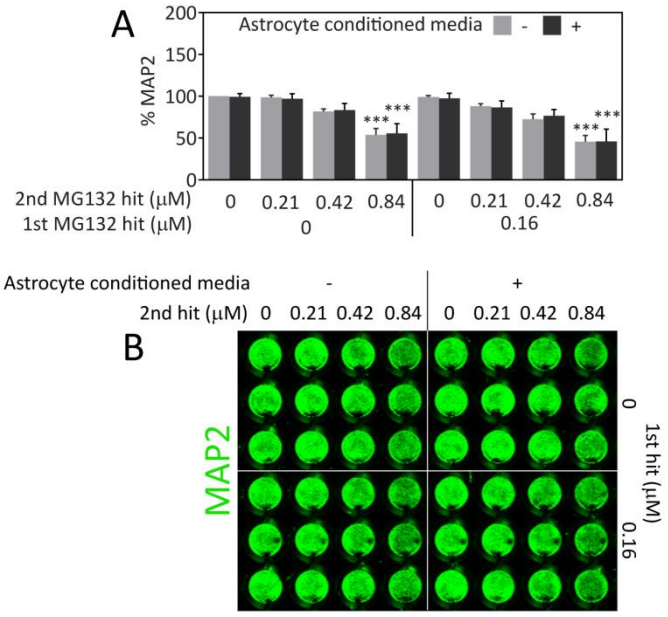

Figure 20. Stressed neurons are not protected from proteotoxicity by astrocyte-conditioned media. A) The 1st MG132 hit or an equivalent v/v of vehicle was added for 24h to wells in the presence of astrocytes (conditioned media) or in their absence (unconditioned media). Conditioned and unconditioned media (still containing 1st hit MG132 or vehicle) were then delivered to neocortical neurons by diluting them 1:1 in neuron media. The 2nd MG132 hit was administered at the time of media transfer. Neuronal viability was measured by the In-Cell Western assay for MAP2 48h after media transfer. **B)** Representative image of MAP2 In-Cell Western. *** $p \leq 0.001$ vs 0 μM 2nd MG132 hit, three-way ANOVA followed by Bonferroni *post hoc* correction Reprinted from "Astrocytes surviving severe stress can still protect neighboring neurons from proteotoxic stress," by A. M. Gleixner, 2015, *Molecular Neurobiology, Epub ahead of print*. Copyright [2015] by A.M Gleixner. Reprinted with permission.

3.2 N-acetyl cysteine-mediated protection of astrocytes against proteotoxicity is dependent upon heat shock protein activity

N-acetyl cysteine attenuates proteotoxicity in astrocytes

N-acetyl cysteine (NAC) has shown beneficial effects in multiple neurological conditions (Adair, et al., 2001; Berk, Copolov, Dean, Lu, Jeavons, Schapkaitz, Anderson-Hunt, Judd, et al., 2008; Berk, Copolov, Dean, Lu, Jeavons, Schapkaitz, Anderson-Hunt, & Bush, 2008; M. E. Hoffer, et al., 2013). These therapeutic effects of NAC are thought to be mediated by antioxidant effects on neurons. As astrocytes are known to support neurons, it is also important to protect astrocytes from protein misfolding stress in neurological conditions so that they can continue to promote neuronal health. Therefore, we sought to determine the therapeutic potential of NAC in astrocytes exposed to proteotoxicity. First, we hypothesized that NAC would prevent MG132 toxicity in cortical astrocytes. Consistent with this expectation, NAC decreased the MG132-induced loss of Hoechst^{+} nuclei in a concentration-dependent manner (Fig 21A). Representative images of Hoechst-stained nuclei and the preservation of cellular morphology by NAC are presented in Figure 21B and C.

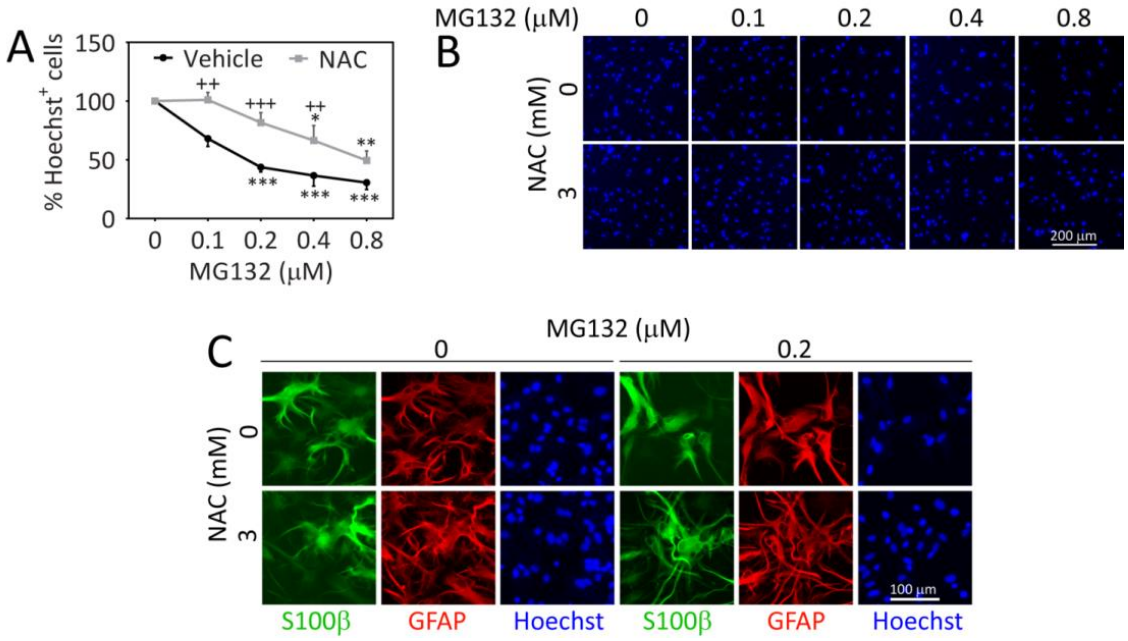

Figure 21. NAC protects astrocytes from MG132 toxicity. Cortical astrocytes were treated with vehicle (DMSO) or a range of MG132 concentrations in the presence of 3 mM NAC or vehicle (H_2O, equivalent v/v). **A)** Viability was determined 48h later by blinded counts of Hoechst$^+$ nuclei. **B)** Representative images of Hoechst$^+$ nuclei. **C)** Representative images of astrocytes stained for S100β (green), glial fibrillary acidic protein (GFAP, red), and Hoechst (blue). Shown are the mean ± SEM of 3 independent experiments. * $p \leq 0.05$, ** $p \leq 0.01$, *** $p \leq 0.001$ versus 0 µM MG132; ++ $p \leq 0.01$, +++ $p \leq 0.001$ versus 0 mM NAC, two-way ANOVA followed by Bonferroni *post hoc* test.

NAC protects astrocytes independent of glutathione synthesis

As mentioned above, proteotoxic stress is often associated with oxidative stress. NAC is known to be a glutathione precursor and can also have direct antioxidant effects (Aruoma, Halliwell, Hoey, & Butler, 1989; E. Hoffer, Baum, Tabak, & Taitelman, 1996). Therefore, we sought to determine whether NAC protects astrocytes from MG132 toxicity through a glutathione-dependent mechanism. MG132 increased total glutathione levels in a concentration-dependent manner and NAC unexpectedly attenuated this effect (Fig 22A & B). These data suggest that NAC protects astrocytes in a glutathione-independent manner. In order to test this directly, we used the glutathione synthesis inhibitor BSO to decrease glutathione levels (Fig 22C &D). As outlined above, the In-Cell Western assay measures total glutathione levels, which include both the reduced and oxidized forms. The reduced form of glutathione is important for defense against oxidative stress. Thus, reduced glutathione levels were also measured in our model. MG132 significantly increased intracellular levels of reduced glutathione, and NAC attenuated the rise in glutathione in response to MG132, consistent with the abovementioned results of the In-Cell Western assay. Reduced glutathione levels were slightly increased in the presence of NAC in cells not exposed to MG132 (Fig 22E). No significant changes in reduced glutathione levels were observed in the extracellular space with the exception of a BSO-induced decrease in reduced glutathione in the NAC-treated group (Fig 22F). These results suggest that MG132 elicits a stress-induced increase in glutathione synthesis but that there may be less need for this compensatory stress response in the presence of NAC.

Next, we tested whether glutathione synthesis is essential for NAC-mediated protection against MG132 toxicity in astrocytes. Glutathione synthesis was inhibited by BSO and astrocyte viability was measured by counting the number of $Hoechst^{+}$ astrocytes. BSO did not abolish or even attenuate the protective effects of NAC (Fig 22G & H). These findings suggest that glutathione synthesis is not essential for NAC-mediated protection against MG132 toxicity.

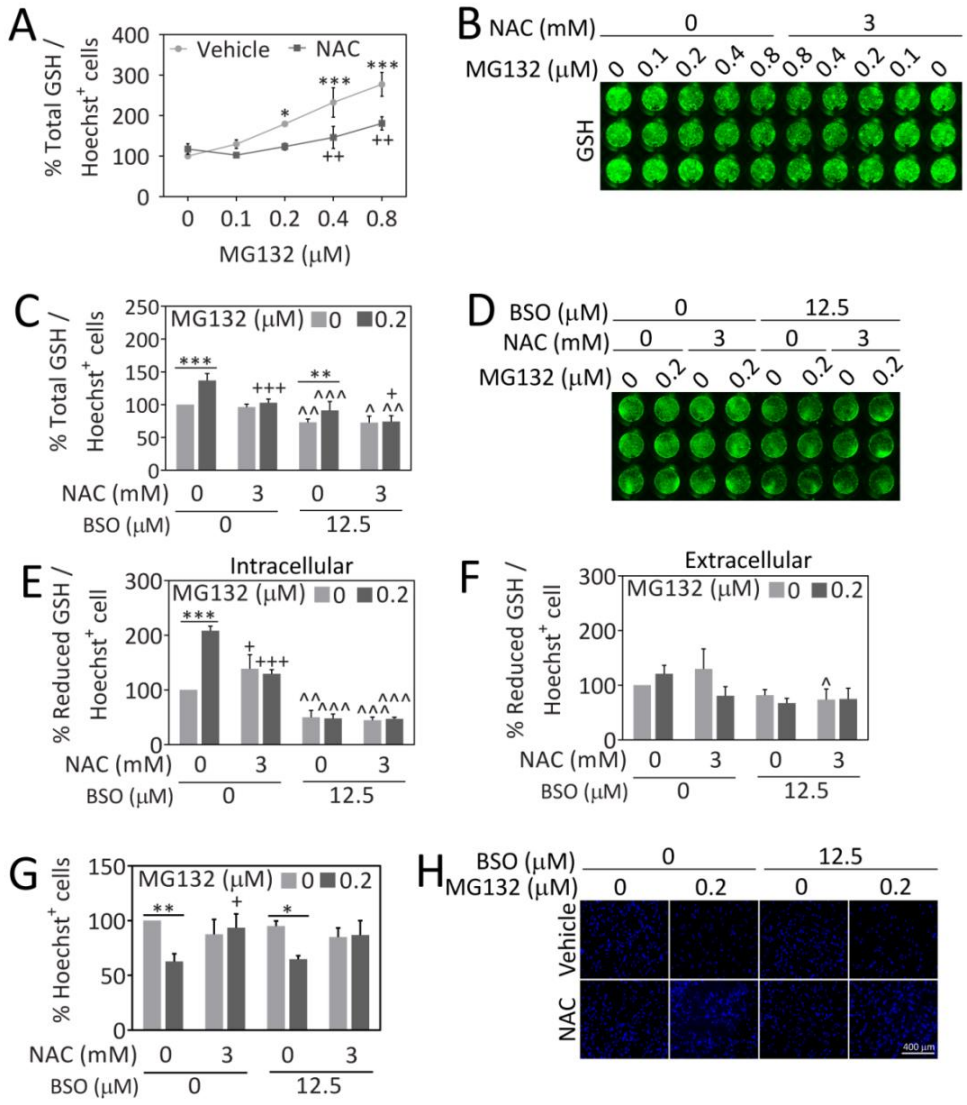

Figure 22. NAC protects astrocytes against MG132 independent of glutathione synthesis. Cortical astrocytes were treated with the indicated MG132 concentrations in the presence of NAC (3 mM) or the equivalent v/v of vehicle. **A)** Total glutathione levels were measured 48h later by the fluorescent In-Cell Western assay. Total glutathione levels are expressed as a function of the number of Hoechst$^+$ cell numbers. **B)** Representative total glutathione In-Cell Western image for data presented in panel A. **C)** Total glutathione levels as a function of the number of Hoechst$^+$ nuclei in the absence and presence of glutathione synthesis inhibitor, buthionine sulfoximine (BSO). **D)** Representative In-Cell Western image of total glutathione levels for data presented in panel C. Intracellular **(E)** and extracellular **(F)** reduced glutathione levels in the absence or presence of BSO were measured by the luminescent GSH-Glo assay**. G)** Blinded counts of the number of Hoechst$^+$ nuclei in the absence or presence of BSO. **H)** Representative images of Hoechst$^+$ nuclei for the data shown in panel G. Shown are the mean and SEM of 3-5 independent experiments. * $p \leq 0.05$, ** $p \leq 0.01$, *** $p \leq 0.001$ versus 0 μM MG132; + $p \leq 0.05$, ++ $p \leq 0.01$, +++ $p \leq 0.01$ versus 0 mM NAC; ^ $p \leq 0.05$, ^^ $p \leq 0.01$, ^^^ $p \leq 0.001$ versus 0 μM BSO, two- or three-way ANOVA followed by Bonferroni *post hoc* correction.

Cysteine thiols protect astrocytes against protein-misfolding stress

We had shown in Figure 22 that NAC did not protect against MG132 toxicity by increasing glutathione levels. In order to elucidate the mechanism underlying NAC-mediated glioprotection, the therapeutic potential of two cysteine isoforms was tested. Cysteine can exist in the L- or D- conformation, with L-cysteine being the biologically active form of cysteine that can be incorporated into glutathione whereas D-cysteine cannot be directly incorporated into glutathione (Corcoran & Wong, 1986). Both forms of cysteine contain a thiol group, which is known to attenuate oxidative stress (Requejo, Hurd, Costa, & Murphy, 2010). Figure 23 illustrates that both D- and L-cysteine (subpanels A & B and C & D, respectively) protect astrocytes against MG132 toxicity.

D-amino acids may be converted to L-amino acids by D-amino acid oxidase (Friedman & Levin, 2012; Sacchi, et al., 2008). Therefore, in order test whether D-cysteine was protective due to conversion to L-cysteine, D-amino acid oxidase was inhibited with sodium benzoate (Gong et al., 2011; Van den Berghe-Snorek & Stankovich, 1985). Sodium benzoate did not affect the protection against MG132 toxicity by D- and L-cysteine (Fig 23E-H). Therefore, we speculate that protection against MG132 toxicity by all three cysteines (NAC, L-cysteine, and D-cysteine) may occur through the thiol that they all have in common.

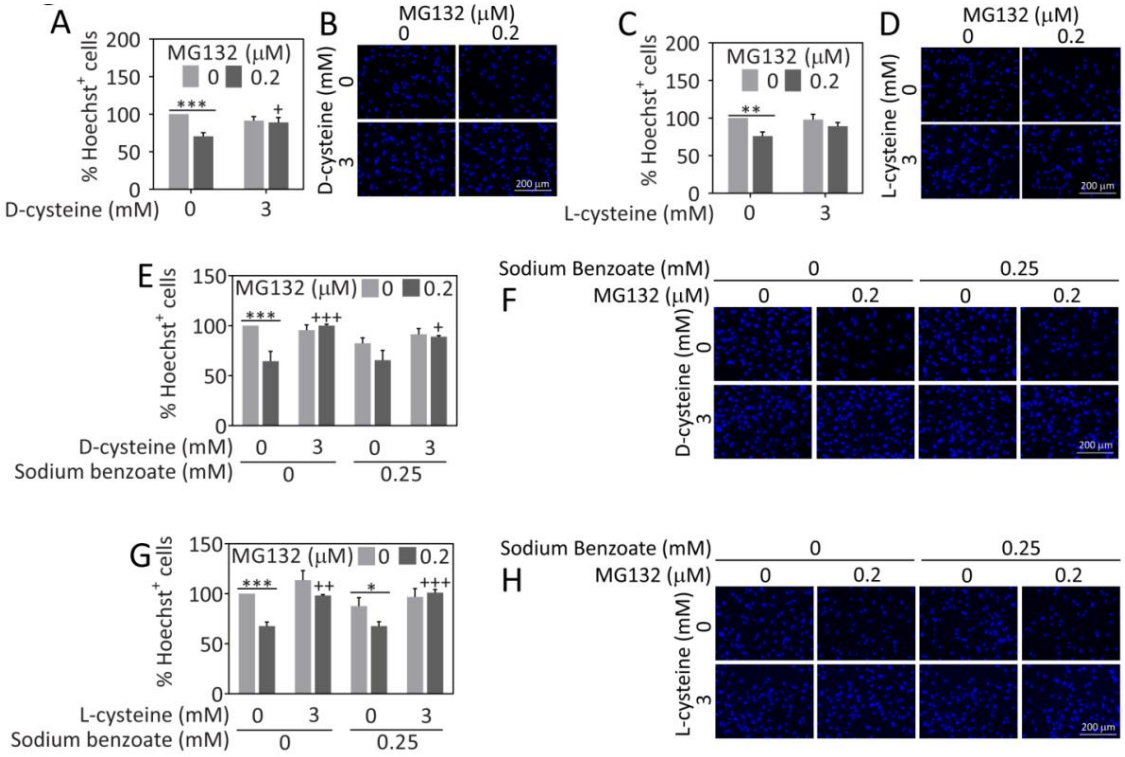

Figure 23. D-cysteine and L-cysteine protect astrocytes against MG132 toxicity. Cortical astrocytes were treated with MG132 or vehicle in the presence of D-cysteine (**A, B**) and L-cysteine (**C, D**) or vehicle. (**E-H**) Sodium benzoate was delivered in conjunction with D- and L-cysteine to inhibit the conversion of D- to L-cysteine by D-amino acid oxidase. Viability was measured 48h later by blinded counts of the number of Hoechst$^+$ nuclei. Representative images of Hoechst$^+$ nuclei are illustrated. Shown are the mean and SEM of 3-6 independent experiments. ** $p \leq 0.01$, *** $p \leq 0.001$ versus 0 μM MG132; + $p \leq 0.05$, ++ $p \leq 0.01$, +++ $p \leq 0.001$ vs 0 mM D-cysteine or L-cysteine, two- or three-way ANOVA followed by Bonferroni *post hoc* test.

NAC attenuates the stress-induced upregulation of several heat shock proteins

We previously showed that NAC protects neuroblastoma cells in a heat shock protein-dependent manner (Jiang, et al., 2013). Thus, here we examined heat shock proteins in MG132- and NAC-treated astrocytes. Proteotoxic stress elicited a significant increase in multiple heat shock proteins but NAC attenuated this effect, in contrast with the findings in neuroblastoma cells (Fig 24). Although NAC attenuated the rise in Hsp70 and HO1 under proteotoxic conditions, these heat shock proteins remain elevated relative to the 0 μM MG132 group in the presence of NAC (Fig 24A & C, respectively). Thus, these heat shock proteins may nevertheless contribute to the protective effects of NAC.

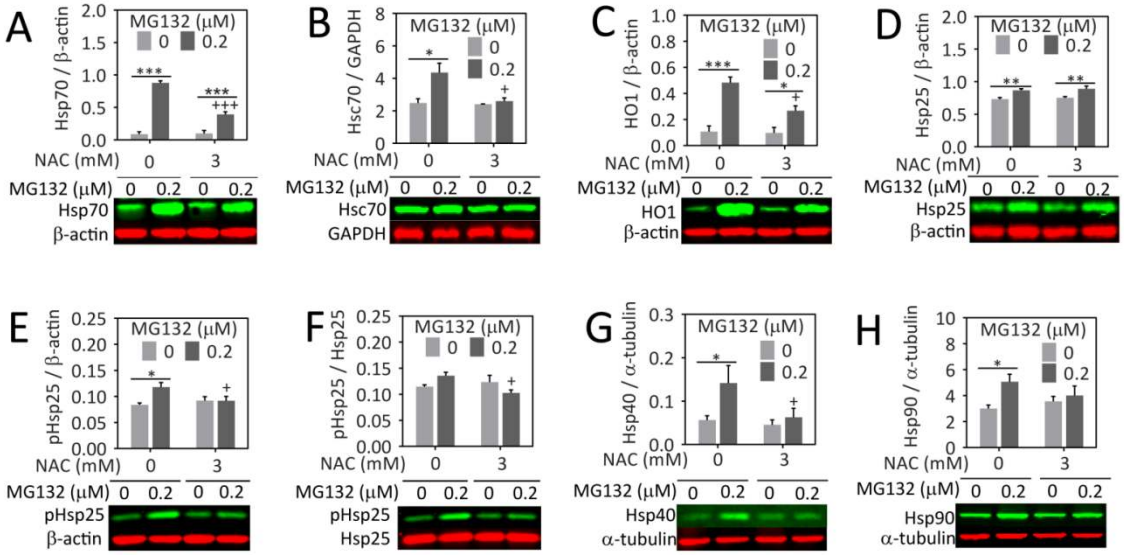

Figure 24. NAC attenuates the MG132-induced increase in heat shock proteins in astrocytes. Cortical astrocytes were treated with MG132 or vehicle in the presence or absence of NAC. Lysates were collected 24h later and heat shock proteins were measured by Western blot analysis. Representative Western blot images are included below each graph. **A)** Heat shock protein 70 (Hsp70), **B)** heat shock cognate 70 (Hsc70), **C)** heme oxygenase 1 (HO1 or heat shock protein 32), **D)** heat shock protein 25 (Hsp25), **E & F)** phosphorylated Hsp25, **G)** heat shock protein 40 (Hsp40), and **H)** heat shock protein 90 (Hsp90). Protein levels are expressed as a function of the loading controls β-actin, GAPDH or α-tubulin, depending upon the species of the antibody for the protein of interest and its MW. Shown are the mean and SEM of 3-5 independent experiments. * $p \leq 0.05$, ** $p \leq 0.01$, *** $p \leq 0.001$ versus 0 μM MG132; + $p \leq 0.05$, +++ $p \leq 0.01$ versus 0 mM NAC, two-way ANOVA followed by Bonferroni *post hoc* test.

Hsp70 and HO1 activity are essential for NAC-mediated protection of astrocytes against proteotoxicity

As mentioned above, Hsp70 is important for defending against proteotoxicity and is increased in response to proteasome inhibition by MG132. Geldanamycin is an Hsp90 inhibitor and is known to increase Hsp70 levels as a result of Hsp90 inhibition (McLean, Klucken, Shin, & Hyman, 2004; Shen, He, Wang, Huang, & Chen, 2005). Thus we tested the hypothesis that geldanamycin protects astrocytes against MG132 toxicity as proof of principle. As expected, we found that geldanamycin abolished MG132 toxicity in astrocytes (Fig 25A & B).

In Figure 24, we had shown that NAC attenuated the MG132-induced rise in Hsp70. However, Hsp70 levels were still significantly higher in the MG132-treated group in the presence of NAC relative to cells not exposed to MG132, suggesting that Hsp70 may still contribute to the protective effects of NAC. Therefore, we next tested the hypothesis that Hsp70 inhibitors would abolish the protective effects of NAC. Consistent with this hypothesis, the protective effects of NAC were attenuated by three independent Hsp70 pharmacological inhibitors with unique mechanisms of action: VER155008 (Fig 26A-C), pifithrin-μ (Fig 26D-F), and MAL3-101 (Fig 26G & H). These findings strongly suggest that Hsp70 activity may be an important factor in the protective effects of NAC. Inhibition of Hsp70 by itself did not increase the susceptibility of astrocytes to MG132 in the absence of NAC. Therefore, it is possible that other heat shock proteins compensate for Hsp70 inhibition in this group and prevent any additional decrease in viability with MG132.

We previously observed that NAC elicited a trend towards an increase in HO1 in MG132-treated neuroblastoma cells (Jiang, et al., 2013). Thus, here we tested the hypothesis that inhibition of HO1 would also attenuate NAC-mediated protection. Consistent with this hypothesis, inhibition of HO1 activity by SnPPx attenuated the protective effects of NAC in astrocytes (Fig 27A & B). Therefore, heat shock protein activity (Hsp32 or HO1 and Hsp70) appears to contribute to the NAC-mediated protection against MG132 toxicity (Fig 26 & 27).

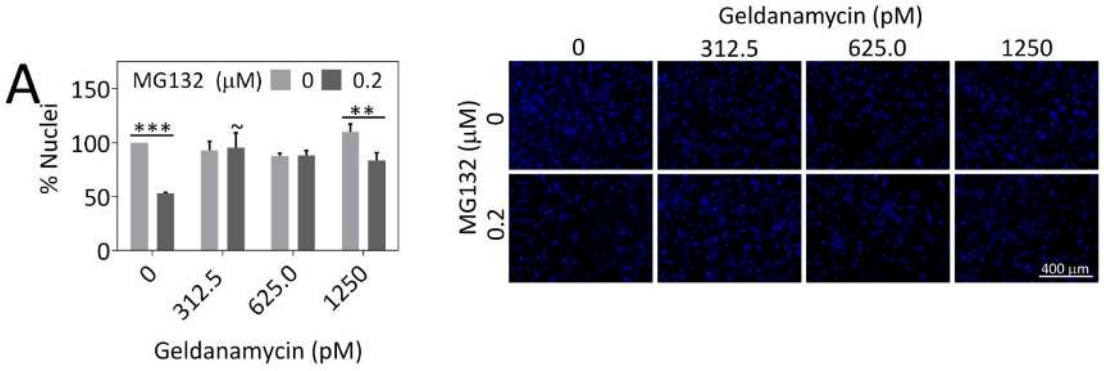

Figure 25. Geldanamycin protects against MG132 toxicity in astrocytes Cortical astrocytes were treated with 0.2 μM MG132 and geldanamycin (312.5, 625, 1250 pM). **A)** Astrocyte viability was determined by blinded counts of Hoechst$^+$ nuclei **B)** Representative image of Hoechst-stained nuclei. ** $p \leq 0.01$, *** $p \leq 0.001$ versus 0 μM MG132; ~ $p \leq 0.05$vs 0 pM geldanamycin two-way ANOVA followed by Bonferroni *post hoc* test.

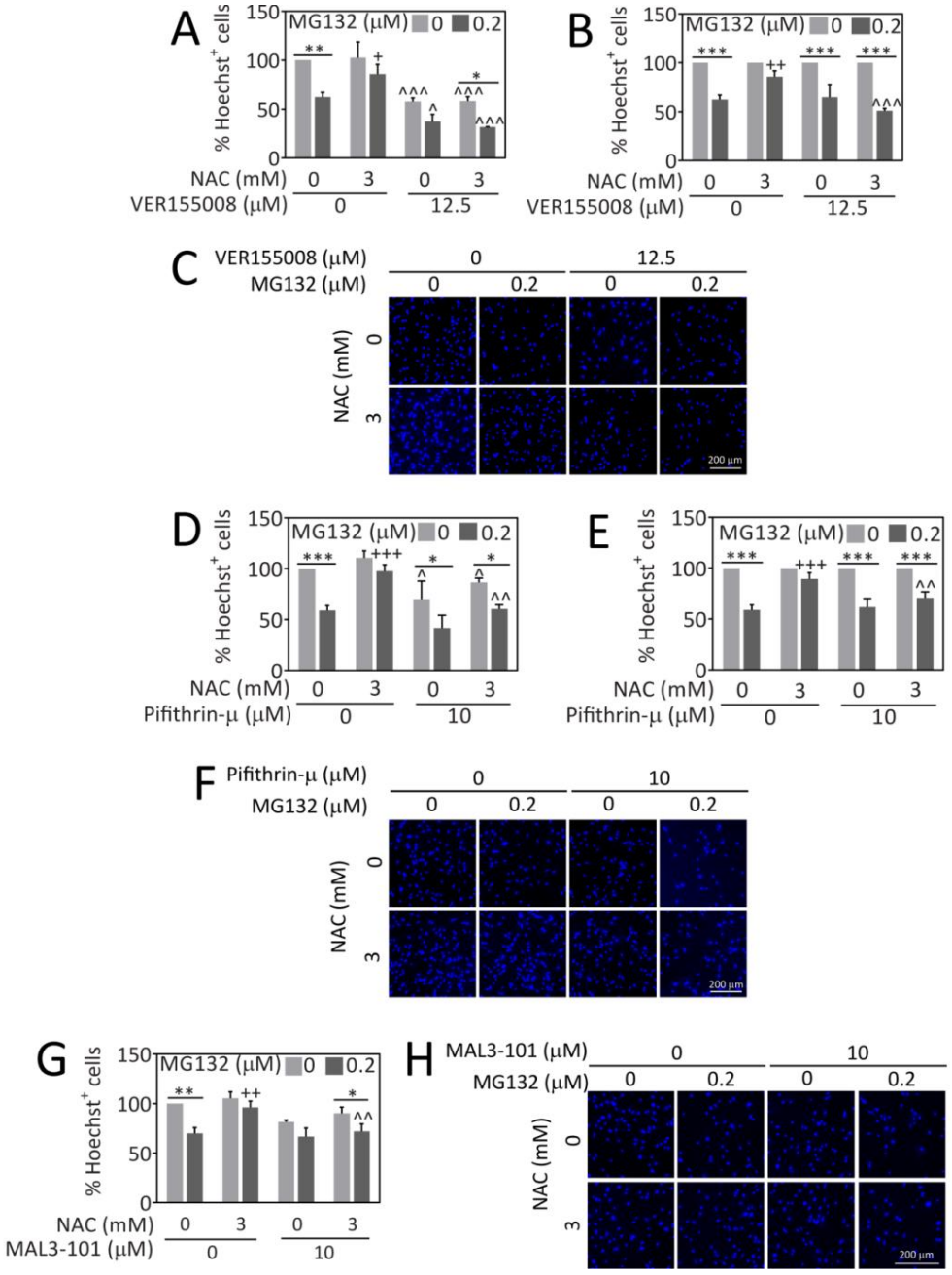

Figure 26. Loss of Hsp70/Hsc70 activity abolishes NAC-mediated protection in astrocytes. Cortical astrocytes were treated with MG132 or vehicle in the presence or absence of NAC and the Hsp70/Hsc70 inhibitors VER155008 (**A-C**), pifithrin-μ or PES (**D-F**), and MAL3-101 (**G-H**). Cell viability was measured by blinded counts of Hoechst-stained nuclei. VER155008 and pifithrin-μ led to loss of basal viability. Thus, data in panels A and D were expressed as a percentage of the 0 μM MG132 group in panels B and E to account for the basal viability loss. Representative images of Hoechst$^+$ nuclei are illustrated in C, F, and H. Shown are the mean and SEM of 3-5 independent experiments. * $p \leq 0.05$, ** $p \leq 0.01$, *** $p \leq 0.001$ versus 0 μM MG132; + $p \leq 0.05$, ++ $p \leq 0.01$, +++ $p \leq 0.001$ versus 0 mM NAC; ^ $p \leq 0.05$, ^^ $p \leq 0.01$, ^^^ $p \leq 0.001$ versus 0 μM VER155008, pifithrin-μ, or MAL3-101, three-way ANOVA followed by Bonferroni *post hoc* correction.

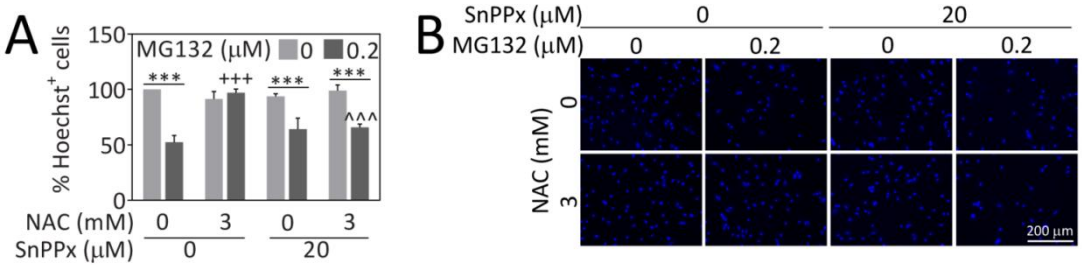

Figure 27. Inhibition of HO1 activity attenuates protective effects of NAC Cortical astrocytes were treated with the indicated concentration of MG132 in the absence and presence of NAC and HO1 inhibitor tin protoporphoryrin (SnPPx). **A)** The relative number of viable astrocytes was determined by blinded counts of Hoechst$^+$ nuclei. **B)** Representative images of Hoechst-stained nuclei. *** $p \leq 0.001$ versus 0 μM MG132; +++ $p \leq 0.001$ versus 0 mM NAC; ^^^ $p \leq 0.001$ versus 0 μM SnPPx three-way ANOVA followed by Bonferroni *post hoc* correction.

NAC attenuates protein-misfolding stress after MG132 treatment

As NAC reduced the toxicity of MG132, we tested the hypothesis that it would also reduce the increase in ubiquitinated proteins normally seen with proteasome inhibitors. Consistent with this hypothesis, NAC abolished the dramatic rise in ubiquitinated proteins in response to MG132 treatment, suggesting that proteotoxicity was robustly attenuated by NAC (Fig 28A). Previous studies by our group have shown that NAC does not reverse MG132-mediated inhibition of proteasome activity in neuroblastoma cells (Jiang, et al., 2013). Those studies suggest that NAC does not reduce the extent of the original insult, but protects cells downstream from the proteasome. Consistent with this notion, NAC did not alter the levels of the proteasomal subunits PA28α and PA700 (42 & 46 kDa subunits) in our model (Fig 25B-D). These findings support the view that the protective effects of NAC are not related to direct alterations in the ubiquitin proteasome system but help mitigate the downstream toxic effects of the proteasome inhibtors.

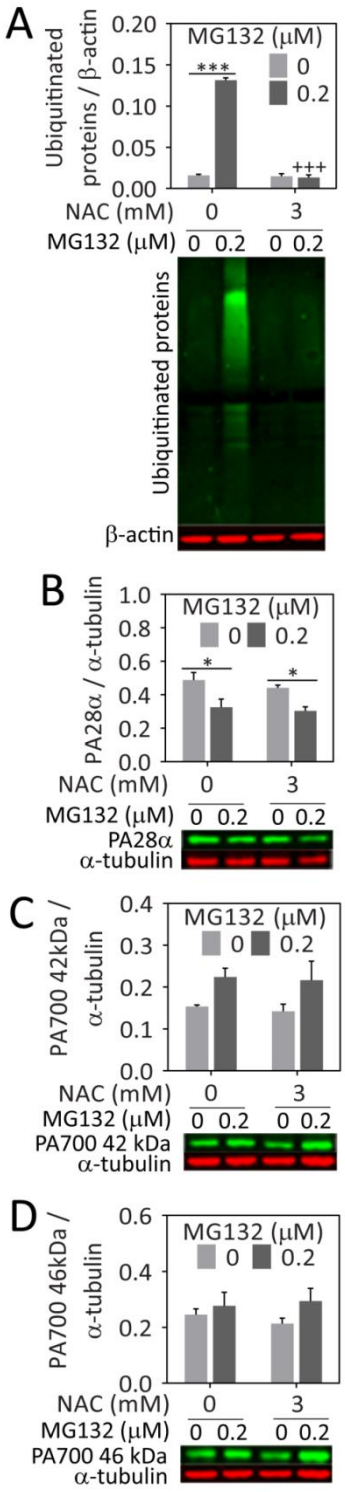

Figure 28. NAC decreases ubiquitinated proteins in astrocytes after MG132 treatment. Cortical astrocytes were treated with MG132 or vehicle. Lysates were collected 24h later and Western blots were performed. Representative images are shown adjacent to the quantification. **A)** Ubiquitinated proteins, **B)** PA28α, **C)** PA700 42 kDa subunit, and **D)** PA700 46 kDa subunit. All proteins are expressed as a fraction of β-actin or α-tubulin levels. Infrared images were pseudocolored green and red. Shown are the mean and SEM of 3 independent experiments. * $p \leq 0.05$, *** $p \leq 0.001$ versus 0 μM MG132; +++ $p \leq 0.001$ versus 0 mM NAC, two-way ANOVA followed by Bonferroni *post hoc* test.

3.3 Impact of aging on heat shock proteins in the female rat

Aging is the best known risk factor for the development of neurodegenerative diseases (Lindsay et al., 2002; Van Den Eeden, et al., 2003). Protein misfolding and oxidative stress are thought to accumulate with advancing age (Alavez, Vantipalli, Zucker, Klang, & Lithgow, 2011; Attems, Walker, & Jellinger, 2014; Cuanalo-Contreras, Mukherjee, & Soto, 2013; David et al., 2010; Driver, Kodavanti, & Mundy, 2000; Mecocci et al., 1993; Muller, Lustgarten, Jang, Richardson, & Van Remmen, 2007). Therefore, aging may contribute to the pathology associated with neurodegeneration. Some heat shock protein defenses are upregulated in neurodegenerative diseases (Schipper, et al., 2006; Schipper, et al., 1998; Uryu et al., 2006; Y. Zhang, James, Middleton, & Davis, 2005). The effect of aging on several heat shock proteins has mostly been measured in male animals (V. Calabrese, et al., 2004; Gupte, et al., 2010; Unno, et al., 2000). However, women have a higher incidence of Alzheimer's disease than men (Fratiglioni, et al., 1997) and a lower incidence of Parkinson's disease (Van Den Eeden, et al., 2003), suggesting that there are sex-related differences in vulnerability to proteotoxicity. Therefore, an examination of heat shock protein changes in aging females is warranted. In the following studies, we used female animals for an extensive examination of various heat shock proteins as a function of age, including those heat shock proteins highly expressed in astrocytes. Heat shock proteins were examined in brain regions known to exhibit pathology in neurodegenerative diseases, such as the substantia nigra, striatum and olfactory bulb. We hypothesized that age-related stress would be associated with an increase in heat shock proteins, based on previous work in

other brain regions (V. Calabrese, et al., 2004; Di Domenico et al., 2010; Dickey, et al., 2009; Schipper, et al., 2006).

Aging elicits distinct patterns of heat shock protein changes that vary depending upon protein type and brain region

A significant increase in Hsp25 was observed in both the striatum and substantia nigra from young to old age (Fig 29a and 30a). For example, the oldest animals (19-22 mo) showed significantly higher Hsp25 levels in the striatum than the youngest animals (2-4 mo). Similarly, 19-22 mo old animals expressed higher Hsp25 levels in the substantia nigra than 2-4 mo old animals as well as 4-6 mo old animals. Hsp25 levels were also higher in the substantia nigra in 19-22 and 16-19 mo old animals than 8-9 mo old animals. Hsp25 was elevated in the olfactory bulb after 4 months of age relative to the 2-4 month old animals (Fig 32A).

Next we measured Hsp60 and Hsp70 levels as a function of age. In the striatum, 19-22 mo old animals expressed higher Hsp60 protein levels than 2-4, 8-9, and 16-19 mo old animals (Fig 29e). Middle (8-9 mo) and old (19-22 mo) animals exhibited higher Hsp70 levels in the olfactory bulb compared to the youngest animals (2-4 mo) (Fig 32C). These findings support the hypothesis that age-related stress increases some heat shock protein defenses in a compensatory fashion.

Proteins tagged specifically for proteasome degradation contain ubiquitin that is linked through lysine 48 (K48-linked ubiquitin) (Sadowski & Sarcevic, 2010). In the striatum, K48-linked ubiquitin was increased from 4-6 mo of age to 16-19 mo of age (Fig 29j). These findings are consistent with the view that there is an age-related decline in the efficiency of the ubiquitin proteasome system.

In our model, some heat shock proteins exhibited a biphasic response to aging, in that there was a rise in heat shock proteins that was reversed with increasing age. For example, in the striatum, HO1 protein levels were higher in 8-9 mo old animals relative to 2-4 mo old animals (Fig 29b). However, HO1 levels were then decreased in the 16-19 and 19-22 mo old animals. A biphasic effect was also observed in Hsp60 levels in the substantia nigra (Fig 30e) and Hsp40 levels in the striatum (Fig 29c). Middle-aged (8-9 mo) animals preserved GRP78 expression, whereas 4-6 and 16-22 mo old animals exhibited lower GRP78 levels. The increase in heat shock protein defenses in middle-aged animals may reverse early signs of proteotoxicity but these responses appear to fail in the oldest groups.

Some heat shock protein defenses were also observed to decrease with advancing age. For example, Hsc70 was decreased in old age in the striatum and olfactory bulb (Fig 29f and 32D). Further, HO1 protein levels were decreased from 2-4 to 16-19 months of age in the substantia nigra (Fig 30b). The co-chaperone Hip was lower in 4-6 and 19-22 month old animals relative to young 2-4 month old animals (Fig 29d). The decrease in Hip observed in 4-6 month old animals may be related to developmental changes whereas lower Hip levels in the oldest animals may be suggestive of age-related declines in some co-chaperone defenses.

Some heat shock proteins were not affected by aging in the striatum, substantia nigra, and olfactory bulb. For example, striatal levels of GRP78, pan-ubiquitinated proteins, and Hsp90 remained unaffected (Figure 29). No significant changes in GRP78, pan-ubiquitinated proteins, Hsp90, Hsp40, Hip, Hsc70, and K48-linked ubiquitin were observed in the substantia nigra (Figure 30). Furthermore, CHIP, HO1, Hsp90, Hip, Hop,

Hsp60, and mitochondrial Hsp70 (mtHsp70) were not significantly altered by aging in the olfactory bulb (Fig 33), Therefore, several heat shock proteins are not upregulated with aging and may require higher levels of proteotoxic stress before a response is elicited.

As Hsp25 was shown to be higher with aging in both the substantia nigra and striatum, we suspected that Hsp25 may be present in the dopaminergic neurons that comprise the nigrostriatal pathway. As expected, a confocal analysis revealed that Hsp25 colocalized with tyrosine hydroxylase staining in young, female rats (Fig 31a-c). Tyrosine hydroxylase is the rate limiting enzyme for dopamine synthesis and can be used as a marker for dopaminergic nigral neurons (Pickel, Joh, Field, Becker, & Reis, 1975). Our findings therefore, suggest that Hsp25 is expressed in dopaminergic neurons. Not surprisingly, Hsp25 was also expressed in cells lacking tyrosine hydroxylase staining, as this protein is known to be ubiquitous and expressed heavily in glia. Age-related increases in Hsp25 in the midbrain may help mitigate age-related proteotoxicity in dopaminergic neurons as well as other cell types such as astrocytes. Other heat shock proteins (HO1 and Hsp60) were also examined using dual-immunofluorescence. However, levels of HO1 and Hsp60 in the substantia nigra were below the limits of immunohistochemical detection. In order avoid false positive conclusions from antibody cross-reactivity, multiple control experiments were conducted. First, tissue sections were incubated with one primary antibody (Hsp25 or tyrosine hydroxylase) only, followed by exposure to both secondary antibodies. For example, Figure 31d-f illustrates nigral staining with mouse antibodies raised against tyrosine hydroxylase antibodies followed by exposure to secondary antibodies raised against both mouse and rabbit IgG molecules.

The lack of staining in the red channel shows that the anti-rabbit secondary antibodies are not cross-reacting inappropriately with the mouse primary antibodies, as we have on occasion observed for various secondary antibodies. The lack of signal in the red channel also shows clearly that the green tyrosine hydroxylase signal is not bleeding through to the red channel during the microscopy. Second, we also ensured that signal was lost when the tissue was incubated in no primary antibodies followed by both secondary antibodies.

In summary, some heat shock proteins were increased with aging in female animals as was originally hypothesized. However, reductions and biphasic changes in heat shock protein changes were also observed. The changes were highly dependent upon the brain region examined, which is not surprising given the heterogeneity of the central nervous system

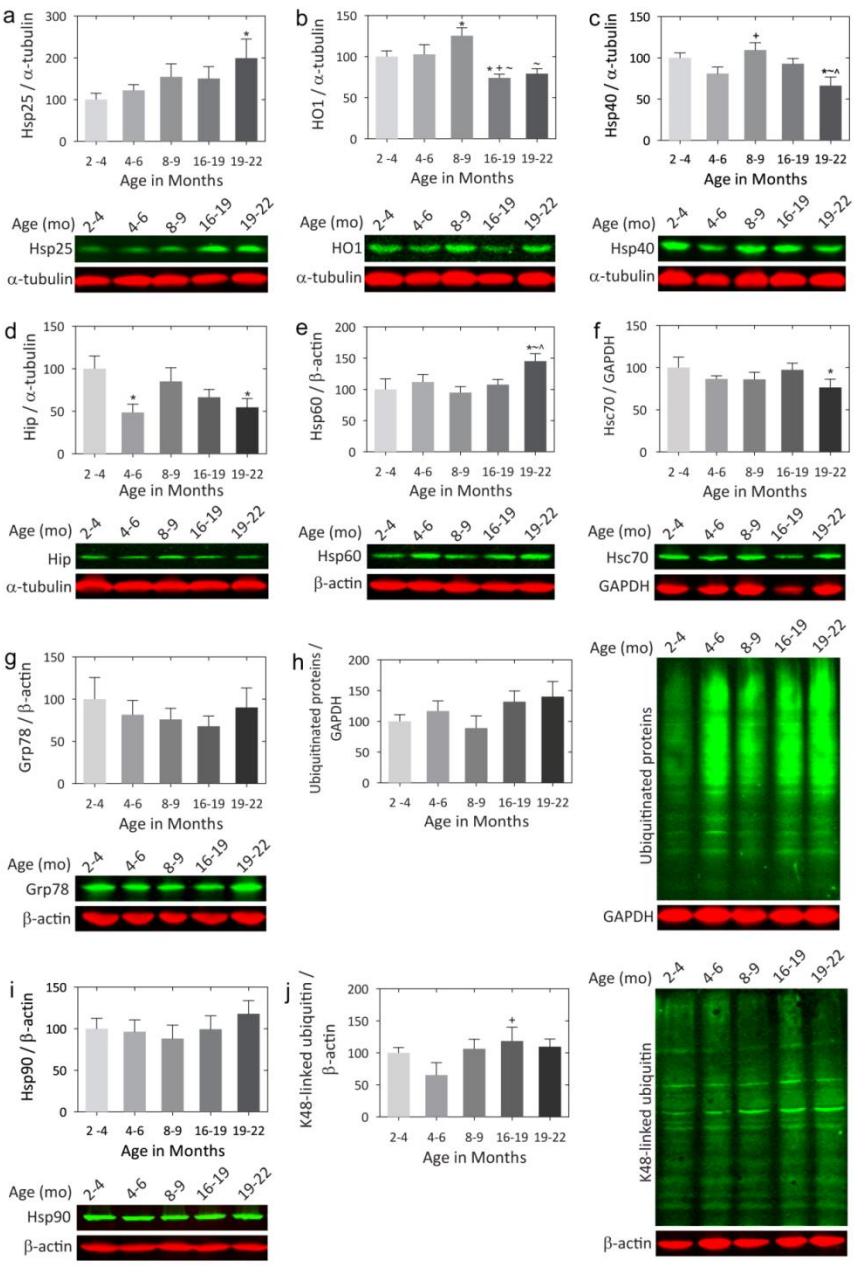

Figure 29. Impact of aging on heat shock proteins and ubiquitin-conjugated proteins in the striatum (caudoputamen). Whole tissue lysates of striatal tissue from female Sprague-Dawley rats were probed by Western blots for the indicated proteins. GAPDH, α-tubulin, or β-actin was used as a protein loading control. * $p \leq 0.05$ versus 2-4 month old, + $p \leq 0.05$ versus 4-6 month old, ~ $p \leq 0.05$ versus 8-9 month old, ^ $p \leq 0.05$ versus 16-19 month old. Reprinted from "Impact of aging on heat shock protein expression in the substantia nigra and striatum of the female rat," by A. M. Gleixner, 2014, *Cell Tissue Research, 357*, 43-54. Copyright [2014] by A.M Gleixner. Reprinted with permission.

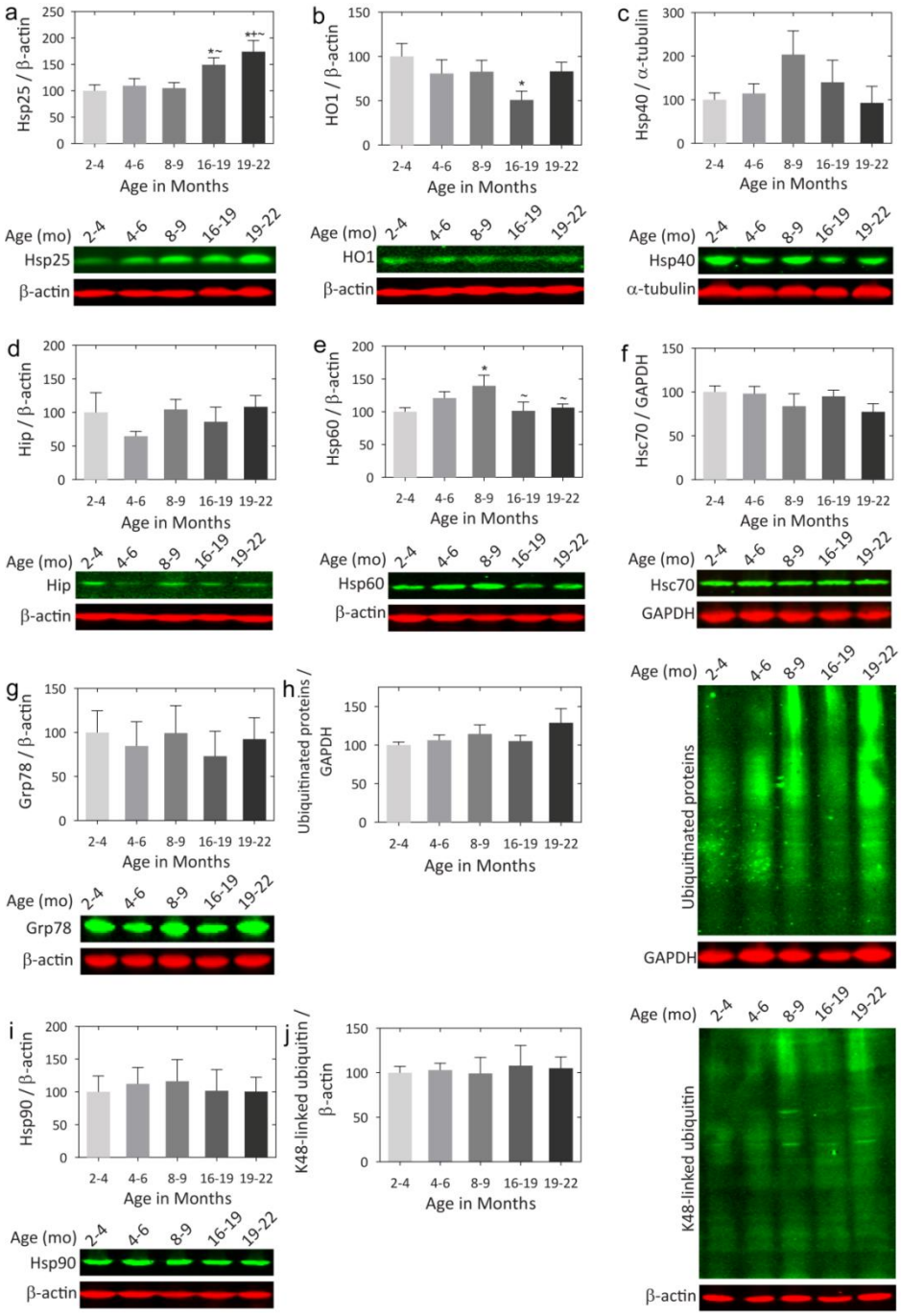

Figure 30. Impact of aging on heat shock proteins and ubiquitin-conjugated proteins in the substantia nigra. Whole tissue lysates of substantia nigra tissue from female Sprague-Dawley rats were probed by Western blots for the indicated proteins. GAPDH, α-tubulin, or β-actin was used as a protein loading control. * $p \leq 0.05$ versus 2-4 month old, + $p \leq 0.05$ versus 4-6 month old, ~ $p \leq 0.05$ versus 8-9 month old, ^ $p \leq 0.05$ versus 16-19 month old. Reprinted from "Impact of aging on heat shock protein expression in the substantia nigra and striatum of the female rat," by A. M. Gleixner, 2014, *Cell Tissue Research, 357*, 43-54. Copyright [2014] by A.M Gleixner. Reprinted with permission.

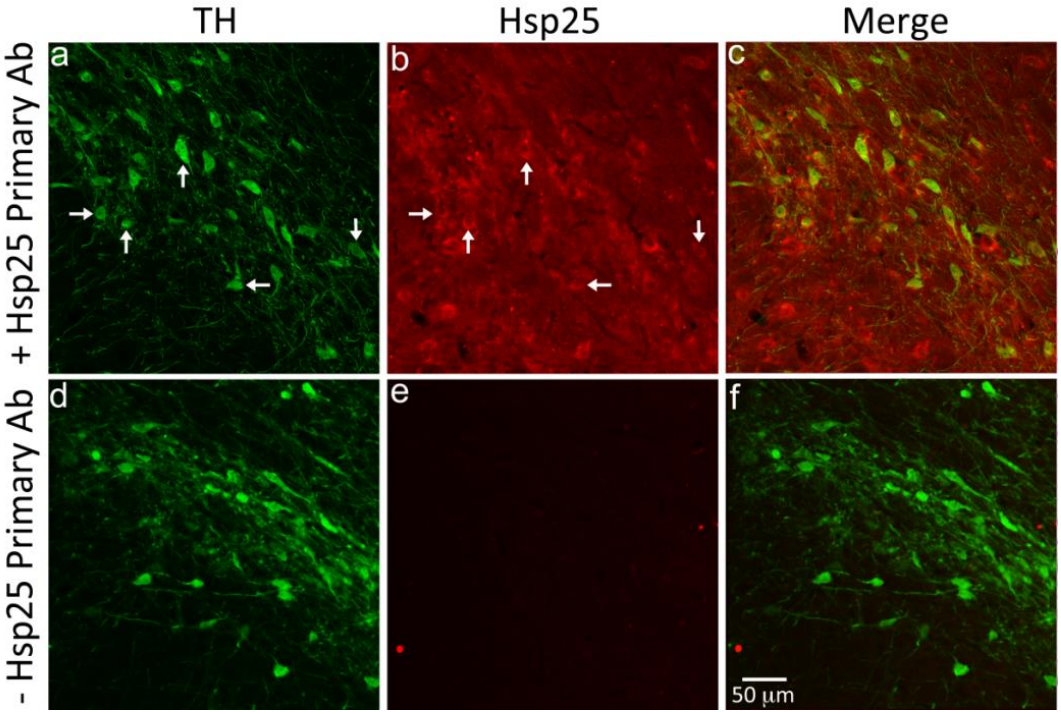

Figure 31. Hsp25 expression in the substantia nigra. Confocal analysis of Hsp25 (red) and TH (green) immunostaining in the substantia nigra, pars compacta of a young female rat (**top panels**). Examples of dual-labeled neurons are indicated by white arrows. The dual-labeled neurons do not appear yellow in the merged image on the right because the Hsp25 signal was weak and the images are not overly manipulated. The **bottom panels** show an adjacent midbrain section that was only incubated in primary antibodies against TH, followed by exposure to the same secondary antibody solutions as in the top panels. Reprinted from "Impact of aging on heat shock protein expression in the substantia nigra and striatum of the female rat," by A. M. Gleixner, 2014, *Cell Tissue Research, 357*, 43-54. Copyright [2014] by A.M Gleixner. Reprinted with permission.

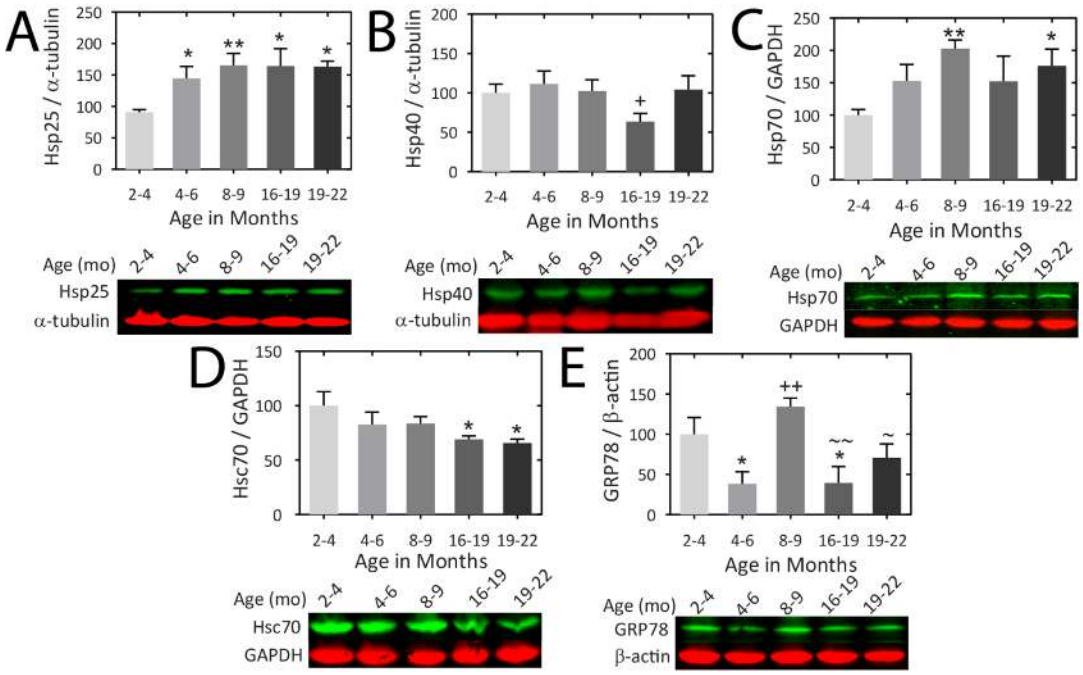

Figure 32. Impact of aging on Hsps and co-chaperones in the olfactory bulb of the female rat. (**A-E**) Infrared Western immunoblots are shown for the indicated Hsps and co-chaperones. Olfactory bulb tissue was harvested from female rats at 2.0-3.9 months, 4.0-6.0 months, 8.0-9.0 months, 16.0-18.9 months, and 19.0-22.0 months of age. GAPDH, α-tubulin, or β-actin was used as a protein loading control, depending on the species of the primary antibodies and the expected molecular weights. n = 3-6 rats per group. * $p \leq 0.05$, ** $p \leq 0.01$, versus 2-4 month old, + $p \leq 0.05$, ++ $p \leq 0.01$ versus 4-6 month old, ~ $p \leq 0.05$, ~~ $p \leq 0.01$ versus 8-9 month old, LSD *post hoc* following one-way ANOVA. Reprinted from "Heat shock protein responses to aging and proteotoxicity in the olfactory bulb," by T.S. Crum, 2014, *Journal of Neurochemistry, 133*, 780-794. Copyright [2014] by T.S.Crum. Reprinted with permission.

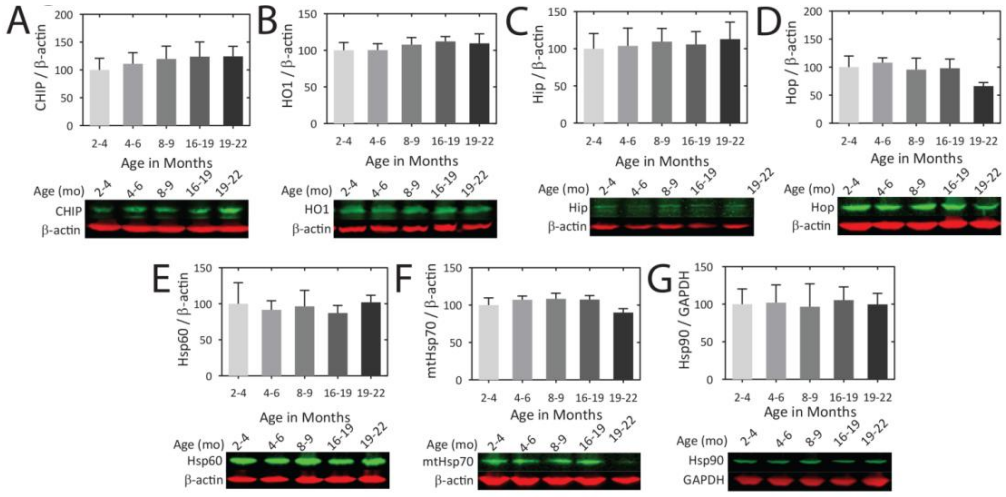

Figure 33. Impact of aging on Hsps and co-chaperones in the olfactory bulb of the female rat. (**A-G**) Infrared Western immunoblots are shown for the indicated Hsps and co-chaperones. Olfactory bulb tissue was harvested from female rats at 2.0-3.9 months, 4.0-6.0 months, 8.0-9.0 months, 16.0-18.9 months, and 19.0-22.0 months of age. GAPDH, α-tubulin, or β-actin was used as a protein loading control, depending on the species of the primary antibody and the expected molecular weight. n = 3-6 rats per group. * $p \leq 0.05$, ** $p \leq 0.01$, versus 2-4 month old, + $p \leq 0.05$, ++ $p \leq 0.01$ versus 4-6 month old, ~ $p \leq 0.05$, ~~ $p \leq 0.01$ versus 8-9 month old, LSD *post hoc* following one-way ANOVA. Reprinted from "Heat shock protein responses to aging and proteotoxicity in the olfactory bulb," by T.S. Crum, 2014, *Journal of Neurochemistry, 133*, 780-794. Copyright [2014] by T.S.Crum. Reprinted with permission.

Chapter 4 Discussion

4.1 Exposure to severe proteotoxic stress elicits tolerance in surviving astrocytes

Protein misfolding stress, or proteotoxicity, is known to affect both neurons and glia in many neurodegenerative disorders, as evidenced by the appearance of protein aggregates in both cell types (Braak et al., 2003; Braak, et al., 2007). Further evidence of proteotoxicity in these conditions lies in the loss of protein quality control systems, such as inhibition of proteasome activity (Cook & Petrucelli, 2009; Q. Huang & Figueiredo-Pereira, 2010). However, the impact of proteotoxicity on glial cells is less well defined than on neurons. Astrocytes are known to harbor misfolded proteins in both Parkinson's and Alzheimer's disease and to exhibit signs of activation without loss of cell numbers (Korolainen, Auriola, Nyman, Alafuzoff, & Pirttila, 2005; Mythri, et al., 2011; Panter, McSwigan, Sheppard, Emory, & Frey, 1985; Schultz, Hubbard, Rub, Braak, & Braak, 2000). These observations suggest that astrocytes are less vulnerable to proteotoxicity in these conditions than neurons. If stressed astrocytes can continue to protect and support neurons, the onset and progression of neurodegenerative disorders may be delayed. Indeed, the slow and protracted nature of these conditions may be explained by both neuronal and glial defense mechanisms that are activated by proteotoxic stress, such as those examined in the present series of investigations.

It is well established that astrocytes can adapt to subtoxic levels of cellular stress, a phenomenon known as preconditioning or tolerance (Pang, et al., 2015; Sen, et al., 2011). For example, many studies have examined astrocytic adaptions to cellular stress at levels that do not elicit any cell death (Chu, Beart, & Jones, 2010; Gao et al., 2014; Rajapakse, Kis, Horiguchi, Snipes, & Busija, 2003). Even though astrocytes are known

for their ability to adapt to a subtoxic, fluctuating environment, astrocytic adaptations to severe cellular stressors are less well understood (Shao & McCarthy, 1994). Therefore, we examined astrocytic responses to severe stress, or stress that is lethal to some fraction of the cellular population under study. We tested the hypothesis that exposure to severe proteotoxicity would render astrocytes less susceptible to subsequent insults. Although astrocytes are not reduced in numbers in neurodegenerative disorders, it was essential to significantly decrease astrocyte viability in our studies in order to answer this question. We therefore applied lethal concentrations of proteasome inhibitors such as MG132 and lactacystin and discovered that cells that managed to survive the first toxic exposure exhibited no additional cell death in response to the second exposure to the same toxin. These findings demonstrate that severely stressed astrocytes are not necessarily weakened. On the contrary, those that survive are more resistant than naïve cells to toxic challenges. This is the first study to reveal that astrocytes can adapt to proteotoxic stress at concentrations that are high enough to kill a significant population of cells. In contrast to these adaptive glial responses, many studies have shown that neurons are weakened by exposure to high levels of stress, a phenomenon referred to as the dual hit hypothesis of neurodegeneration (Boger, et al., 2010; Sulzer, 2007; Unnithan, et al., 2012; Zhu, et al., 2007).

Next we sought to determine the mechanism underlying the protective effects of severe stress in astrocytes. For these studies we focused on heat shock proteins and glutathione, because heat shock proteins are elevated in astrocytes in Parkinson's disease while glutathione defenses are increased in resistant brain regions such as the frontal cortex in this condition (Braak, Del Tredici, Sandmann-Kiel, Rub, & Schultz, 2001;

Mythri, et al., 2011; Schipper, et al., 1998). Therefore, we hypothesized that the first hit would upregulate heat shock protein and glutathione defenses. As expected, severely stressed astrocytes exhibited higher levels of glutathione defenses and several heat shock proteins 24h after the first hit (Fig 13 and 14). Similarly, both types of molecules were upregulated 24h after the second hit. In order to test whether heat shock protein and glutathione defenses mediated the protective effects induced by severe stress, we used the pharmacological inhibitors VER155008, SnPPx, and BSO to inhibit Hsp70, Hsp32 (HO1), and glutathione, respectively. We observed that inhibition of glutathione but not Hsp70 or HO1 completely abolished astrocyte stress tolerance (Fig 14 and 17). These findings are consistent with the observation that astrocytes are one of the major sources of glutathione in the brain (Makar, et al., 1994; Slivka, et al., 1987) and that glutathione levels are upregulated in stressed astrocytes in neurodegenerative conditions (Mythri, et al., 2011). Although one study demonstrated that heat shock protein 70 can increase glutathione redox cycling (Guo, et al., 2007), we did not gather evidence that loss of Hsp70 activity altered the ability of stressed astrocytes to resist subsequent proteotoxic insults or that it negatively affected glutathione defenses (Fig 14). Instead, there was a dramatic increase in glutathione levels in astrocytes treated with VER155008, which may help explain why this compound failed to abolish stress resistance in this model. It remains possible that the activity of Hsp70 and HO1 was insufficiently blocked, although the reduction in basal survival with the inhibitors does not support this view. We were unable to verify the efficacy of VER155008, as the assays for Hsp70 ATPase activity are only specific when using pure recombinant Hsp70 and not when examining cellular lysates containing multiple types of ATPases other than Hsp70. HO1 activity can be

measured in cellular samples because of its unique conversion of toxic heme to bilirubin (Drummond & Kappas, 1981; Yoshinaga, et al., 1982). Preliminary data showed that the HO1 inhibitor SnPPx decreased enzymatic activity as expected. Another possibility for the negative findings with Hsp70 and HO1 inhibitors is compensatory upregulation of other heat shock proteins. For example, preliminary data in our lab has shown that Hsp90 and HO1 levels are elevated in the presence of VER155008.

As mentioned earlier, glutathione levels are preserved in astrocytes in brain regions highly susceptible to Parkinson's disease (Damier, et al., 1993; Mythri, et al., 2011). Furthermore, patients with the disease exhibit higher glutathione levels in resilient brain regions in comparison to control individuals. Similarly, we observed a stress-induced increase in glutathione levels that contributed significantly to astrocyte resistance. Elimination of xenobiotics by glutathione in the presence of glutathione S-transferase may also contribute to astrocyte stress tolerance. As mentioned above, glutathione S-transferases are enzymes that vary by their N-terminal domain amino acid sequence (Mazzetti, et al., 2015). Both glutathione S-transferase μ and π are expressed in astrocytes. The 1st MG132 hit increased glutathione S-transferase μ but not glutathione S-transferase π levels in astrocytes (Fig 14). The absence of glutathione S-transferase μ is associated with an earlier age of onset of Parkinson's disease (Ahmadi et al., 2000). Furthermore, glutathione S-transferase μ null genotypes have been associated with a higher incidence of Alzheimer's disease (Piacentini et al., 2012). We also observed a stress-induced increase in glutamate cysteine ligase, which plays a role in glutathione synthesis. Taken together, these findings suggest that glutathione defenses are essential for the protection of astrocytes from severe proteotoxic stress and that the absence of

glutathione defenses may increase the likelihood of developing neurodegenerative diseases.

In the present study, we measured viability by performing blinded cell counts of Hoechst-stained nuclei and measuring ATP levels. ATP levels are not always in proportion to cell numbers and are therefore only interpreted as an indicator of metabolic fitness (Posimo, et al., 2014; Titler, et al., 2013). We were unable to use In-Cell Western assays for the astrocytic marker GFAP as a third viability assay, because stressed astrocytes are known to upregulate GFAP expression (Posimo, et al., 2014; Titler, et al., 2013). One potential caveat of relying on the Hoechst assay is that it stains all nuclei present, including those undergoing apoptosis. The Hoechst-positive nuclei of cells undergoing apoptosis are often condensed, fragmented, and/or brightly stained (Abdel Wahab, Abdul, Alzubairi, Mohamed Elhassan, & Mohan, 2009; Syed Abdul Rahman, Abdul Wahab, & Abd Malek, 2013). Therefore, cells with nuclei under 50 μm^2 in area were not included in our results. We also investigated the frequency distribution of the number of cells with specific nuclear sizes or staining intensities (Fig 11). Median and average nuclear sizes were not significantly reduced by the first hit, supporting the view that the cells surviving the first hit are indeed viable (Fig 9). However, average nuclear size was slightly decreased after two MG132 insults, suggesting cells were stressed and perhaps undergoing apoptosis. Therefore, we performed the TUNEL assay for apoptotic cells but discovered that the first MG132 hit did not change the number of TUNEL-positive cells. The second MG132 hit significantly increased the number of TUNEL-positive cells in both the control and previously stressed groups, but the total numbers of apoptotic cells were low (~10%), suggesting that the vast majority of cells counted after

dual hits are indeed viable. It is also important to note here that we were excluding the small, dying cells in our viability assays. These findings are entirely consistent with our observations that astrocytes survived dual hits even when the interval between the first and second hits was increased to 96h and when the interval between the second hit and the time of assay was increased to 72h. Had the cells been progressing towards cell death, we would not expect to have continued to see protection in the latter studies.

An examination of the scatterplots of nuclear size versus staining intensity suggests that the first hit eliminated cells with small nuclear sizes (50-150 μm^2) and bright staining intensities (greater than 20 arbitrary units for mean gray value). Indeed, cells with small nuclei were more likely to die and wash off the plate at the time of assay than cells with larger nuclei, as shown in Figure 11. Small, bright cells may be in the process of dying and the MG132 treatment may force them beyond the threshold needed to survive. These findings of preferential loss of the smaller cells continue to support the hypothesis that MG132 treatment kills the most vulnerable cells and leaves behind the more resistant survivors.

Based on a large body of work, astrocytes are no longer considered a relatively uniform population of cells (Hewett, 2009; Y. Zhang & Barres, 2010). In addition to regional differences in the properties of astrocytes, astrocytes within a given brain region are also structurally and functionally diverse. As argued by Hewett, astrocyte adaptability or plasticity contributes to this diversity (cite the man again!!). Early studies had already established that astrocytes can be divided into protoplasmic and fibrous groups, which are found in gray and white matter, respectively, and exhibit unique morphological characteristics (R. H. Miller & Raff, 1984). Astrocyte heterogeneity has been

hypothesized to contribute to the differential vulnerability of specific brain regions to neurodegenerative disorders. For example, astrocytic glutathione levels are higher in the cerebral cortex relative to the substantia nigra in Parkinson's disease and may explain the relative resistance of the former brain region to pathology in this condition. Even within the cortex itself, astrocytes exhibit heterogeneity, as they do not uniformly express the GFAP and S100β markers (Emsley & Macklis, 2006). This heterogeneity may also be reflected in the differential expression of S100β and GFAP in our cortical astrocyte cultures; that is, a small number of cells in our cultures only expressed one of these two markers. Further evidence of astrocyte heterogeneity in our model is the fundamental observation that some astrocytes succumbed to the first hit of MG132 whereas others survived this insult and were resistant to further injury. As mentioned above, we observed higher vulnerability of astrocytes with small, brightly stained nuclei relative to astrocytes with large nuclei. An important goal for future studies would be to determine the unique protein profiles of these two distinct groups. One might speculate that the cells with larger nuclei have undergone some degree of hypertrophy *in vitro*, a classic anatomical sign of cellular stress, and that they are more likely to engage the enzymes responsible for glutathione synthesis and redox cycling, such as glutamate cysteine ligase, glutathione reductase, and glutathione peroxidase. Alternatively, cortical astrocytes may naturally include both large and small cells and these in vivo features may be retained under in vitro culturing conditions. It is worth noting that the astrocytes that survived MG132 exhibited marked changes in their qualitative appearance, shifting from a stellate shape to a bipolar, fusiform, or rounded shape, and expressing higher levels of GFAP (Figure 2). Consistent with the view that astrocyte heterogeneity influences their ability to develop

stress tolerance, there are reports of differential vulnerabilities of cortical astrocyte subpopulations after diffuse traumatic brain injury (Hill, Barbarese, & McIntosh, 1996).

Previous work suggests that preconditioned astrocytes can still support neuronal functions (Sen, et al., 2011). However, it is not clear whether severely stressed astrocyte survivors promote or prevent neuronal injury. Some authors have hypothesized the reverse, namely that injured astrocytes exacerbate neuronal injury (Fogal, Li, Lobner, McCullough, & Hewett, 2007; Gouix, et al., 2014; Jana & Pahan, 2010; Pertusa, Garcia-Matas, Rodriguez-Farre, Sanfeliu, & Cristofol, 2007). Thus, we sought to determine whether stressed astrocyte survivors can protect neurons from proteotoxicity. As expected, we observed that severely stressed astrocytes can still protect neighboring neurons from proteotoxic injury. Although glutathione was essential for astrocytic stress resistance, astrocytes did not rely on glutathione defenses in order to protect neurons from proteotoxicity. This finding was unexpected because previous work has shown that astrocytes protect neurons by releasing glutathione precursors into the extracellular space (Dringen, et al., 2000; Dringen, et al., 1999). Hsp70 is also known to be released from astrocytes via exosomes and may decrease proteotoxicity in other models through this transcellular process (Taylor, et al., 2007). However, neither inhibition of Hsp70 by VER155008 nor glutathione by buthionine sulfoximine attenuated astrocyte-mediated neuroprotection in our hands. It is possible that VER155008 may not be as effective in the mixed cultures as it is in the neuron-only group simply because there are more cells present. However, the stressed astrocyte group with lower cell numbers was more protective than the unstressed astrocyte group with higher cell numbers, suggesting that greater uptake of inhibitors at lower cell densities did not confound our interpretations.

The astrocyte-mediated neuroprotection in our model appeared to be dependent upon cell-cell contacts and not a diffusible factor (Fig 20). For example, the neuroprotective effects may occur through the diffusion of a small molecule via gap junctions (Kozoriz et al., 2010; Nakase, Sohl, Theis, Willecke, & Naus, 2004). Alternatively, astrocytes may protect neurons by the uptake of excess glutamate from the extracellular space, which would require them to be present at the time of neuronal excitotoxicity (Romera et al., 2007). Astrocyte-conditioned medium was concentrated by ultra-centrifugation concentrating devices in a preliminary study but showed the same results as unconcentrated medium. One possible explanation of these findings is that glutathione may diffuse through the concentrating device owing to its small size. If this were the case, it would not be delivered to the neurons in the conditioned media exchange experiments and we would fail to observe neuroprotection. Alternatively, astrocytes may release the diffusible factor immediately following the proteotoxic insult and this factor may be degraded in the 24h interval between the MG132 insult and conditioned media exchange.

As mentioned earlier, GFAP is a highly stress-responsive cytoskeletal protein thought to be primarily expressed by astrocytes (Eng, Ghirnikar, & Lee, 2000). Changes in GFAP expression levels have been attributed to astrocytosis and/or astrocyte hypertrophy(Eng, et al., 2000). Mutations in GFAP have been reported in Alexander's disease (Tang, Perng, Wilk, Quinlan, & Goldman, 2010). In this condition, $GFAP^{+}$ protein aggregates may be associated with a toxic gain of astrocyte function (Brenner et al., 2001; Messing, Brenner, Feany, Nedergaard, & Goldman, 2012). However, attenuation of astrocyte reactivity can also be detrimental to neurological recovery after

injury (Liu et al., 2014) and astrocyte cytoskeletal proteins and cellular reactivity are thought to be essential for maintaining the astrocyte neurosupportive functions. For example, recent studies demonstrate that loss of GFAP increases neuronal loss in the brain (Schreiner et al., 2015). Although forced overexpression of GFAP is associated with early death in mice (Messing et al., 1998), many studies suggest that physiological GFAP upregulation serves to preserve homeostasis. For example, GFAP is essential for mitigating traumatic brain injury (Nawashiro, Messing, Azzam, & Brenner, 1998). Furthermore, motor neurons in the spinal cord become dysfunctional in the absence of GFAP (Schreiner, et al., 2015). All of these studies are consistent with the findings of the present study that reactive astrocytes can continue to support neurons, even under conditions of severe injury and after synergistic loss proteasome and Hsp70 chaperone functions.

In conclusion, our studies suggest that astrocytes can adapt to severe proteotoxicity, a form of plasticity that may have evolved so that this cell type retains its capacity to support neuronal functions. Thus, neurons surrounded by reactive astrocytes may be able to survive for longer periods under conditions of proteotoxic stress. It may be difficult to generate severely stressed astrocytes in an *in vivo* model because the elimination of even small numbers of astrocytes might incapacitate some neuronal functions (Wagner et al., 2006). For example, compromises in astrocytic function may contribute to neurodegeneration in Alexander's disease (Brenner, et al., 2001; Messing, et al., 2012). A more targeted approach to eliciting severe proteotoxicity in astrocytes alone and one that does not elicit astrocyte death seems warranted.

Study limitations

A number of limitations, in addition to the ones alluded to above, must be conceded. First, all pharmacological inhibitors exert nonspecific effects at high concentrations. As a result of this concern, we used concentrations that are established in the literature, but this does not preclude some off-target effects. One approach to blocking heat shock protein activity more specifically in the future might be to use RNA interference. However, this method would not circumvent potential compensatory responses of other proteins. For example, other heat shock protein family members may be upregulated in response to loss of Hsp70 function. It is also important to note that MG132 inhibits proteases such as cathepsin A, cathepsin B, and calpain 1 in addition to its inhibition of the proteasome, as mentioned in the Introduction (Rivett & Gardner, 2000). However, the inhibition of these proteases would still contribute to proteotoxic effects. For this reason, our model is described as one of loss of protein homeostasis, defined as proteotoxicity, rather than selective proteasome inhibition (Morimoto, 2008).

Second, one might argue that the astrocytes surviving MG132 do not mount any active defenses against proteotoxicity but are simply inherently less susceptible to this toxin from the very beginning. If the stressed cells were always inherently less susceptible, one would expect these cells to have elevated defensive molecules at all times relative to untreated cells. If this were indeed the case, one would not expect to observe the transient upregulation of Hsp70, HO1, and ubiquitinated proteins after the first hit as we did. Furthermore, stressed astrocytes exhibited robust increases in Hsp70, HO1, and ubiquitinated proteins after the second hit whether or not they had previously been stressed, suggesting that we had not selected for a population of cells that were refractory to the effect of the toxin. Finally, if astrocytes had not mounted any defenses in

response to MG132, then inhibition of the stress-induced increase in glutathione would not have rendered them vulnerable to the toxic effects of dual MG132 hits. In effect, glutathione loss unmasks the toxic impact of the second hit. All these data support the view that the astrocytes mount active defenses in response to proteotoxicity.

In our studies, astrocytes were able to attenuate proteotoxicity in neurons despite being exposed to high concentrations of MG132 prior to the introduction of neurons (Fig 18A and 19A). These findings are the first to demonstrate that severely stressed astrocytes surviving a lethal insult can still protect neighboring neurons from proteotoxic injury although there are greatly reduced in numbers. It is possible that the effects of MG132 in the neuron-astrocyte coculture group may be attenuated simply because there are greater numbers of cells present to take up the MG132 than the neuron-only cultures. However, as mentioned above, this hypothesis is not consistent with the observation that astrocytes previously exposed to MG132 (and therefore reduced in numbers) are even more protective than the unstressed astrocytes (with greater numbers) in the experiments delivering MG132 and VER155008 simultaneously or MG132 and BSO simultaneously (Fig 19 and 18).

4.2 N-acetyl cysteine protects against protein-misfolding stress in an Hsp70-dependent manner

NAC has been shown to exert some beneficial effects in patients with psychiatric and neurodegenerative diseases, perhaps by reducing oxidative stress (Adair, et al., 2001; Berk, Copolov, Dean, Lu, Jeavons, Schapkaitz, Anderson-Hunt, Judd, et al., 2008; Berk, Copolov, Dean, Lu, Jeavons, Schapkaitz, Anderson-Hunt, & Bush, 2008; M. E. Hoffer, et al., 2013). In experimental Parkinson's disease, NAC has been shown to decrease α-synuclein^{+} aggregates, an established sign of protein-misfolding stress, perhaps by raising glutathione defenses (Clark et al., 2010). Various doses and delivery methods have been used to administer NAC in the clinic. Soldiers experiencing blast injuries were administered 4 grams of NAC daily for 4 days after injury followed by 3 grams daily for the remainder of the study (M. E. Hoffer, et al., 2013). Rather strikingly, this regimen doubled the chances of resolution of neurological symptoms from 42% to 86%. A similar oral dose of NAC was given to Alzheimer's disease patients in capsule form (50 mg/kg/day) (Adair, et al., 2001). NAC was shown to increase brain glutathione levels in Parkinson's disease patients when delivered at 150 mg/kg by intravenous infusion for one hour (Holmay, et al., 2013). However, NAC is thought to have an oral bioavailability of only 9.1% (Olsson, Johansson, Gabrielsson, & Bolme, 1988). On the other hand, many studies have shown that orally delivered NAC can have protective effects on neurons *in vivo* and increase brain glutathione levels in experimental models of neurological disorders, suggesting it crosses the blood-brain barrier in sufficient quantities (Grant, Odlaug, & Kim, 2009; R. W. Hurd, Wilder, Helveston, & Uthman, 1996; Lavoie et al., 2008). Nevertheless, chemical modifications to NAC have been investigated due to

perceived poor bioavailability (Giustarini, Milzani, Dalle-Donne, Tsikas, & Rossi, 2012; Sunitha et al., 2013). Either way, the effective *in vitro* concentration (3 mM) used in the present investigation likely surpasses concentrations delivered to cells in *in vivo* studies. It is possible that higher concentrations are needed *in vitro* than *in vivo* because of high basal levels of oxidative stress under *in vitro* culturing conditions (Halliwell, 2014). Further studies are warranted to continue to improve NAC bioavailability.

NAC has already been shown to decrease cellular stress in astrocytes in experimental models of ischemia and pain (Bernabucci et al., 2012; Gabryel, Toborek, & Malecki, 2005). As mentioned previously, astrocytes exhibit protein-misfolding stress in neurodegenerative diseases (Allen & Barres, 2009; Braak, et al., 2007; Kimelberg & Nedergaard, 2010). Because astrocytes help preserve neuronal function, it is important to identify therapies that protect astrocytes from protein-misfolding stress in order to mitigate loss of neuroprotective features. Our study demonstrates that NAC might be one such candidate. Other studies in the Leak lab have shown that NAC can also protect cortical neurons and neuroblastoma cells against proteotoxic and oxidative stress, supporting the view that the protective effects of NAC are generalizable across multiple experimental models (Posimo, et al., 2013; Unnithan, et al., 2012; Unnithan et al., 2014). The generalizability across different models improves the chances of success in the clinic.

As mentioned above, previous studies in the Leak lab have shown that NAC protects neuroblastoma cells against MG132 (Jiang, et al., 2013). In those studies, MG132 was effective at inhibiting the chymotrypsin-like activity of the proteasome in the presence or absence of NAC. Furthermore, in our astrocyte study, expression of

proteasomal subunits was not altered by NAC treatment. In contrast, the dramatic MG132-mediated rise in ubiquitin-conjugated proteins was abolished by NAC in both neuroblastoma cells and astrocytes. Taken together, these findings suggest that NAC decreases proteotoxicity through a mechanism independent of direct effects on proteasome activity. Had NAC directly reduced the effects of MG132 on the proteasome, we would not have been able to conclude that it protects against protein misfolding stress because the toxin would simply be less effective in the NAC-treated group. Instead, NAC may be reducing the burden of misfolded, ubiquitinated proteins by improving chaperone and antioxidant defenses (see below).

Neurodegenerative diseases are characterized by both protein-misfolding and oxidative stress, which propel and propagate each other and amplify the injury. For example, proteasome inhibition has been shown to increase oxidative stress (Maharjan, et al., 2014). NAC is thought to provide the rate-limiting component in glutathione synthesis (E. Hoffer, et al., 1996). However, in our astrocytes, NAC was protective independent of glutathione synthesis, as its therapeutic potential was not abolished by buthionine sulfoximine. Unexpectedly, NAC attenuated the MG132-mediated rise in glutathione. However, NAC has been observed to attenuate stress-induced rises in glutathione in other models, demonstrating that our findings are not entirely unprecedented (Tchantchou, Graves, Rogers, Ortiz, & Shea, 2005). Although NAC attenuated proteotoxicity independent of glutathione synthesis, NAC may nevertheless reduce oxidative stress in astrocytes by the direct antioxidant activity of the thiol group (Aruoma, et al., 1989). This may prevent oxidative damage to proteins, including Hsp70 and other chaperones, and as a result, decrease proteotoxicity. Furthermore, if NAC

directly reduces oxidative stress, this may explain the mitigation of the stress-induced rise in glutathione levels.

The cysteine of NAC can exist in two isomeric forms: L-cysteine and D-cysteine. Both forms of the amino acid can reduce oxidative stress through redox cycling of the cysteine sulfhydryl group. L-cysteine but not D-cysteine can be incorporated into glutathione. In our studies, both L-cysteine and D-cysteine were shown to protect astrocytes against MG132 toxicity, as was observed with NAC. Some amino acids can be converted from the D- to L-isoform by D-amino acid oxidase (Friedman & Levin, 2012; Sacchi, et al., 2008). Thus, D-cysteine may decrease proteotoxic stress by first being converted to L-cysteine followed by incorporation into glutathione. However, inhibition of D-amino acid oxidase with sodium benzoate did not alter the protective effect of D-cysteine in our study (Katane, et al., 2013; Van den Berghe-Snorek & Stankovich, 1985), suggesting that the conversion reaction was not significant in our model. Future studies are needed to confirm that L-cysteine is directly protective and not protective through interconversion to glutathione, perhaps by using buthionine sulfoximine to inhibit cysteine incorporation into glutathione. Nevertheless, all the data collected thus far in our model are consistent with the view that protection by NAC is not dependent upon glutathione synthesis. Thus, we speculate that the robust protection by NAC may depend upon the cysteine sulfhydryl group, which is also present in both L-cysteine and D-cysteine.

Thiol exchange reactions can facilitate activation of transcription factors such as Nrf2 and HSF1 (Dinkova-Kostova, 2012). For example, NAC might be expected to react with cysteine residues on Keap1. As a result, Keap1-mediated degradation of Nrf2 would

be attenuated, enabling its translocation from the cytoplasm to the nucleus and the transcription of genes such as HO1 and HSPA1B, which encodes Hsp70 (Hu, et al., 2006; Kwak, et al., 2003; Qi et al., 2013). Similarly, thiol exchange reactions between NAC and the cysteine residues in HSF1 might elicit transcription of Hsp70 genes. However, our studies showed that NAC attenuated MG132-mediated increases in HO1 and Hsp70 expression. Contrary to the results observed in astrocytes, other studies in our lab have shown that NAC increases Hsp70 in N2a cells (Jiang, et al., 2013) and in cortical neurons (unpublished findings). The reasons underlying this discrepancy are still under investigation.

Although NAC attenuated the MG132-mediated rises in Hsp70 and HO1, we investigated whether inhibition of Hsp70 and HO1 activity attenuated NAC-mediated protection because changes in protein levels do not always coincide with changes in activity. Three pharmacological inhibitors for Hsp70 (VER155008, pifithrin-μ, and MAL3-101) with different mechanisms of action and one pharmacological inhibitor of HO1 (SnPPx) activity all attenuated astrocytic protection by NAC. These findings suggest that Hsp70 and/or HO1 activity is important for NAC-mediated protection. It remains possible that NAC preserves Hsp70 or HO1 activity under conditions of oxidative stress by direct antioxidant action. For example, NAC may prevent oxidative damage to these proteins. Other studies in the Leak lab have also shown that Hsp70 inhibitors abolish NAC-mediated protection in N2a cells, cortical neurons, and hippocampal neurons, suggesting that NAC protects multiple cell types in an Hsp70-dependent manner.

Heat shock proteins such as Hsp70 and HO1 are known to be higher in patients with neurodegenerative diseases relative to control subjects, probably because the stimuli to induce their expression include proteotoxic and oxidative stress (Schipper, et al., 2006; Schipper, et al., 1998; Wu et al., 2004). The upregulation of these heat shock protein molecules may be a compensatory response to damage to some fraction of the heat shock protein pool, resulting in a loss of negative feedback on heat shock protein gene transcription and translation. NAC may protect in part by reducing further damage to heat shock proteins and in turn, this may enable more efficient refolding and degradation by Hsp70 and superior heme degradation by HO1. Based on the dramatic reduction in ubiquitinated proteins and the potential facilitation of Hsp70 refolding activity, NAC is expected to slow or halt further accumulation of protein aggregates in patients with neurodegenerative conditions.

As described above, measurements of Hsp70 activity are not feasible in cellular lysates because many molecules in these lysates exhibit ATPase activity in addition to Hsp70. It is therefore not possible to assess whether NAC protects astrocytes by increasing Hsp70 activity in the astrocyte model. To address this gap, one might assess the activity of pure, recombinant Hsp70 in the presence of NAC (Z. Lu & Cyr, 1998), although such experiments would not establish a definitive mechanism in the astrocyte model. Cysteine residues on Hsp70 are susceptible to oxidative damage that might hinder ATPase activity (Miyata, et al., 2012). If NAC reverses damage to Hsp70, this would suggest that NAC decreases proteotoxicity by preserving normal Hsp70 function.

As mentioned above, all pharmacological inhibitors have off-target effects at high concentrations. Therefore, multiple pharmacological inhibitors were used to examine the

role of Hsp70 activity in NAC-mediated protection against MG132. VER155008 and pifithrin-μ are known to inhibit autophagy, but this may occur through inhibition of Hsc70 (Budina-Kolomets et al., 2013; Leu, et al., 2011), because Hsc70 escorts proteins to the lysosome for autophagic degradation (Arias & Cuervo, 2011). Despite potentially nonspecific effects, the overlapping effects of the inhibitors suggest that Hsp70 activity loss is indeed responsible for reducing NAC-mediated protection. In other words, it would be unlikely that all three inhibitors have the same non-specific effects.

In conclusion, protein aggregate buildup may be attenuated by NAC through the thiol-mediated prevention of disulfide bond formation (Samuni, Goldstein, Dean, & Berk, 2013). The accumulation of protein aggregates may also be reversed in the presence of Hsp70 (Chittoor-Vinod, Lee, Judge, & Notterpek, 2015). Our studies reveal that NAC-mediated protection of astrocytes is dependent upon Hsp70 activity. Preservation of astrocyte function by NAC would be expected to contribute to neuronal homeostasis and slow down the neurodegenerative process.

4.3 Natural aging elicits changes in heat shock proteins in multiple brain regions

Heat shock proteins are important for restoring protein homeostasis under conditions of proteotoxic stress. Perez and colleagues found that longevity is determined in part by protein stability and resistance to oxidative damage (Perez et al., 2009). Some studies have shown that heat shock protein defenses wane with advancing age while others have shown age-related increases in heat shock proteins (Alladi, et al., 2010; Dickey, et al., 2009; Ewing & Maines, 2006; Gupte, et al., 2010; C. K. Lee, Weindruch, & Prolla, 2000; Paz Gavilan, et al., 2006). The impact of aging in the substantia nigra and striatum on heat shock proteins has been previously examined (V. Calabrese, et al., 2004; Ewing & Maines, 2006; Gupte, et al., 2010; Unno, et al., 2000). However, all of these animal studies were conducted in males. Thus, the present study is the first to assess the relationship between natural aging and heat shock protein expression in the substantia nigra, striatum, and olfactory bulb in female rats.

In this study, some heat shock proteins, such as Hsp25 and Hsp70, were observed to increase with advancing age. These increases may be the result of compensatory responses to age-related proteotoxic and oxidative stress. For example, cells may elevate heat shock protein levels to reverse or slow the detrimental effects of age-related loss of proteasome activity (Martinez-Vicente, et al., 2005). As misfolded proteins are ubiquinated prior to proteasomal degradation, proteotoxic stress was measured by assessing ubiquitin-conjugated proteins in our studies. The statistical trends towards age-related increases in pan ubiquitin-conjugated proteins in the substantia nigra and striatum are suggestive of an increase in proteotoxic stress. Furthermore, K48-linked ubiquitin in the striatum was higher in older animals in comparison to 4-6 month old rats. However,

no significant increases in K48-linked ubiquitin levels were observed in the substantia nigra. K48-linked ubiquitin is a more direct assessment of proteotoxicity than pan ubiquitin as some molecules are ubiquitinated without being targeted to the proteasome. For example, linkages between ubiquitin molecules at lysine 63 signal endocytosis, kinase activation, and DNA damage, and not proteasomal degradation (Sadowski & Sarcevic, 2010). Measuring proteasome activity would be an important goal for future aging studies in our model.

The female Sprague Dawley rat has been shown to have a lifespan ranging from 193-1100 days (Davis, Stevenson, & Busch, 1956). The oldest animals in our study were sacrificed at 22 months because some began to exhibit poor health and die. Even older animals might have exhibited a more robust increase in proteotoxic stress. In future studies we would need to house a large number of animals to account for high rates of spontaneous death after two years of age.

A thorough understanding of age-related disruptions to proteostasis and the response of heat shock proteins to these changes is important for the identification of new therapeutic targets. However, some authors have argued that aging animal models have poor predictive validity. Sengupta and colleagues reviewed factors such as teeth, sexual development, and musculoskeletal systems as important for relating rat age to human age (Sengupta, 2013). Based upon these factors, the authors suggested that rats encounter developmental stages at different rates than humans and therefore, caution must be exerted when correlating rat to human ages. In other words, changes in heat shock protein expression at specific rat ages may be difficult to extrapolate to human developmental stages.

Depending upon the brain region examined, some heat shock protein defenses, such as Hsp40 and Hsc70 were observed to wane with advancing age. These effects would be expected to contribute to a progressive accumulation of protein aggregates. Despite declines in expression of these heat shock proteins, age-related increases in ubiquitinated proteins were small in size, suggesting that other heat shock proteins may have compensated for deficits in these proteins. Thus, the overall severity of age-related proteotoxicity is likely to be the result of the concerted efforts of multiple heat shock protein defenses and proteasomal and autophagic clearance mechanisms.

In our work, we have shown that the relationships between aging and heat shock proteins are highly dependent upon brain region. For example, Hsp25 increased in the female rat olfactory bulb, striatum, and substantia nigra with aging. For example, Hsp25 was higher in 4-22 month animals in comparison to the youngest animals in the olfactory bulb. This may be suggestive of developmental changes in Hsp25 expression. As both the striatum and the nigra exhibited a rise in Hsp25, we hypothesized that Hsp25 may be present within the dopaminergic neurons that form the nigrostriatal pathway. Confocal analyses confirmed that Hsp25 was present in tyrosine hydroxylase^{+} dopaminergic neurons of the substantia nigra. In addition, Hsp25 was also present in cells not expressing tyrosine hydroxylase, as one might expect given the ubiquitous nature of this heat shock protein. If the number of dopaminergic neurons decrease with aging as has been reported in some models, the rise in Hsp25 observed in the present study may be attributed to Hsp25 expression within other cell types (Gibb & Lees, 1991).

As mentioned above, the confocal analysis suggests that Hsp25 is expressed in both dopaminergic and non-dopaminergic cells in the ventral mesencephalon. Some of

the Hsp25-expressing non-dopaminergic cells are expected to be glial in nature, as Hsp25 is known to be highly expressed in astrocytes (Chen & Swanson, 2003; Stetler, Gao, Signore, Cao, & Chen, 2009). Hsp25 expression has been shown to be increased in various models of neurological disorders and with natural aging (Crum et al., 2015a; Gleixner, et al., 2014; Gupte, et al., 2010; Strey et al., 2004). For example, Hsp25 expression within glial cells is increased in transgenic models of amyotrophic lateral sclerosis (Wang, Martin, Gonzales, Borchelt, & Lee, 2008). Future studies to investigate the differential impact of aging and proteotoxicity on Hsp25 levels in glial and neurons are warranted, as they may provide insight into the differential susceptibility of various cell types to proteotoxicity.

Several authors have speculated that the olfactory bulb is especially vulnerable to protein inclusions in neurological disorders because of greater exposure to environmental pathogens than deeper brain regions. For example, α-synuclein^{+} aggregates appear in the olfactory bulb long before they emerge in the ventral mesencephalon in Parkinson's disease (Hawkes, Del Tredici, & Braak, 2009). Based on these histological observations, one would expect to see heat shock protein changes in the olfactory bulb before similar changes appear within the nigrostriatal pathway in Parkinson's patients. Future studies to test this hypothesis might help correlate the emergence of Lewy pathology with stress responses in heat shock proteins. Such findings would also be consistent with histological studies showing that Lewy bodies contain high levels of Hsp70 molecules (Shin, Klucken, Patterson, Hyman, & McLean, 2005).

Some heat shock protein responses to aging differed between the substantia nigra and striatum. For example, HO1 was decreased with aging in the substantia nigra,

whereas a biphasic response in HO1 levels was observed in the striatum. The discrepancy between the nigral and striatal HO1 changes may suggest that HO1 is present in cells other than dopaminergic neurons of the nigrostriatal pathway. Despite our repeated efforts to address this question, multiple antibodies against HO1 were ineffective by immunohistochemistry and only worked in Western blot analyses.

An age-related decline in Hsc70 was observed in both the olfactory bulb and the striatum. As mentioned above, Hsc70 recognizes proteins with the KFERQ-like sequence and escorts them to the lysosome for chaperone-mediated autophagic degradation (Boya, Reggiori, & Codogno, 2013). A loss of Hsc70 expression with aging would therefore be expected to contribute to autophagic stress. As expression of the membrane protein LAMP2A is thought to reflect levels of chaperone mediated autophagy (Boya, et al., 2013), future studies to measure LAMP2A protein levels to assess age-related changes in autophagy in the olfactory bulb and striatum might be valuable.

For our *in vivo* studies, we used female rats. Advancing age leads to cessation of estrous cycling in female rats (Sone et al., 2007). It is possible that fluctuations in the estrous cycle may have contributed to some of the high variability observed in some of the heat proteins. Estrous cycling is already known to have an impact on Hsp25 expression (Steffl, Telgen, Schweiger, & Amselgruber, 2010). Similarly, Hsp70 expression levels also fluctuate with the estrous cycle (Muthukumar et al., 2014). In order to reduce variability, vaginal smears to determine the phase of the estrous cycle might be helpful. However, if the data were stratified according to the estrous cycle, we would need many more animals in each group.

In conclusion, aging is the most important risk factor for the development of neurodegenerative diseases, all of which are characterized by loss of proteostasis and changes in heat shock proteins (Alladi, et al., 2010; Dickey, et al., 2009; Ewing & Maines, 2006; Gupte, et al., 2010; Keller, Hanni, & Markesbery, 2000b; Keller, Huang, et al., 2000; C. K. Lee, et al., 2000; Martinez-Vicente, et al., 2005; Paz Gavilan, et al., 2006; Van Den Eeden, et al., 2003). However, not all aged individuals suffer from neurodegenerative diseases and it is therefore important to understand heat shock protein defenses in the absence of pathological changes. It is worth noting that our study of the relationship between normal aging and heat shock proteins was only correlative and did not establish any causal links. In order to assess the importance of the observed changes in heat shock proteins, knockout, knockdown, or antagonism experiments would be necessary. Alternatively, the proteins in question might be overexpressed to determine if this increases lifespan and protects against insults in experimental models. The information garnered in the present study would be useful in guiding such future investigations.

Chapter 5 Bibliography

Abdel Wahab, S. I., Abdul, A. B., Alzubairi, A. S., Mohamed Elhassan, M., & Mohan, S. (2009). In vitro ultramorphological assessment of apoptosis induced by zerumbone on (HeLa). *J Biomed Biotechnol, 2009*, 769568. doi: 10.1155/2009/769568

Abramovitz, M., Homma, H., Ishigaki, S., Tansey, F., Cammer, W., & Listowsky, I. (1988). Characterization and localization of glutathione-S-transferases in rat brain and binding of hormones, neurotransmitters, and drugs. *J Neurochem, 50*(1), 50-57.

Acunzo, J., Katsogiannou, M., & Rocchi, P. (2012). Small heat shock proteins HSP27 (HspB1), alphaB-crystallin (HspB5) and HSP22 (HspB8) as regulators of cell death. *Int J Biochem Cell Biol, 44*(10), 1622-1631. doi: 10.1016/j.biocel.2012.04.002

Adair, J. C., Knoefel, J. E., & Morgan, N. (2001). Controlled trial of N-acetylcysteine for patients with probable Alzheimer's disease. *Neurology, 57*(8), 1515-1517.

Adam, C., Baeurle, A., Brodsky, J. L., Wipf, P., Schrama, D., Becker, J. C., & Houben, R. (2014). The HSP70 Modulator MAL3-101 Inhibits Merkel Cell Carcinoma. *PLoS One, 9*(4), e92041. doi: 10.1371/journal.pone.0092041

Adams, J. D., Jr., Klaidman, L. K., Odunze, I. N., Shen, H. C., & Miller, C. A. (1991). Alzheimer's and Parkinson's disease. Brain levels of glutathione, glutathione disulfide, and vitamin E. *Mol Chem Neuropathol, 14*(3), 213-226.

Adler, V., Yin, Z., Fuchs, S. Y., Benezra, M., Rosario, L., Tew, K. D., . . . Ronai, Z. (1999). Regulation of JNK signaling by GSTp. *EMBO J, 18*(5), 1321-1334. doi: 10.1093/emboj/18.5.1321

Ahmadi, A., Fredrikson, M., Jerregard, H., Akerback, A., Fall, P. A., Rannug, A., . . . Soderkvist, P. (2000). GSTM1 and mEPHX polymorphisms in Parkinson's disease and age of onset. *Biochem Biophys Res Commun, 269*(3), 676-680. doi: 10.1006/bbrc.2000.2338

Alavez, S., Vantipalli, M. C., Zucker, D. J., Klang, I. M., & Lithgow, G. J. (2011). Amyloid-binding compounds maintain protein homeostasis during ageing and extend lifespan. *Nature, 472*(7342), 226-229. doi: 10.1038/nature09873

Alexandrova, A., Petrov, L., Georgieva, A., Kirkova, M., & Kukan, M. (2008a). Effects of proteasome inhibitor, MG132, on proteasome activity and oxidative status of rat liver. *Cell Biochem Funct, 26*(3), 392-398. doi: 10.1002/cbf.1459

Alexandrova, A., Petrov, L., Georgieva, A., Kirkova, M., & Kukan, M. (2008b). Effects of proteasome inhibitor, MG132, on proteasome activity and oxidative status of rat liver. [Research Support, Non-U.S. Gov't]. *Cell biochemistry and function, 26*(3), 392-398. doi: 10.1002/cbf.1459

Alladi, P. A., Mahadevan, A., Vijayalakshmi, K., Muthane, U., Shankar, S. K., & Raju, T. R. (2010). Ageing enhances alpha-synuclein, ubiquitin and endoplasmic reticular stress protein expression in the nigral neurons of Asian Indians. *Neurochem Int, 57*(5), 530-539. doi: 10.1016/j.neuint.2010.06.018

Allen, N. J., & Barres, B. A. (2009). Neuroscience: Glia - more than just brain glue. *Nature, 457*(7230), 675-677. doi: 10.1038/457675a

Anglade, P., Vyas, S., Javoy-Agid, F., Herrero, M. T., Michel, P. P., Marquez, J., . . . Agid, Y. (1997). Apoptosis and autophagy in nigral neurons of patients with Parkinson's disease. *Histol Histopathol, 12*(1), 25-31.

Aquilano, K., Baldelli, S., & Ciriolo, M. R. (2014). Glutathione: new roles in redox signaling for an old antioxidant. *Front Pharmacol, 5*, 196. doi: 10.3389/fphar.2014.00196

Arias, E., & Cuervo, A. M. (2011). Chaperone-mediated autophagy in protein quality control. [Research Support, N.I.H., Extramural Research Support, Non-U.S. Gov't Review]. *Current opinion in cell biology, 23*(2), 184-189. doi: 10.1016/j.ceb.2010.10.009

Aronica, E., Catania, M. V., Geurts, J., Yankaya, B., & Troost, D. (2001). Immunohistochemical localization of group I and II metabotropic glutamate receptors in control and amyotrophic lateral sclerosis human spinal cord: upregulation in reactive astrocytes. *Neuroscience, 105*(2), 509-520.

Arumugam, T. V., Phillips, T. M., Cheng, A., Morrell, C. H., Mattson, M. P., & Wan, R. (2010). Age and energy intake interact to modify cell stress pathways and stroke outcome. *Ann Neurol, 67*(1), 41-52. doi: 10.1002/ana.21798

Aruoma, O. I., Halliwell, B., Hoey, B. M., & Butler, J. (1989). The antioxidant action of N-acetylcysteine: its reaction with hydrogen peroxide, hydroxyl radical, superoxide, and hypochlorous acid. [Research Support, Non-U.S. Gov't]. *Free Radic Biol Med, 6*(6), 593-597.

Attems, J., Lintner, F., & Jellinger, K. A. (2005). Olfactory involvement in aging and Alzheimer's disease: an autopsy study. *J Alzheimers Dis, 7*(2), 149-157; discussion 173-180.

Attems, J., Walker, L., & Jellinger, K. A. (2014). Olfactory bulb involvement in neurodegenerative diseases. *Acta Neuropathol, 127*(4), 459-475. doi: 10.1007/s00401-014-1261-7

Baker, D. A., McFarland, K., Lake, R. W., Shen, H., Tang, X. C., Toda, S., & Kalivas, P. W. (2003). Neuroadaptations in cystine-glutamate exchange underlie cocaine relapse. *Nat Neurosci, 6*(7), 743-749. doi: 10.1038/nn1069

Balaburski, G. M., Leu, J. I., Beeharry, N., Hayik, S., Andrake, M. D., Zhang, G., . . . Murphy, M. E. (2013). A modified HSP70 inhibitor shows broad activity as an anticancer agent. *Mol Cancer Res, 11*(3), 219-229. doi: 10.1158/1541-7786.MCR-12-0547-T

Bannai, S., & Kitamura, E. (1980). Transport interaction of L-cystine and L-glutamate in human diploid fibroblasts in culture. *J Biol Chem, 255*(6), 2372-2376.

Beere, H. M., Wolf, B. B., Cain, K., Mosser, D. D., Mahboubi, A., Kuwana, T., . . . Green, D. R. (2000). Heat-shock protein 70 inhibits apoptosis by preventing recruitment of procaspase-9 to the Apaf-1 apoptosome. *Nat Cell Biol, 2*(8), 469-475. doi: 10.1038/35019501

Bell, K. F., Al-Mubarak, B., Fowler, J. H., Baxter, P. S., Gupta, K., Tsujita, T., . . . Hardingham, G. E. (2011). Mild oxidative stress activates Nrf2 in astrocytes, which contributes to neuroprotective ischemic preconditioning. *Proc Natl Acad Sci U S A, 108*(1), E1-2; author reply E3-4. doi: 10.1073/pnas.1015229108

Berk, M., Copolov, D., Dean, O., Lu, K., Jeavons, S., Schapkaitz, I., . . . Bush, A. I. (2008). N-acetyl cysteine as a glutathione precursor for schizophrenia--a double-

blind, randomized, placebo-controlled trial. [Clinical Trial, Multicenter Study, Randomized Controlled Trial, Research Support, Non-U.S. Gov't]. *Biological psychiatry, 64*(5), 361-368. doi: 10.1016/j.biopsych.2008.03.004

Berk, M., Copolov, D. L., Dean, O., Lu, K., Jeavons, S., Schapkaitz, I., . . . Bush, A. I. (2008). N-acetyl cysteine for depressive symptoms in bipolar disorder--a double-blind randomized placebo-controlled trial. [Multicenter Study, Randomized Controlled Trial, Research Support, Non-U.S. Gov't]. *Biological psychiatry, 64*(6), 468-475. doi: 10.1016/j.biopsych.2008.04.022

Bernabucci, M., Notartomaso, S., Zappulla, C., Fazio, F., Cannella, M., Motolese, M., . . . Nicoletti, F. (2012). N-Acetyl-cysteine causes analgesia by reinforcing the endogenous activation of type-2 metabotropic glutamate receptors. *Mol Pain, 8*, 77. doi: 10.1186/1744-8069-8-77

Boger, H. A., Granholm, A. C., McGinty, J. F., & Middaugh, L. D. (2010). A dual-hit animal model for age-related parkinsonism. [Research Support, N.I.H., Extramural Review]. *Prog Neurobiol, 90*(2), 217-229. doi: 10.1016/j.pneurobio.2009.10.013

Boya, P., Reggiori, F., & Codogno, P. (2013). Emerging regulation and functions of autophagy. *Nat Cell Biol, 15*(7), 713-720. doi: 10.1038/ncb2788

Braak, H., Del Tredici, K., Rub, U., de Vos, R. A., Jansen Steur, E. N., & Braak, E. (2003). Staging of brain pathology related to sporadic Parkinson's disease. *Neurobiol Aging, 24*(2), 197-211.

Braak, H., Del Tredici, K., Sandmann-Kiel, D., Rub, U., & Schultz, C. (2001). Nerve cells expressing heat-shock proteins in Parkinson's disease. *Acta Neuropathol, 102*(5), 449-454.

Braak, H., Ghebremedhin, E., Rub, U., Bratzke, H., & Del Tredici, K. (2004). Stages in the development of Parkinson's disease-related pathology. *Cell Tissue Res, 318*(1), 121-134. doi: 10.1007/s00441-004-0956-9

Braak, H., Rub, U., Gai, W. P., & Del Tredici, K. (2003). Idiopathic Parkinson's disease: possible routes by which vulnerable neuronal types may be subject to neuroinvasion by an unknown pathogen. *J Neural Transm, 110*(5), 517-536. doi: 10.1007/s00702-002-0808-2

Braak, H., Rub, U., Schultz, C., & Del Tredici, K. (2006). Vulnerability of cortical neurons to Alzheimer's and Parkinson's diseases. *J Alzheimers Dis, 9*(3 Suppl.), 35-44.

Braak, H., Sastre, M., & Del Tredici, K. (2007). Development of alpha-synuclein immunoreactive astrocytes in the forebrain parallels stages of intraneuronal pathology in sporadic Parkinson's disease. *Acta Neuropathol, 114*(3), 231-241. doi: 10.1007/s00401-007-0244-3

Braun, H. A., Umbreen, S., Groll, M., Kuckelkorn, U., Mlynarczuk, I., Wigand, M. E., . . . Schmidt, B. (2005). Tripeptide mimetics inhibit the 20 S proteasome by covalent bonding to the active threonines. *J Biol Chem, 280*(31), 28394-28401. doi: 10.1074/jbc.M502453200

Braunstein, M. J., Scott, S. S., Scott, C. M., Behrman, S., Walter, P., Wipf, P., . . . Batuman, O. (2011). Antimyeloma Effects of the Heat Shock Protein 70 Molecular Chaperone Inhibitor MAL3-101. *Journal of oncology, 2011*, 232037. doi: 10.1155/2011/232037

Brenner, M., Johnson, A. B., Boespflug-Tanguy, O., Rodriguez, D., Goldman, J. E., & Messing, A. (2001). Mutations in GFAP, encoding glial fibrillary acidic protein, are associated with Alexander disease. *Nat Genet, 27*(1), 117-120. doi: 10.1038/83679

Budina-Kolomets, A., Balaburski, G. M., Bondar, A., Beeharry, N., Yen, T., & Murphy, M. E. (2013). Comparison of the activity of three different HSP70 inhibitors on apoptosis, cell cycle arrest, autophagy inhibition, and HSP90 function. *Cancer biology & therapy, 15*(2).

Bukau, B., & Horwich, A. L. (1998). The Hsp70 and Hsp60 chaperone machines. *Cell, 92*(3), 351-366.Caceres, A., Banker, G., Steward, O., Binder, L., & Payne, M. (1984). MAP2 is localized to the dendrites of hippocampal neurons which develop in culture. *Brain Res, 315*(2), 314-318.

Calabrese, E. J. (2008). Astrocytes: adaptive responses to low doses of neurotoxins. [Review]. *Critical reviews in toxicology, 38*(5), 463-471. doi: 10.1080/10408440802004023

Calabrese, E. J., Bachmann, K. A., Bailer, A. J., Bolger, P. M., Borak, J., Cai, L., . . . Mattson, M. P. (2007). Biological stress response terminology: Integrating the concepts of adaptive response and preconditioning stress within a hormetic dose-response framework. *Toxicol Appl Pharmacol, 222*(1), 122-128. doi: 10.1016/j.taap.2007.02.015

Calabrese, V., Scapagnini, G., Ravagna, A., Colombrita, C., Spadaro, F., Butterfield, D. A., & Giuffrida Stella, A. M. (2004). Increased expression of heat shock proteins in rat brain during aging: relationship with mitochondrial function and glutathione redox state. *Mech Ageing Dev, 125*(4), 325-335. doi: 10.1016/j.mad.2004.01.003

Cammer, W., & Zhang, H. (1993). Atypical localization of the oligodendrocytic isoform (PI) of glutathione-S-transferase in astrocytes during cuprizone intoxication. *J Neurosci Res, 36*(2), 183-190. doi: 10.1002/jnr.490360208

Cecarini, V., Bonfili, L., Cuccioloni, M., Mozzicafreddo, M., Rossi, G., Keller, J. N., . . . Eleuteri, A. M. (2014). Wild type and mutant amyloid precursor proteins influence downstream effects of proteasome and autophagy inhibition. *Biochim Biophys Acta, 1842*(2), 127-134. doi: 10.1016/j.bbadis.2013.11.002

Chatterjee, M., Andrulis, M., Stuhmer, T., Muller, E., Hofmann, C., Steinbrunn, T., . . . Bargou, R. C. (2013). The PI3K/Akt signaling pathway regulates the expression of Hsp70, which critically contributes to Hsp90-chaperone function and tumor cell survival in multiple myeloma. [Research Support, Non-U.S. Gov't]. *Haematologica, 98*(7), 1132-1141. doi: 10.3324/haematol.2012.066175

Chaudhuri, K. R., Healy, D. G., & Schapira, A. H. (2006). Non-motor symptoms of Parkinson's disease: diagnosis and management. *Lancet Neurol, 5*(3), 235-245. 10.1016/S1474-4422(06)70373-8

Chen, Y., & Swanson, R. A. (2003). Astrocytes and brain injury. *J Cereb Blood Flow Metab, 23*(2), 137-149.

Chittoor-Vinod, V. G., Lee, S., Judge, S. M., & Notterpek, L. (2015). Inducible HSP70 is critical in preventing the aggregation and enhancing the processing of PMP22. *ASN Neuro, 7*(1). doi: 10.1177/1759091415569909

Cho, S. G., Lee, Y. H., Park, H. S., Ryoo, K., Kang, K. W., Park, J., . . . Choi, E. J. (2001). Glutathione S-transferase mu modulates the stress-activated signals by

suppressing apoptosis signal-regulating kinase 1. *J Biol Chem, 276*(16), 12749-12755. doi: 10.1074/jbc.M005561200

Chu, P. W., Beart, P. M., & Jones, N. M. (2010). Preconditioning protects against oxidative injury involving hypoxia-inducible factor-1 and vascular endothelial growth factor in cultured astrocytes. [Research Support, Non-U.S. Gov't]. *Eur J Pharmacol, 633*(1-3), 24-32. doi: 10.1016/j.ejphar.2010.02.008

Ciechanover, A., & Schwartz, A. L. (1994). The ubiquitin-mediated proteolytic pathway: mechanisms of recognition of the proteolytic substrate and involvement in the degradation of native cellular proteins. *FASEB J, 8*(2), 182-191.

Clare, D. K., & Saibil, H. R. (2013). ATP-driven molecular chaperone machines. *Biopolymers, 99*(11), 846-859. doi: 10.1002/bip.22361

Clark, J., Clore, E. L., Zheng, K., Adame, A., Masliah, E., & Simon, D. K. (2010). Oral N-acetyl-cysteine attenuates loss of dopaminergic terminals in alpha-synuclein overexpressing mice. *PLoS One, 5*(8), e12333. doi: 10.1371/journal.pone.0012333

Cook, C., & Petrucelli, L. (2009). A critical evaluation of the ubiquitin-proteasome system in Parkinson's disease. *Biochim Biophys Acta, 1792*(7), 664-675. doi: 10.1016/j.bbadis.2009.01.012

Corcoran, G. B., & Wong, B. K. (1986). Role of glutathione in prevention of acetaminophen-induced hepatotoxicity by N-acetyl-L-cysteine in vivo: studies with N-acetyl-D-cysteine in mice. *J Pharmacol Exp Ther, 238*(1), 54-61.

Crouch, S. P., Kozlowski, R., Slater, K. J., & Fletcher, J. (1993). The use of ATP bioluminescence as a measure of cell proliferation and cytotoxicity. *J Immunol Methods, 160*(1), 81-88.

Crum, T. S., Gleixner, A. M., Posimo, J. M., Mason, D. M., Broeren, M. T., Heinemann, S. D., . . . Leak, R. K. (2015a). Heat shock protein responses to aging and proteotoxicity in the olfactory bulb. *J Neurochem, 133*(6), 780-794. doi: 10.1111/jnc.13041

Crum, T. S., Gleixner, A. M., Posimo, J. M., Mason, D. M., Broeren, M. T., Heinemann, S. D., . . . Leak, R. K. (2015b). Heat shock protein responses to aging and proteotoxicity in the olfactory bulb. *J Neurochem. 133*(6), 780-794. doi: 10.1111/jnc.13041

Cuanalo-Contreras, K., Mukherjee, A., & Soto, C. (2013). Role of protein misfolding and proteostasis deficiency in protein misfolding diseases and aging. *Int J Cell Biol, 2013*, 638083. doi: 10.1155/2013/638083

Cuervo, A. M., Stefanis, L., Fredenburg, R., Lansbury, P. T., & Sulzer, D. (2004). Impaired degradation of mutant alpha-synuclein by chaperone-mediated autophagy. *Science, 305*(5688), 1292-1295. doi: 10.1126/science.1101738

Damier, P., Hirsch, E. C., Zhang, P., Agid, Y., & Javoy-Agid, F. (1993). Glutathione peroxidase, glial cells and Parkinson's disease. *Neuroscience, 52*(1), 1-6.

Dasuri, K., Ebenezer, P. J., Zhang, L., Fernandez-Kim, S. O., Uranga, R. M., Gavilan, E., . . . Keller, J. N. (2010). Selective vulnerability of neurons to acute toxicity after proteasome inhibitor treatment: implications for oxidative stress and insolubility of newly synthesized proteins. *Free Radic Biol Med, 49*(8), 1290-1297. doi: 10.1016/j.freeradbiomed.2010.07.014

David, D. C., Ollikainen, N., Trinidad, J. C., Cary, M. P., Burlingame, A. L., & Kenyon, C. (2010). Widespread protein aggregation as an inherent part of aging in C. elegans. *PLoS Biol, 8*(8), e1000450. doi: 10.1371/journal.pbio.1000450

Davies, K. J. (1987). Protein damage and degradation by oxygen radicals. I. general aspects. *J Biol Chem, 262*(20), 9895-9901.

Davis, R. K., Stevenson, G. T., & Busch, K. A. (1956). Tumor incidence in normal Sprague-Dawley female rats. *Cancer Res, 16*(3), 194-197.

Deveraux, Q., Ustrell, V., Pickart, C., & Rechsteiner, M. (1994). A 26 S protease subunit that binds ubiquitin conjugates. *J Biol Chem, 269*(10), 7059-7061.

Di Domenico, F., Sultana, R., Tiu, G. F., Scheff, N. N., Perluigi, M., Cini, C., & Butterfield, D. A. (2010). Protein levels of heat shock proteins 27, 32, 60, 70, 90 and thioredoxin-1 in amnestic mild cognitive impairment: an investigation on the role of cellular stress response in the progression of Alzheimer disease. *Brain Res, 1333*, 72-81. doi: 10.1016/j.brainres.2010.03.085

Dickey, C., Kraft, C., Jinwal, U., Koren, J., Johnson, A., Anderson, L., . . . Lewis, J. (2009). Aging analysis reveals slowed tau turnover and enhanced stress response in a mouse model of tauopathy. *Am J Pathol, 174*(1), 228-238. doi: 10.2353/ajpath.2009.080764

Ding, W. X., Ni, H. M., Gao, W., Yoshimori, T., Stolz, D. B., Ron, D., & Yin, X. M. (2007). Linking of autophagy to ubiquitin-proteasome system is important for the regulation of endoplasmic reticulum stress and cell viability. *Am J Pathol, 171*(2), 513-524. 10.2353/ajpath.2007.070188

Dinkova-Kostova, A. T. (2012). The Role of Sulfhydryl Reactivity of Small Molecules for the Activation of the KEAP1/NRF2 Pathway and the Heat Shock Response. [Review]. *Scientifica, 2012*, 606104. doi: 10.6064/2012/606104

Dringen, R. (2000). Metabolism and functions of glutathione in brain. *Prog Neurobiol, 62*(6), 649-671. Dringen, R., Gutterer, J. M., & Hirrlinger, J. (2000). Glutathione metabolism in brain metabolic interaction between astrocytes and neurons in the defense against reactive oxygen species. *Eur J Biochem, 267*(16), 4912-4916.

Dringen, R., Pfeiffer, B., & Hamprecht, B. (1999). Synthesis of the antioxidant glutathione in neurons: supply by astrocytes of CysGly as precursor for neuronal glutathione. *J Neurosci, 19*(2), 562-569.

Driver, A. S., Kodavanti, P. R., & Mundy, W. R. (2000). Age-related changes in reactive oxygen species production in rat brain homogenates. *Neurotoxicol Teratol, 22*(2), 175-181. Drummond, G. S., & Kappas, A. (1981). Prevention of neonatal hyperbilirubinemia by tin protoporphyrin IX, a potent competitive inhibitor of heme oxidation. *Proc Natl Acad Sci U S A, 78*(10), 6466-6470.

Elmore, S. (2007). Apoptosis: a review of programmed cell death. *Toxicol Pathol, 35*(4), 495-516. doi: 10.1080/01926230701320337

Emsley, J. G., & Macklis, J. D. (2006). Astroglial heterogeneity closely reflects the neuronal-defined anatomy of the adult murine CNS. *Neuron Glia Biol, 2*(3), 175-186. doi: 10.1017/S1740925X06000202

Eng, L. F., Ghirnikar, R. S., & Lee, Y. L. (2000). Glial fibrillary acidic protein: GFAP-thirty-one years (1969-2000). *Neurochem Res, 25*(9-10), 1439-1451.

Ewing, J. F., & Maines, M. D. (2006). Regulation and expression of heme oxygenase enzymes in aged-rat brain: age related depression in HO-1 and HO-2 expression

and altered stress-response. *J Neural Transm, 113*(4), 439-454. doi: 10.1007/s00702-005-0408-z

Fewell, S. W., Smith, C. M., Lyon, M. A., Dumitrescu, T. P., Wipf, P., Day, B. W., & Brodsky, J. L. (2004). Small molecule modulators of endogenous and co-chaperone-stimulated Hsp70 ATPase activity. *J Biol Chem, 279*(49), 51131-51140. doi: 10.1074/jbc.M404857200

Floyd, R. A., & Carney, J. M. (1992). Free radical damage to protein and DNA: mechanisms involved and relevant observations on brain undergoing oxidative stress. *Ann Neurol, 32 Suppl*, S22-27.

Fogal, B., Li, J., Lobner, D., McCullough, L. D., & Hewett, S. J. (2007). System x(c)- activity and astrocytes are necessary for interleukin-1 beta-mediated hypoxic neuronal injury. *J Neurosci, 27*(38), 10094-10105. doi: 10.1523/JNEUROSCI.2459-07.2007

Fourquet, S., Guerois, R., Biard, D., & Toledano, M. B. (2010). Activation of NRF2 by nitrosative agents and H2O2 involves KEAP1 disulfide formation. *J Biol Chem, 285*(11), 8463-8471. doi: 10.1074/jbc.M109.051714

Franklin, C. C., Backos, D. S., Mohar, I., White, C. C., Forman, H. J., & Kavanagh, T. J. (2009). Structure, function, and post-translational regulation of the catalytic and modifier subunits of glutamate cysteine ligase. *Mol Aspects Med, 30*(1-2), 86-98. doi: 10.1016/j.mam.2008.08.009

Fratiglioni, L., Viitanen, M., von Strauss, E., Tontodonati, V., Herlitz, A., & Winblad, B. (1997). Very old women at highest risk of dementia and Alzheimer's disease: incidence data from the Kungsholmen Project, Stockholm. *Neurology, 48*(1), 132-138.

Friedman, M., & Levin, C. E. (2012). Nutritional and medicinal aspects of D-amino acids. *Amino Acids, 42*(5), 1553-1582. doi: 10.1007/s00726-011-0915-1

Gabryel, B., Toborek, T., & Malecki, A. (2005). Immunosuppressive immunophilin ligands attenuate damage in cultured rat astrocytes depleted of glutathione and exposed to simulated ischemia in vitro. Comparison with N-acetylcysteine. [Research Support, Non-U.S. Gov't]. *Neurotoxicology, 26*(3), 373-384. doi: 10.1016/j.neuro.2005.03.004

Gao, C., Wang, C., Liu, B., Wu, H., Yang, Q., Jin, J., . . . Zhang, H. (2014). Intermittent hypoxia preconditioning-induced epileptic tolerance by upregulation of monocarboxylate transporter 4 expression in rat hippocampal astrocytes. *Neurochem Res, 39*(11), 2160-2169. doi: 10.1007/s11064-014-1411-2

Garnier, P., Demougeot, C., Bertrand, N., Prigent-Tessier, A., Marie, C., & Beley, A. (2001). Stress response to hypoxia in gerbil brain: HO-1 and Mn SOD expression and glial activation. *Brain Res, 893*(1-2), 301-309.Gatz, M., Reynolds, C. A., Fratiglioni, L., Johansson, B., Mortimer, J. A., Berg, S., . . . Pedersen, N. L. (2006). Role of genes and environments for explaining Alzheimer disease. *Arch Gen Psychiatry, 63*(2), 168-174. doi: 10.1001/archpsyc.63.2.168

Gavrieli, Y., Sherman, Y., & Ben-Sasson, S. A. (1992). Identification of programmed cell death in situ via specific labeling of nuclear DNA fragmentation. *J Cell Biol, 119*(3), 493-501.

George Paxinos, C. W. (1998). *The rat brain in stereotaxic coordinates*. San Diego, CA: Academic Press.

Gibb, W. R., & Lees, A. J. (1991). Anatomy, pigmentation, ventral and dorsal subpopulations of the substantia nigra, and differential cell death in Parkinson's disease. *J Neurol Neurosurg Psychiatry, 54*(5), 388-396.

Giustarini, D., Milzani, A., Dalle-Donne, I., Tsikas, D., & Rossi, R. (2012). N-Acetylcysteine ethyl ester (NACET): a novel lipophilic cell-permeable cysteine derivative with an unusual pharmacokinetic feature and remarkable antioxidant potential. *Biochem Pharmacol, 84*(11), 1522-1533. doi: 10.1016/j.bcp.2012.09.010

Gleixner, A. M., Pulugulla, S. H., Pant, D. B., Posimo, J. M., Crum, T. S., & Leak, R. K. (2014). Impact of aging on heat shock protein expression in the substantia nigra and striatum of the female rat. *Cell Tissue Res, 357*(1), 43-54. doi: 10.1007/s00441-014-1852-6

Gong, N., Gao, Z. Y., Wang, Y. C., Li, X. Y., Huang, J. L., Hashimoto, K., & Wang, Y. X. (2011). A series of D-amino acid oxidase inhibitors specifically prevents and reverses formalin-induced tonic pain in rats. *J Pharmacol Exp Ther, 336*(1), 282-293. doi: 10.1124/jpet.110.172353

Gouix, E., Buisson, A., Nieoullon, A., Kerkerian-Le Goff, L., Tauskela, J. S., Blondeau, N., & Had-Aissouni, L. (2014). Oxygen glucose deprivation-induced astrocyte dysfunction provokes neuronal death through oxidative stress. *Pharmacol Res, 87*, 8-17. doi: 10.1016/j.phrs.2014.06.002

Granato, M., Lacconi, V., Peddis, M., Lotti, L. V., Renzo, L. D., Gonnella, R., . . . Cirone, M. (2013). HSP70 inhibition by 2-phenylethynesulfonamide induces lysosomal cathepsin D release and immunogenic cell death in primary effusion lymphoma. *Cell Death Dis, 4*, e730. doi: 10.1038/cddis.2013.263

Grant, J. E., Odlaug, B. L., & Kim, S. W. (2009). N-acetylcysteine, a glutamate modulator, in the treatment of trichotillomania: a double-blind, placebo-controlled study. *Arch Gen Psychiatry, 66*(7), 756-763. doi: 10.1001/archgenpsychiatry.2009.60

Griffith, O. W. (1982). Mechanism of action, metabolism, and toxicity of buthionine sulfoximine and its higher homologs, potent inhibitors of glutathione synthesis. *J Biol Chem, 257*(22), 13704-13712.

Griffith, O. W., & Meister, A. (1979). Potent and specific inhibition of glutathione synthesis by buthionine sulfoximine (S-n-butyl homocysteine sulfoximine). *J Biol Chem, 254*(16), 7558-7560.

Gundersen, V. (2010). Protein aggregation in Parkinson's disease. [Review]. *Acta neurologica Scandinavica. Supplementum*, (190), 82-87. doi: 10.1111/j.1600-0404.2010.01382.x

Guo, S., Wharton, W., Moseley, P., & Shi, H. (2007). Heat shock protein 70 regulates cellular redox status by modulating glutathione-related enzyme activities. *Cell Stress Chaperones, 12*(3), 245-254.

Gupte, A. A., Morris, J. K., Zhang, H., Bomhoff, G. L., Geiger, P. C., & Stanford, J. A. (2010). Age-related changes in HSP25 expression in basal ganglia and cortex of F344/BN rats. *Neurosci Lett, 472*(2), 90-93. doi: 10.1016/j.neulet.2010.01.049

Halliwell, B. (2014). Cell culture, oxidative stress, and antioxidants: avoiding pitfalls. *Biomed J, 37*(3), 99-105. doi: 10.4103/2319-4170.128725

Hardy, J., & Selkoe, D. J. (2002). The amyloid hypothesis of Alzheimer's disease: progress and problems on the road to therapeutics. *Science, 297*(5580), 353-356. doi: 10.1126/science.1072994

Hatic, H., Kane, M. J., Saykally, J. N., & Citron, B. A. (2012). Modulation of transcription factor Nrf2 in an in vitro model of traumatic brain injury. [Research Support, Non-U.S. Gov'tResearch Support, U.S. Gov't, Non-P.H.S.]. *Journal of neurotrauma, 29*(6), 1188-1196. doi: 10.1089/neu.2011.1806

Hawkes, C. H., Del Tredici, K., & Braak, H. (2009). Parkinson's disease: the dual hit theory revisited. *Ann N Y Acad Sci, 1170*, 615-622. doi: 10.1111/j.1749-6632.2009.04365.x

Hebert, L. E., Weuve, J., Scherr, P. A., & Evans, D. A. (2013). Alzheimer disease in the United States (2010-2050) estimated using the 2010 census. *Neurology, 80*(19), 1778-1783. doi: 10.1212/WNL.0b013e31828726f5

Hewett, J. A. (2009). Determinants of regional and local diversity within the astroglial lineage of the normal central nervous system. *J Neurochem, 110*(6), 1717-1736. doi: 10.1111/j.1471-4159.2009.06288.x

Hill, S. J., Barbarese, E., & McIntosh, T. K. (1996). Regional heterogeneity in the response of astrocytes following traumatic brain injury in the adult rat. *J Neuropathol Exp Neurol, 55*(12), 1221-1229.

Hoffer, E., Baum, Y., Tabak, A., & Taitelman, U. (1996). N-acetylcysteine increases the glutathione content and protects rat alveolar type II cells against paraquat-induced cytotoxicity. *Toxicol Lett, 84*(1), 7-12.

Hoffer, M. E., Balaban, C., Slade, M. D., Tsao, J. W., & Hoffer, B. (2013). Amelioration of acute sequelae of blast induced mild traumatic brain injury by N-acetyl cysteine: a double-blind, placebo controlled study. *PLoS One, 8*(1), e54163. doi: 10.1371/journal.pone.0054163

Holmay, M. J., Terpstra, M., Coles, L. D., Mishra, U., Ahlskog, M., Oz, G., . . . Tuite, P. J. (2013). N-Acetylcysteine boosts brain and blood glutathione in Gaucher and Parkinson diseases. *Clin Neuropharmacol, 36*(4), 103-106. doi: 10.1097/WNF.0b013e31829ae713

Hu, R., Xu, C., Shen, G., Jain, M. R., Khor, T. O., Gopalkrishnan, A., . . . Kong, A. N. (2006). Gene expression profiles induced by cancer chemopreventive isothiocyanate sulforaphane in the liver of C57BL/6J mice and C57BL/6J/Nrf2 (-/-) mice. [Research Support, N.I.H., Extramural]. *Cancer Lett, 243*(2), 170-192. doi: 10.1016/j.canlet.2005.11.050

Huang, C. S., Chang, L. S., Anderson, M. E., & Meister, A. (1993). Catalytic and regulatory properties of the heavy subunit of rat kidney gamma-glutamylcysteine synthetase. *J Biol Chem, 268*(26), 19675-19680.

Huang, Q., & Figueiredo-Pereira, M. E. (2010). Ubiquitin/proteasome pathway impairment in neurodegeneration: therapeutic implications. *Apoptosis, 15*(11), 1292-1311. doi: 10.1007/s10495-010-0466-z

Hurd, M. D., Martorell, P., & Langa, K. M. (2013). Monetary costs of dementia in the United States. *N Engl J Med, 369*(5), 489-490. doi: 10.1056/NEJMc1305541

Hurd, R. W., Wilder, B. J., Helveston, W. R., & Uthman, B. M. (1996). Treatment of four siblings with progressive myoclonus epilepsy of the Unverricht-Lundborg type with N-acetylcysteine. *Neurology, 47*(5), 1264-1268.

Huryn, D. M., Brodsky, J. L., Brummond, K. M., Chambers, P. G., Eyer, B., Ireland, A. W., . . . Wipf, P. (2011). Chemical methodology as a source of small-molecule checkpoint inhibitors and heat shock protein 70 (Hsp70) modulators. [Research Support, N.I.H., Extramural Research Support, Non-U.S. Gov't]. *Proc Natl Acad Sci U S A, 108*(17), 6757-6762. doi: 10.1073/pnas.1015251108

Hussain, S. G., & Ramaiah, K. V. (2007). Reduced eIF2alpha phosphorylation and increased proapoptotic proteins in aging. *Biochem Biophys Res Commun, 355*(2), 365-370. doi: 10.1016/j.bbrc.2007.01.156

Jackman, N. A., Melchior, S. E., Hewett, J. A., & Hewett, S. J. (2012). Non-cell autonomous influence of the astrocyte system xc- on hypoglycaemic neuronal cell death. *ASN Neuro, 4*(1). doi: 10.1042/AN20110030

Jacobson, A. D., Zhang, N. Y., Xu, P., Han, K. J., Noone, S., Peng, J., & Liu, C. W. (2009). The lysine 48 and lysine 63 ubiquitin conjugates are processed differently by the 26 s proteasome. *J Biol Chem, 284*(51), 35485-35494. doi: 10.1074/jbc.M109.052928

Jana, A., & Pahan, K. (2010). Fibrillar amyloid-beta-activated human astroglia kill primary human neurons via neutral sphingomyelinase: implications for Alzheimer's disease. *J Neurosci, 30*(38), 12676-12689. doi: 10.1523/JNEUROSCI.1243-10.2010

Jenner, P. (1992). Parkinson's disease: pathological mechanisms and actions of piribedil. *J Neurol, 239*(Suppl. 1), S2-8.

Jenner, P., Dexter, D. T., Sian, J., Schapira, A. H., & Marsden, C. D. (1992). Oxidative stress as a cause of nigral cell death in Parkinson's disease and incidental Lewy body disease. The Royal Kings and Queens Parkinson's Disease Research Group. *Ann Neurol, 32*(Supp. L), S82-87.

Jiang, Y., Rumble, J. L., Gleixner, A. M., Unnithan, A. S., Pulugulla, S. H., Posimo, J. M., . . . Leak, R. K. (2013). N-Acetyl cysteine blunts proteotoxicity in a heat shock protein-dependent manner. *Neuroscience, 255*, 19-32. doi: 10.1016/j.neuroscience.2013.09.049

Johnson, J. A., el Barbary, A., Kornguth, S. E., Brugge, J. F., & Siegel, F. L. (1993). Glutathione S-transferase isoenzymes in rat brain neurons and glia. *J Neurosci, 13*(5), 2013-2023.

Katane, M., Osaka, N., Matsuda, S., Maeda, K., Kawata, T., Saitoh, Y., . . . Homma, H. (2013). Identification of novel D-amino acid oxidase inhibitors by in silico screening and their functional characterization in vitro. *J Med Chem, 56*(5), 1894-1907. doi: 10.1021/jm3017865

Kaushik, S., & Cuervo, A. M. (2012). Chaperone-mediated autophagy: a unique way to enter the lysosome world. *Trends Cell Biol, 22*(8), 407-417. doi: 10.1016/j.tcb.2012.05.006

Keller, J. N., Gee, J., & Ding, Q. (2002). The proteasome in brain aging. *Ageing Res Rev, 1*(2), 279-293. Keller, J. N., Hanni, K. B., & Markesbery, W. R. (2000a). Impaired proteasome function in Alzheimer's disease. *J Neurochem, 75*(1), 436-439.

Keller, J. N., Hanni, K. B., & Markesbery, W. R. (2000b). Possible involvement of proteasome inhibition in aging: implications for oxidative stress. *Mech Ageing Dev, 113*(1), 61-70.

Keller, J. N., Huang, F. F., & Markesbery, W. R. (2000). Decreased levels of proteasome activity and proteasome expression in aging spinal cord. *Neuroscience, 98*(1), 149-156. Kilpatrick, K., Novoa, J. A., Hancock, T., Guerriero, C. J., Wipf, P., Brodsky, J. L., & Segatori, L. (2013). Chemical Induction of Hsp70 Reduces alpha-Synuclein Aggregation in Neuroglioma Cells. *ACS Chem Biol, 8*(7), 1460-1468. doi: 10.1021/cb400017h

Kimelberg, H. K., & Nedergaard, M. (2010). Functions of astrocytes and their potential as therapeutic targets. *Neurotherapeutics, 7*(4), 338-353. doi: 10.1016/j.nurt.2010.07.006

Kish, S. J., Shannak, K., Rajput, A., Deck, J. H., & Hornykiewicz, O. (1992). Aging produces a specific pattern of striatal dopamine loss: implications for the etiology of idiopathic Parkinson's disease. *J Neurochem, 58*(2), 642-648.

Kisselev, A. F., & Goldberg, A. L. (2001). Proteasome inhibitors: from research tools to drug candidates. *Chem Biol, 8*(8), 739-758.

Kondoh, Y., & Osada, H. (2013). High-throughput screening identifies small molecule inhibitors of molecular chaperones. *Current pharmaceutical design, 19*(3), 473-492.

Korolainen, M. A., Auriola, S., Nyman, T. A., Alafuzoff, I., & Pirttila, T. (2005). Proteomic analysis of glial fibrillary acidic protein in Alzheimer's disease and aging brain. *Neurobiol Dis, 20*(3), 858-870. doi: 10.1016/j.nbd.2005.05.021

Korolchuk, V. I., Menzies, F. M., & Rubinsztein, D. C. (2010). Mechanisms of cross-talk between the ubiquitin-proteasome and autophagy-lysosome systems. *FEBS Lett, 584*(7), 1393-1398. doi: 10.1016/j.febslet.2009.12.047

Kowal, S. L., Dall, T. M., Chakrabarti, R., Storm, M. V., & Jain, A. (2013). The current and projected economic burden of Parkinson's disease in the United States. *Mov Disord, 28*(3), 311-318. doi: 10.1002/mds.25292

Kozoriz, M. G., Bechberger, J. F., Bechberger, G. R., Suen, M. W., Moreno, A. P., Maass, K., . . . Naus, C. C. (2010). The connexin43 C-terminal region mediates neuroprotection during stroke. *J Neuropathol Exp Neurol, 69*(2), 196-206. doi: 10.1097/NEN.0b013e3181cd44df

Kwak, M. K., Wakabayashi, N., Itoh, K., Motohashi, H., Yamamoto, M., & Kensler, T. W. (2003). Modulation of gene expression by cancer chemopreventive dithiolethiones through the Keap1-Nrf2 pathway. Identification of novel gene clusters for cell survival. [Research Support, U.S. Gov't, P.H.S.]. *J Biol Chem, 278*(10), 8135-8145. doi: 10.1074/jbc.M211898200

Lancaster, G. I., & Febbraio, M. A. (2005). Exosome-dependent trafficking of HSP70: a novel secretory pathway for cellular stress proteins. *J Biol Chem, 280*(24), 23349-23355. doi: 10.1074/jbc.M502017200

Lanneau, D., Wettstein, G., Bonniaud, P., & Garrido, C. (2010). Heat shock proteins: cell protection through protein triage. *ScientificWorldJournal, 10*, 1543-1552. doi: 10.1100/tsw.2010.152

Lavoie, S., Murray, M. M., Deppen, P., Knyazeva, M. G., Berk, M., Boulat, O., . . . Do, K. Q. (2008). Glutathione precursor, N-acetyl-cysteine, improves mismatch negativity in schizophrenia patients. *Neuropsychopharmacology, 33*(9), 2187-2199. doi: 10.1038/sj.npp.1301624

Le Prince, G., Delaere, P., Fages, C., Duyckaerts, C., Hauw, J. J., & Tardy, M. (1993). Alterations of glial fibrillary acidic protein mRNA level in the aging brain and in senile dementia of the Alzheimer type. *Neurosci Lett, 151*(1), 71-73.

Leak, R. K. (2014). Adaptation and sensitization to proteotoxic stress. *Dose-response : a publication of International Hormesis Society, 12*(1), 24-56. doi: 10.2203/dose-response.13-016.Leak

Leak, R. K., Castro, S. L., Jaumotte, J. D., Smith, A. D., & Zigmond, M. J. (2010). Assaying multiple biochemical variables from the same tissue sample. *J Neurosci Methods, 191*(2), 234-238. doi: 10.1016/j.jneumeth.2010.06.023

Lecker, S. H., Goldberg, A. L., & Mitch, W. E. (2006). Protein degradation by the ubiquitin-proteasome pathway in normal and disease states. *J Am Soc Nephrol, 17*(7), 1807-1819. doi: 10.1681/ASN.2006010083

Lee, C. K., Weindruch, R., & Prolla, T. A. (2000). Gene-expression profile of the ageing brain in mice. *Nat Genet, 25*(3), 294-297. doi: 10.1038/77046

Lee, D. H., & Goldberg, A. L. (1998). Proteasome inhibitors: valuable new tools for cell biologists. *Trends Cell Biol, 8*(10), 397-403.

Lee, H. C., & Wei, Y. H. (2012). Mitochondria and aging. *Adv Exp Med Biol, 942*, 311-327. doi: 10.1007/978-94-007-2869-1_14

Leu, J. I., Pimkina, J., Frank, A., Murphy, M. E., & George, D. L. (2009). A small molecule inhibitor of inducible heat shock protein 70. *Mol Cell, 36*(1), 15-27. doi: 10.1016/j.molcel.2009.09.023

Leu, J. I., Pimkina, J., Pandey, P., Murphy, M. E., & George, D. L. (2011). HSP70 inhibition by the small-molecule 2-phenylethynesulfonamide impairs protein clearance pathways in tumor cells. *Mol Cancer Res, 9*(7), 936-947. doi: 10.1158/1541-7786.MCR-11-0019

Lindersson, E., Beedholm, R., Hojrup, P., Moos, T., Gai, W., Hendil, K. B., & Jensen, P. H. (2004). Proteasomal inhibition by alpha-synuclein filaments and oligomers. *J Biol Chem, 279*(13), 12924-12934. doi: 10.1074/jbc.M306390200

Lindsay, J., Laurin, D., Verreault, R., Hebert, R., Helliwell, B., Hill, G. B., & McDowell, I. (2002). Risk factors for Alzheimer's disease: a prospective analysis from the Canadian Study of Health and Aging. *Am J Epidemiol, 156*(5), 445-453.

Liu, Z., Li, Y., Cui, Y., Roberts, C., Lu, M., Wilhelmsson, U., . . . Chopp, M. (2014). Beneficial effects of gfap/vimentin reactive astrocytes for axonal remodeling and motor behavioral recovery in mice after stroke. *Glia, 62*(12), 2022-2033. doi: 10.1002/glia.22723

Lu, S. C. (2009). Regulation of glutathione synthesis. *Mol Aspects Med, 30*(1-2), 42-59. doi: 10.1016/j.mam.2008.05.005

Lu, S. C. (2013). Glutathione synthesis. *Biochim Biophys Acta, 1830*(5), 3143-3153. doi: 10.1016/j.bbagen.2012.09.008

Lu, Z., & Cyr, D. M. (1998). Protein folding activity of Hsp70 is modified differentially by the hsp40 co-chaperones Sis1 and Ydj1. *J Biol Chem, 273*(43), 27824-27830.

Maharjan, S., Oku, M., Tsuda, M., Hoseki, J., & Sakai, Y. (2014). Mitochondrial impairment triggers cytosolic oxidative stress and cell death following proteasome inhibition. *Sci Rep, 4*, 5896. doi: 10.1038/srep05896

Maher, P. (2005). The effects of stress and aging on glutathione metabolism. *Ageing Res Rev, 4*(2), 288-314. doi: 10.1016/j.arr.2005.02.005

Makar, T. K., Nedergaard, M., Preuss, A., Gelbard, A. S., Perumal, A. S., & Cooper, A. J. (1994). Vitamin E, ascorbate, glutathione, glutathione disulfide, and enzymes of glutathione metabolism in cultures of chick astrocytes and neurons: evidence that astrocytes play an important role in antioxidative processes in the brain. *J Neurochem, 62*(1), 45-53.

Maragakis, N. J., & Rothstein, J. D. (2006). Mechanisms of Disease: astrocytes in neurodegenerative disease. *Nat Clin Pract Neurol, 2*(12), 679-689. doi: 10.1038/ncpneuro0355

Markesbery, W. R. (1997). Oxidative stress hypothesis in Alzheimer's disease. *Free Radic Biol Med, 23*(1), 134-147.

Martinez-Vicente, M., Sovak, G., & Cuervo, A. M. (2005). Protein degradation and aging. *Exp Gerontol, 40*(8-9), 622-633. doi: 10.1016/j.exger.2005.07.005

Massey, A. J., Williamson, D. S., Browne, H., Murray, J. B., Dokurno, P., Shaw, T., . . . Wood, M. (2010). A novel, small molecule inhibitor of Hsc70/Hsp70 potentiates Hsp90 inhibitor induced apoptosis in HCT116 colon carcinoma cells. *Cancer Chemother Pharmacol, 66*(3), 535-545. doi: 10.1007/s00280-009-1194-3

Mateo, I., Infante, J., Sanchez-Juan, P., Garcia-Gorostiaga, I., Rodriguez-Rodriguez, E., Vazquez-Higuera, J. L., . . . Combarros, O. (2010). Serum heme oxygenase-1 levels are increased in Parkinson's disease but not in Alzheimer's disease. *Acta Neurol Scand, 121*(2), 136-138. doi: 10.1111/j.1600-0404.2009.01261.x

Mayer, M. P., & Bukau, B. (2005). Hsp70 chaperones: cellular functions and molecular mechanism. *Cell Mol Life Sci, 62*(6), 670-684. doi: 10.1007/s00018-004-4464-6

Mazzetti, A. P., Fiorile, M. C., Primavera, A., & Lo Bello, M. (2015). Glutathione transferases and neurodegenerative diseases. *Neurochem Int, 82*, 10-18. doi: 10.1016/j.neuint.2015.01.008

McCormack, A. L., Di Monte, D. A., Delfani, K., Irwin, I., DeLanney, L. E., Langston, W. J., & Janson, A. M. (2004). Aging of the nigrostriatal system in the squirrel monkey. *J Comp Neurol, 471*(4), 387-395. doi: 10.1002/cne.20036

McCormack, A. L., Thiruchelvam, M., Manning-Bog, A. B., Thiffault, C., Langston, J. W., Cory-Slechta, D. A., & Di Monte, D. A. (2002). Environmental risk factors and Parkinson's disease: selective degeneration of nigral dopaminergic neurons caused by the herbicide paraquat. *Neurobiol Dis, 10*(2), 119-127.McLean, P. J., Klucken, J., Shin, Y., & Hyman, B. T. (2004). Geldanamycin induces Hsp70 and prevents alpha-synuclein aggregation and toxicity in vitro. *Biochem Biophys Res Commun, 321*(3), 665-669. doi: 10.1016/j.bbrc.2004.07.021

McNaught, K. S., Belizaire, R., Isacson, O., Jenner, P., & Olanow, C. W. (2003). Altered proteasomal function in sporadic Parkinson's disease. *Exp Neurol, 179*(1), 38-46.

McNaught, K. S., & Jenner, P. (2001). Proteasomal function is impaired in substantia nigra in Parkinson's disease. *Neurosci Lett, 297*(3), 191-194.

McNaught, K. S., Shashidharan, P., Perl, D. P., Jenner, P., & Olanow, C. W. (2002). Aggresome-related biogenesis of Lewy bodies. *Eur J Neurosci, 16*(11), 2136-2148.

Mecocci, P., MacGarvey, U., Kaufman, A. E., Koontz, D., Shoffner, J. M., Wallace, D. C., & Beal, M. F. (1993). Oxidative damage to mitochondrial DNA shows marked age-dependent increases in human brain. *Ann Neurol, 34*(4), 609-616. doi: 10.1002/ana.410340416

Mega, M. S., Cummings, J. L., Fiorello, T., & Gornbein, J. (1996). The spectrum of behavioral changes in Alzheimer's disease. *Neurology, 46*(1), 130-135.
Meister, A., & Anderson, M. E. (1983). Glutathione. *Annu Rev Biochem, 52*, 711-760. doi: 10.1146/annurev.bi.52.070183.003431
Messing, A., Brenner, M., Feany, M. B., Nedergaard, M., & Goldman, J. E. (2012). Alexander disease. *J Neurosci, 32*(15), 5017-5023. doi: 10.1523/JNEUROSCI.5384-11.2012
Messing, A., Head, M. W., Galles, K., Galbreath, E. J., Goldman, J. E., & Brenner, M. (1998). Fatal encephalopathy with astrocyte inclusions in GFAP transgenic mice. *Am J Pathol, 152*(2), 391-398.
Middeldorp, J., & Hol, E. M. (2011). GFAP in health and disease. *Prog Neurobiol, 93*(3), 421-443. doi: 10.1016/j.pneurobio.2011.01.005
Miller, F. D., & Gauthier, A. S. (2007). Timing is everything: making neurons versus glia in the developing cortex. *Neuron, 54*(3), 357-369. doi: 10.1016/j.neuron.2007.04.019
Miller, R. H., & Raff, M. C. (1984). Fibrous and protoplasmic astrocytes are biochemically and developmentally distinct. *J Neurosci, 4*(2), 585-592.
Miyata, Y., Rauch, J. N., Jinwal, U. K., Thompson, A. D., Srinivasan, S., Dickey, C. A., & Gestwicki, J. E. (2012). Cysteine reactivity distinguishes redox sensing by the heat-inducible and constitutive forms of heat shock protein 70. *Chem Biol, 19*(11), 1391-1399. doi: 10.1016/j.chembiol.2012.07.026
Morimoto, R. I. (2008). Proteotoxic stress and inducible chaperone networks in neurodegenerative disease and aging. *Genes Dev, 22*(11), 1427-1438. doi: 10.1101/gad.1657108
Muller, F. L., Lustgarten, M. S., Jang, Y., Richardson, A., & Van Remmen, H. (2007). Trends in oxidative aging theories. *Free Radic Biol Med, 43*(4), 477-503. doi: 10.1016/j.freeradbiomed.2007.03.034
Muthukumar, S., Rajkumar, R., Karthikeyan, K., Liao, C. C., Singh, D., Akbarsha, M. A., & Archunan, G. (2014). Buffalo cervico-vaginal fluid proteomics with special reference to estrous cycle: heat shock protein (HSP)-70 appears to be an estrus indicator. *Biol Reprod, 90*(5), 97. doi: 10.1095/biolreprod.113.113852
Mythri, R. B., Venkateshappa, C., Harish, G., Mahadevan, A., Muthane, U. B., Yasha, T. C., . . . Shankar, S. K. (2011). Evaluation of markers of oxidative stress, antioxidant function and astrocytic proliferation in the striatum and frontal cortex of Parkinson's disease brains. *Neurochem Res, 36*(8), 1452-1463. doi: 10.1007/s11064-011-0471-9
Nakase, T., Sohl, G., Theis, M., Willecke, K., & Naus, C. C. (2004). Increased apoptosis and inflammation after focal brain ischemia in mice lacking connexin43 in astrocytes. *Am J Pathol, 164*(6), 2067-2075. doi:10.1016/S0002-9440(10)63765-0
Nawashiro, H., Messing, A., Azzam, N., & Brenner, M. (1998). Mice lacking GFAP are hypersensitive to traumatic cerebrospinal injury. *Neuroreport, 9*(8), 1691-1696.
Nixon, R. A., Wegiel, J., Kumar, A., Yu, W. H., Peterhoff, C., Cataldo, A., & Cuervo, A. M. (2005). Extensive involvement of autophagy in Alzheimer disease: an immuno-electron microscopy study. *J Neuropathol Exp Neurol, 64*(2), 113-122.

Olsson, B., Johansson, M., Gabrielsson, J., & Bolme, P. (1988). Pharmacokinetics and bioavailability of reduced and oxidized N-acetylcysteine. *Eur J Clin Pharmacol, 34*(1), 77-82.

Ostrowska, H., Wojcik, C., Omura, S., & Worowski, K. (1997). Lactacystin, a specific inhibitor of the proteasome, inhibits human platelet lysosomal cathepsin A-like enzyme. *Biochem Biophys Res Commun, 234*(3), 729-732. doi: 10.1006/bbrc.1997.6434

Owen, J. B., & Butterfield, D. A. (2010). Measurement of oxidized/reduced glutathione ratio. *Methods Mol Biol, 648*, 269-277. doi: 10.1007/978-1-60761-756-3_18

Pang, Y., Chai, C. R., Gao, K., Jia, X. H., Kong, J. G., Chen, X. Q., . . . Yu, A. C. (2015). Ischemia preconditioning protects astrocytes from ischemic injury through 14-3-3gamma. *J Neurosci Res, 93*(10), 1507-1518. doi: 10.1002/jnr.23574

Panter, S. S., McSwigan, J. D., Sheppard, J. R., Emory, C. R., & Frey, W. H., 2nd. (1985). Glial fibrillary acidic protein and Alzheimer's disease. *Neurochem Res, 10*(12), 1567-1576.

Paz Gavilan, M., Vela, J., Castano, A., Ramos, B., del Rio, J. C., Vitorica, J., & Ruano, D. (2006). Cellular environment facilitates protein accumulation in aged rat hippocampus. *Neurobiol Aging, 27*(7), 973-982. doi: 10.1016/j.neurobiolaging.2005.05.010

Pearce, R. K., Owen, A., Daniel, S., Jenner, P., & Marsden, C. D. (1997). Alterations in the distribution of glutathione in the substantia nigra in Parkinson's disease. *J Neural Transm, 104*(6-7), 661-677.

Perez, V. I., Buffenstein, R., Masamsetti, V., Leonard, S., Salmon, A. B., Mele, J., . . . Chaudhuri, A. (2009). Protein stability and resistance to oxidative stress are determinants of longevity in the longest-living rodent, the naked mole-rat. *Proc Natl Acad Sci U S A, 106*(9), 3059-3064. doi: 10.1073/pnas.0809620106

Pertusa, M., Garcia-Matas, S., Rodriguez-Farre, E., Sanfeliu, C., & Cristofol, R. (2007). Astrocytes aged in vitro show a decreased neuroprotective capacity. *J Neurochem, 101*(3), 794-805. doi: 10.1111/j.1471-4159.2006.04369.x

Petty, R. D., Sutherland, L. A., Hunter, E. M., & Cree, I. A. (1995). Comparison of MTT and ATP-based assays for the measurement of viable cell number. *J Biolumin Chemilumin, 10*(1), 29-34. doi: 10.1002/bio.1170100105

Piacentini, S., Polimanti, R., Squitti, R., Ventriglia, M., Cassetta, E., Vernieri, F., . . . Fuciarelli, M. (2012). GSTM1 null genotype as risk factor for late-onset Alzheimer's disease in Italian patients. *J Neurol Sci, 317*(1-2), 137-140. doi: 10.1016/j.jns.2012.01.026

Pickart, C. M. (2001). Mechanisms underlying ubiquitination. *Annu Rev Biochem, 70*, 503-533. doi:10.1146/annurev.biochem.70.1.503

Pickel, V. M., Joh, T. H., Field, P. M., Becker, C. G., & Reis, D. J. (1975). Cellular localization of tyrosine hydroxylase by immunohistochemistry. *J Histochem Cytochem, 23*(1), 1-12.

Ponsen, M. M., Stoffers, D., Booij, J., van Eck-Smit, B. L., Wolters, E., & Berendse, H. W. (2004). Idiopathic hyposmia as a preclinical sign of Parkinson's disease. *Ann Neurol, 56*(2), 173-181. doi: 10.1002/ana.20160

Posimo, J. M., Titler, A. M., Choi, H. J., Unnithan, A. S., & Leak, R. K. (2013). Neocortex and allocortex respond differentially to cellular stress in vitro and aging in vivo. *PLoS One, 8*(3), e58596. doi: 10.1371/journal.pone.0058596

Posimo, J. M., Unnithan, A. S., Gleixner, A. M., Choi, H. J., Jiang, Y., Pulugulla, S. H., & Leak, R. K. (2014). Viability assays for cells in culture. *J Vis Exp*(83), e50645. doi: 10.3791/50645

Qi, W., White, M. C., Choi, W., Guo, C., Dinney, C., McConkey, D. J., & Siefker-Radtke, A. (2013). Inhibition of inducible heat shock protein-70 (hsp72) enhances bortezomib-induced cell death in human bladder cancer cells. *PLoS One, 8*(7), e69509. doi: 10.1371/journal.pone.0069509

Rajapakse, N., Kis, B., Horiguchi, T., Snipes, J., & Busija, D. (2003). Diazoxide pretreatment induces delayed preconditioning in astrocytes against oxygen glucose deprivation and hydrogen peroxide-induced toxicity. [Research Support, Non-U.S. Gov'tResearch Support, U.S. Gov't, P.H.S.]. *J Neurosci Res, 73*(2), 206-214. doi: 10.1002/jnr.10657

Ravagnan, L., Gurbuxani, S., Susin, S. A., Maisse, C., Daugas, E., Zamzami, N., . . . Kroemer, G. (2001). Heat-shock protein 70 antagonizes apoptosis-inducing factor. *Nat Cell Biol, 3*(9), 839-843. doi: 10.1038/ncb0901-839

Raz, N., Rodrigue, K. M., Kennedy, K. M., Head, D., Gunning-Dixon, F., & Acker, J. D. (2003). Differential aging of the human striatum: longitudinal evidence. *AJNR Am J Neuroradiol, 24*(9), 1849-1856.

Renkawek, K., Stege, G. J., & Bosman, G. J. (1999). Dementia, gliosis and expression of the small heat shock proteins hsp27 and alpha B-crystallin in Parkinson's disease. *Neuroreport, 10*(11), 2273-2276.

Requejo, R., Hurd, T. R., Costa, N. J., & Murphy, M. P. (2010). Cysteine residues exposed on protein surfaces are the dominant intramitochondrial thiol and may protect against oxidative damage. *FEBS J, 277*(6), 1465-1480. doi: 10.1111/j.1742-4658.2010.07576.x

Rideout, H. J., Larsen, K. E., Sulzer, D., & Stefanis, L. (2001). Proteasomal inhibition leads to formation of ubiquitin/alpha-synuclein-immunoreactive inclusions in PC12 cells. *J Neurochem, 78*(4), 899-908.

Rideout, H. J., & Stefanis, L. (2002). Proteasomal inhibition-induced inclusion formation and death in cortical neurons require transcription and ubiquitination. *Mol Cell Neurosci, 21*(2), 223-238.

Rivett, A. J., & Gardner, R. C. (2000). Proteasome inhibitors: from in vitro uses to clinical trials. *J Pept Sci, 6*(9), 478-488. doi: 10.1002/1099-1387(200009)6:9<478::AID-PSC285>3.0.CO;2-F

Romera, C., Hurtado, O., Mallolas, J., Pereira, M. P., Morales, J. R., Romera, A., . . . Moro, M. A. (2007). Ischemic preconditioning reveals that GLT1/EAAT2 glutamate transporter is a novel PPARgamma target gene involved in neuroprotection. *J Cereb Blood Flow Metab, 27*(7), 1327-1338. doi: 10.1038/sj.jcbfm.9600438

Sacchi, S., Bernasconi, M., Martineau, M., Mothet, J. P., Ruzzene, M., Pilone, M. S., . . . Molla, G. (2008). pLG72 modulates intracellular D-serine levels through its interaction with D-amino acid oxidase: effect on schizophrenia susceptibility. *J Biol Chem, 283*(32), 22244-22256. doi: 10.1074/jbc.M709153200

Sadowski, M., & Sarcevic, B. (2010). Mechanisms of mono- and poly-ubiquitination: Ubiquitination specificity depends on compatibility between the E2 catalytic core and amino acid residues proximal to the lysine. *Cell Div, 5*, 19. doi: 10.1186/1747-1028-5-19

Saibil, H. (2013). Chaperone machines for protein folding, unfolding and disaggregation. *Nat Rev Mol Cell Biol, 14*(10), 630-642. doi: 10.1038/nrm3658

Salvi, A., Carrupt, P., Tillement, J., & Testa, B. (2001). Structural damage to proteins caused by free radicals: asessment, protection by antioxidants, and influence of protein binding. *Biochem Pharmacol, 61*(10), 1237-1242.

Samuni, Y., Goldstein, S., Dean, O. M., & Berk, M. (2013). The chemistry and biological activities of N-acetylcysteine. *Biochim Biophys Acta, 1830*(8), 4117-4129. doi: 10.1016/j.bbagen.2013.04.016

Sato, H., Tamba, M., Okuno, S., Sato, K., Keino-Masu, K., Masu, M., & Bannai, S. (2002). Distribution of cystine/glutamate exchange transporter, system x(c)-, in the mouse brain. *J Neurosci, 22*(18), 8028-8033.Sawada, H., Kohno, R., Kihara, T., Izumi, Y., Sakka, N., Ibi, M., . . . Shimohama, S. (2004). Proteasome mediates dopaminergic neuronal degeneration, and its inhibition causes alpha-synuclein inclusions. *J Biol Chem, 279*(11), 10710-10719.

Saykally, J. N., Rachmany, L., Hatic, H., Shaer, A., Rubovitch, V., Pick, C. G., & Citron, B. A. (2012). The nuclear factor erythroid 2-like 2 activator, tert-butylhydroquinone, improves cognitive performance in mice after mild traumatic brain injury. [Research Support, Non-U.S. Gov't Research Support, U.S. Gov't, Non-P.H.S.]. *Neuroscience, 223*, 305-314. doi: 10.1016/j.neuroscience.2012.07.070

Schipper, H. M. (2011). Heme oxygenase-1 in Alzheimer disease: a tribute to Moussa Youdim. *J Neural Transm, 118*(3), 381-387. doi: 10.1007/s00702-010-0436-1

Schipper, H. M., Bennett, D. A., Liberman, A., Bienias, J. L., Schneider, J. A., Kelly, J., & Arvanitakis, Z. (2006). Glial heme oxygenase-1 expression in Alzheimer disease and mild cognitive impairment. *Neurobiol Aging, 27*(2), 252-261. doi: 10.1016/j.neurobiolaging.2005.01.016

Schipper, H. M., Liberman, A., & Stopa, E. G. (1998). Neural heme oxygenase-1 expression in idiopathic Parkinson's disease. *Exp Neurol, 150*(1), 60-68. doi: 10.1006/exnr.1997.6752

Schipper, H. M., Song, W., Zukor, H., Hascalovici, J. R., & Zeligman, D. (2009). Heme oxygenase-1 and neurodegeneration: expanding frontiers of engagement. *J Neurochem, 110*(2), 469-485. doi: 10.1111/j.1471-4159.2009.06160.x

Schlecht, R., Scholz, S. R., Dahmen, H., Wegener, A., Sirrenberg, C., Musil, D., . . . Bukau, B. (2013). Functional analysis of Hsp70 inhibitors. *PLoS One, 8*(11), e78443. doi: 10.1371/journal.pone.0078443

Schreiner, B., Romanelli, E., Liberski, P., Ingold-Heppner, B., Sobottka-Brillout, B., Hartwig, T., . . . Becher, B. (2015). Astrocyte Depletion Impairs Redox Homeostasis and Triggers Neuronal Loss in the Adult CNS. *Cell Rep, 12*(9), 1377-1384. doi: 10.1016/j.celrep.2015.07.051

Schultz, C., Dick, E. J., Cox, A. B., Hubbard, G. B., Braak, E., & Braak, H. (2001). Expression of stress proteins alpha B-crystallin, ubiquitin, and hsp27 in pallido-nigral spheroids of aged rhesus monkeys. *Neurobiol Aging, 22*(4), 677-

682.Schultz, C., Hubbard, G. B., Rub, U., Braak, E., & Braak, H. (2000). Age-related progression of tau pathology in brains of baboons. *Neurobiol Aging, 21*(6), 905-912.

Seidel, K., Vinet, J., Dunnen, W. F., Brunt, E. R., Meister, M., Boncoraglio, A., . . . Carra, S. (2012). The HSPB8-BAG3 chaperone complex is upregulated in astrocytes in the human brain affected by protein aggregation diseases. *Neuropathol Appl Neurobiol, 38*(1), 39-53. doi: 10.1111/j.1365-2990.2011.01198.x

Sen, E., Basu, A., Willing, L. B., Uliasz, T. F., Myrkalo, J. L., Vannucci, S. J., . . . Levison, S. W. (2011). Pre-conditioning induces the precocious differentiation of neonatal astrocytes to enhance their neuroprotective properties. *ASN Neuro, 3*(3), e00062. doi: 10.1042/AN20100029

Sengupta, P. (2013). The Laboratory Rat: Relating Its Age With Human's. *Int J Prev Med, 4*(6), 624-630.

Shao, Y., & McCarthy, K. D. (1994). Plasticity of astrocytes. *Glia, 11*(2), 147-155. doi: 10.1002/glia.440110209

Shen, H. Y., He, J. C., Wang, Y., Huang, Q. Y., & Chen, J. F. (2005). Geldanamycin induces heat shock protein 70 and protects against MPTP-induced dopaminergic neurotoxicity in mice. *J Biol Chem, 280*(48), 39962-39969. doi: 10.1074/jbc.M505524200

Shin, Y., Klucken, J., Patterson, C., Hyman, B. T., & McLean, P. J. (2005). The co-chaperone carboxyl terminus of Hsp70-interacting protein (CHIP) mediates alpha-synuclein degradation decisions between proteasomal and lysosomal pathways. *J Biol Chem, 280*(25), 23727-23734. doi: 10.1074/jbc.M503326200

Shirley, R. B., Kaddour-Djebbar, I., Patel, D. M., Lakshmikanthan, V., Lewis, R. W., & Kumar, M. V. (2005). Combination of proteasomal inhibitors lactacystin and MG132 induced synergistic apoptosis in prostate cancer cells. *Neoplasia, 7*(12), 1104-1111.

Shringarpure, R., Grune, T., Mehlhase, J., & Davies, K. J. (2003). Ubiquitin conjugation is not required for the degradation of oxidized proteins by proteasome. *J Biol Chem, 278*(1), 311-318. doi: 10.1074/jbc.M206279200

Sian, J., Dexter, D. T., Lees, A. J., Daniel, S., Agid, Y., Javoy-Agid, F., . . . Marsden, C. D. (1994). Alterations in glutathione levels in Parkinson's disease and other neurodegenerative disorders affecting basal ganglia. *Ann Neurol, 36*(3), 348-355. doi: 10.1002/ana.410360305

Slivka, A., Mytilineou, C., & Cohen, G. (1987). Histochemical evaluation of glutathione in brain. *Brain Res, 409*(2), 275-284. Sofic, E., Lange, K. W., Jellinger, K., & Riederer, P. (1992). Reduced and oxidized glutathione in the substantia nigra of patients with Parkinson's disease. *Neurosci Lett, 142*(2), 128-130.

Sofroniew, M. V., & Vinters, H. V. (2010). Astrocytes: biology and pathology. *Acta Neuropathol, 119*(1), 7-35. doi: 10.1007/s00401-009-0619-8

Sone, K., Yamamoto-Sawamura, T., Kuwahara, S., Nishijima, K., Ohno, T., Aoyama, H., & Tanaka, S. (2007). Changes of estrous cycles with aging in female F344/n rats. *Exp Anim, 56*(2), 139-148.Spillantini, M. G., Crowther, R. A., Jakes, R., Hasegawa, M., & Goedert, M. (1998). alpha-Synuclein in filamentous inclusions

of Lewy bodies from Parkinson's disease and dementia with lewy bodies. *Proc Natl Acad Sci U S A, 95*(11), 6469-6473.

Steffl, M., Telgen, L., Schweiger, M., & Amselgruber, W. M. (2010). Estrous cycle-dependent activity of neutrophils in the porcine endometrium: possible involvement of heat shock protein 27 and lactoferrin. *Anim Reprod Sci, 121*(1-2), 159-166. doi: 10.1016/j.anireprosci.2010.05.018

Stetler, R. A., Gao, Y., Signore, A. P., Cao, G., & Chen, J. (2009). HSP27: mechanisms of cellular protection against neuronal injury. *Curr Mol Med, 9*(7), 863-872.

Strey, C. W., Spellman, D., Stieber, A., Gonatas, J. O., Wang, X., Lambris, J. D., & Gonatas, N. K. (2004). Dysregulation of stathmin, a microtubule-destabilizing protein, and up-regulation of Hsp25, Hsp27, and the antioxidant peroxiredoxin 6 in a mouse model of familial amyotrophic lateral sclerosis. *Am J Pathol, 165*(5), 1701-1718. doi: 10.1016/S0002-9440(10)63426-8

Sulzer, D. (2007). Multiple hit hypotheses for dopamine neuron loss in Parkinson's disease. [Research Support, N.I.H., ExtramuralResearch Support, Non-U.S. Gov'tReview]. *Trends in neurosciences, 30*(5), 244-250. doi: 10.1016/j.tins.2007.03.009

Sun, F., Anantharam, V., Zhang, D., Latchoumycandane, C., Kanthasamy, A., & Kanthasamy, A. G. (2006). Proteasome inhibitor MG-132 induces dopaminergic degeneration in cell culture and animal models. *Neurotoxicology, 27*(5), 807-815.

Sun, R., Luo, Y., Li, J., Wang, Q., Chen, X., Guan, K., & Yu, Z. (2015). Ammonium chloride inhibits autophagy of hepatocellular carcinoma cells through SMAD2 signaling. *Tumour Biol, 36*(2), 1173-1177. doi: 10.1007/s13277-014-2699-x

Sunitha, K., Hemshekhar, M., Thushara, R. M., Santhosh, M. S., Yariswamy, M., Kemparaju, K., & Girish, K. S. (2013). N-Acetylcysteine amide: a derivative to fulfill the promises of N-Acetylcysteine. *Free Radic Res, 47*(5), 357-367. doi: 10.3109/10715762.2013.781595

Syed Abdul Rahman, S. N., Abdul Wahab, N., & Abd Malek, S. N. (2013). In Vitro Morphological Assessment of Apoptosis Induced by Antiproliferative Constituents from the Rhizomes of Curcuma zedoaria. *Evid Based Complement Alternat Med, 2013*, 257108. doi: 10.1155/2013/257108

Taguchi, K., Motohashi, H., & Yamamoto, M. (2011). Molecular mechanisms of the Keap1-Nrf2 pathway in stress response and cancer evolution. *Genes Cells, 16*(2), 123-140. doi: 10.1111/j.1365-2443.2010.01473.x

Tang, G., Perng, M. D., Wilk, S., Quinlan, R., & Goldman, J. E. (2010). Oligomers of mutant glial fibrillary acidic protein (GFAP) Inhibit the proteasome system in alexander disease astrocytes, and the small heat shock protein alphaB-crystallin reverses the inhibition. *J Biol Chem, 285*(14), 10527-10537. doi: 10.1074/jbc.M109.067975

Taylor, A. R., Robinson, M. B., Gifondorwa, D. J., Tytell, M., & Milligan, C. E. (2007). Regulation of heat shock protein 70 release in astrocytes: role of signaling kinases. *Dev Neurobiol, 67*(13), 1815-1829. doi: 10.1002/dneu.20559

Tchantchou, F., Graves, M., Rogers, E., Ortiz, D., & Shea, T. B. (2005). N-acteyl cysteine alleviates oxidative damage to central nervous system of ApoE-deficient mice following folate and vitamin E-deficiency. *J Alzheimers Dis, 7*(2), 135-138; discussion 173-180.

Titler, A. M., Posimo, J. M., & Leak, R. K. (2013). Astrocyte plasticity revealed by adaptations to severe proteotoxic stress. *Cell Tissue Res, 352*(3), 427-443. doi: 10.1007/s00441-013-1571-4

Tone, S., Sugimoto, K., Tanda, K., Suda, T., Uehira, K., Kanouchi, H., . . . Earnshaw, W. C. (2007). Three distinct stages of apoptotic nuclear condensation revealed by time-lapse imaging, biochemical and electron microscopy analysis of cell-free apoptosis. *Exp Cell Res, 313*(16), 3635-3644. doi: 10.1016/j.yexcr.2007.06.018

Tynan, R. J., Beynon, S. B., Hinwood, M., Johnson, S. J., Nilsson, M., Woods, J. J., & Walker, F. R. (2013). Chronic stress-induced disruption of the astrocyte network is driven by structural atrophy and not loss of astrocytes. *Acta Neuropathol, 126*(1), 75-91. doi: 10.1007/s00401-013-1102-0

Unnithan, A. S., Choi, H. J., Titler, A. M., Posimo, J. M., & Leak, R. K. (2012). Rescue from a two hit, high-throughput model of neurodegeneration with N-acetyl cysteine. *Neurochem Int, 61*(3), 356-368. doi: 10.1016/j.neuint.2012.06.001

Unnithan, A. S., Jiang, Y., Rumble, J. L., Pulugulla, S. H., Posimo, J. M., Gleixner, A. M., & Leak, R. K. (2014). N-acetyl cysteine prevents synergistic, severe toxicity from two hits of oxidative stress. *Neurosci Lett, 560*, 71-76. doi: 10.1016/j.neulet.2013.12.023

Unno, K., Asakura, H., Shibuya, Y., Kaiho, M., Okada, S., & Oku, N. (2000). Increase in basal level of Hsp70, consisting chiefly of constitutively expressed Hsp70 (Hsc70) in aged rat brain. *J Gerontol A Biol Sci Med Sci, 55*(7), B329-335.

Uryu, K., Richter-Landsberg, C., Welch, W., Sun, E., Goldbaum, O., Norris, E. H., . . . Trojanowski, J. Q. (2006). Convergence of heat shock protein 90 with ubiquitin in filamentous alpha-synuclein inclusions of alpha-synucleinopathies. *Am J Pathol, 168*(3), 947-961.Van den Berghe-Snorek, S., & Stankovich, M. T. (1985). Thermodynamic control of D-amino acid oxidase by benzoate binding. *J Biol Chem, 260*(6), 3373-3379.

Van Den Eeden, S. K., Tanner, C. M., Bernstein, A. L., Fross, R. D., Leimpeter, A., Bloch, D. A., & Nelson, L. M. (2003). Incidence of Parkinson's disease: variation by age, gender, and race/ethnicity. *Am J Epidemiol, 157*(11), 1015-1022.

Venkateshappa, C., Harish, G., Mahadevan, A., Srinivas Bharath, M. M., & Shankar, S. K. (2012). Elevated oxidative stress and decreased antioxidant function in the human hippocampus and frontal cortex with increasing age: implications for neurodegeneration in Alzheimer's disease. *Neurochem Res, 37*(8), 1601-1614. doi: 10.1007/s11064-012-0755-8

Venkateshappa, C., Harish, G., Mythri, R. B., Mahadevan, A., Bharath, M. M., & Shankar, S. K. (2012). Increased oxidative damage and decreased antioxidant function in aging human substantia nigra compared to striatum: implications for Parkinson's disease. *Neurochem Res, 37*(2), 358-369. doi: 10.1007/s11064-011-0619-7

Wagner, B., Natarajan, A., Grunaug, S., Kroismayr, R., Wagner, E. F., & Sibilia, M. (2006). Neuronal survival depends on EGFR signaling in cortical but not midbrain astrocytes. *EMBO J, 25*(4), 752-762. doi: 10.1038/sj.emboj.7600988

Wakabayashi, K., Hayashi, S., Yoshimoto, M., Kudo, H., & Takahashi, H. (2000). NACP/alpha-synuclein-positive filamentous inclusions in astrocytes and

oligodendrocytes of Parkinson's disease brains. [Research Support, Non-U.S. Gov't]. *Acta Neuropathol, 99*(1), 14-20.

Walter, P., & Ron, D. (2011). The unfolded protein response: from stress pathway to homeostatic regulation. *Science, 334*(6059), 1081-1086. doi: 10.1126/science.1209038

Wang, J., Martin, E., Gonzales, V., Borchelt, D. R., & Lee, M. K. (2008). Differential regulation of small heat shock proteins in transgenic mouse models of neurodegenerative diseases. *Neurobiol Aging, 29*(4), 586-597. doi: 10.1016/j.neurobiolaging.2006.11.009

Warner, T. T., & Schapira, A. H. (2003). Genetic and environmental factors in the cause of Parkinson's disease. *Ann Neurol, 53 Suppl 3*, S16-23; discussion S23-15. doi: 10.1002/ana.10487

Wu, Y. R., Wang, C. K., Chen, C. M., Hsu, Y., Lin, S. J., Lin, Y. Y., . . . Lee-Chen, G. J. (2004). Analysis of heat-shock protein 70 gene polymorphisms and the risk of Parkinson's disease. *Hum Genet, 114*(3), 236-241. doi: 10.1007/s00439-003-1050-1

Xu, J., Huang, G., Zhang, K., Sun, J., Xu, T., Li, R., . . . Xu, W. (2014). Nrf2 activation in astrocytes contributes to spinal cord ischemic tolerance induced by hyperbaric oxygen preconditioning. *J Neurotrauma, 31*(15), 1343-1353. doi: 10.1089/neu.2013.3222

Yoshinaga, T., Sassa, S., & Kappas, A. (1982). Purification and properties of bovine spleen heme oxygenase. Amino acid composition and sites of action of inhibitors of heme oxidation. *J Biol Chem, 257*(13), 7778-7785.

Yu, S. W., Wang, H., Poitras, M. F., Coombs, C., Bowers, W. J., Federoff, H. J., . . . Dawson, V. L. (2002). Mediation of poly(ADP-ribose) polymerase-1-dependent cell death by apoptosis-inducing factor. *Science, 297*(5579), 259-263. doi: 10.1126/science.1072221

Zhan, R., Leng, X., Liu, X., Wang, X., Gong, J., Yan, L., . . . Qian, L. J. (2009). Heat shock protein 70 is secreted from endothelial cells by a non-classical pathway involving exosomes. *Biochem Biophys Res Commun, 387*(2), 229-233. doi: 10.1016/j.bbrc.2009.06.095

Zhang, D. D., & Hannink, M. (2003). Distinct cysteine residues in Keap1 are required for Keap1-dependent ubiquitination of Nrf2 and for stabilization of Nrf2 by chemopreventive agents and oxidative stress. *Mol Cell Biol, 23*(22), 8137-8151.

Zhang, Y., & Barres, B. A. (2010). Astrocyte heterogeneity: an underappreciated topic in neurobiology. *Curr Opin Neurobiol, 20*(5), 588-594. doi: 10.1016/j.conb.2010.06.005

Zhang, Y., James, M., Middleton, F. A., & Davis, R. L. (2005). Transcriptional analysis of multiple brain regions in Parkinson's disease supports the involvement of specific protein processing, energy metabolism, and signaling pathways, and suggests novel disease mechanisms. *Am J Med Genet B Neuropsychiatr Genet, 137B*(1), 5-16. doi: 10.1002/ajmg.b.30195

Zhou, J., Coles, L. D., Kartha, R. V., Nash, N., Mishra, U., Lund, T. C., & Cloyd, J. C. (2015). Intravenous Administration of Stable-Labeled N-Acetylcysteine Demonstrates an Indirect Mechanism for Boosting Glutathione and Improving Redox Status. *J Pharm Sci*. doi: 10.1002/jps.24482

Zhu, X., Lee, H. G., Perry, G., & Smith, M. A. (2007). Alzheimer disease, the two-hit hypothesis: an update. [Review]. *Biochim Biophys Acta, 1772*(4), 494-502. doi: 10.1016/j.bbadis.2006.10.014